MEDICAL UNIVERSITY OF VIENNA

Insights into the Brain Extracellular Matrix Through Identification of a Novel Neurodevelopmental Disorder

Doctoral thesis at the Medical University of Vienna

for obtaining the academic degree

Doctor of Philosophy

Submitted by

Christopher Fell, MSc

Supervisor:

Vanja Nagy, PhD

Ludwig Boltzmann Institute for Rare and Undiagnosed Diseases (LBI-RUD)

Research Centre for Molecular Medicine (CeMM) of the Austrian Academy of Sciences

Vienna, February 2022

Table of Contents

Declaration

The work in this thesis was performed at several academic institutions with contributions from various collaborators. In the following section, all contributions will be listed.

Chapter 3 is intended for publication as Fell, C.W.*, Hagelkruys, A.* *et al* and is currently available as a BioRxiv preprint. Most of the experimental work was carried out in the lab of Vanja Nagy (LBI-RUD, Vienna) and Josef Penninger (IMBA, Vienna). The manuscript authors contributed as following: the author of this thesis performed human qPCRs, all experiments relating to human cells (generation of cell lines, flow cytometry, internalisation, immunofluorescence), primary neuron experiments, RNA-sequencing and analysis experiments, curated patient information and liaised with collaborators. AH generated mouse cell lines, performed mouse qPCRs, Western blots and maintenance of mouse colonies. AC performed electrophysiology experiments. MH performed Western blots. LL and JSSL performed Drosophila experiments. JS performed HPLC. AAP performed molecular docking simulations. SM performed flow cytometry in mouse cells. MAT performed mouse pain phenotyping. TK assisted with curation of patient data, RNA-sequencing analysis and analysis of exome data. MMM and JJ analysed exome data. KAT, HY and JW cared for patients and provided clinical information. TLA performed ISH experiments. GW generated plasmid constructs. JBM performed ELISA experiments. VN performed mouse learning phenotyping. MB, UH, NP, BZ, FJM, JMP and VN supervised and provided resources. The author of this thesis and VN wrote the manuscript with input from all collaborators.

All chapters of this thesis were written by the author.

Acknowledgements

First and foremost, the work in this thesis would not have been possible without the support and guidance from my supervisor, Vanja Nagy. I'd like to thank her for her trust, giving me the freedom to develop, for the fruitful scientific discussions, and for her unwavering support in pushing me onto my future steps. I'd also like to thank past and present members of the Nagy lab for making the lab an enjoyable place to come to work. A special shoutout also to Boztug lab members, Rico Ardy in particular, for helping me get started in the lab and for teaching me tips and tricks that have benefitted me ever since.

I've been lucky enough to be part of two fantastic institutes, LBI-RUD and CeMM. I'd like to thank Kaan Boztug, Georg Stary, Giulio Superti-Furga, Anita Ender and all LBI-RUD and CeMM management and faculty for establishing an environment in which I have grown both scientifically and personally. I'll cherish my time at both institutes and will always look back with fond memories. A special thank you also to Joanna Loizou, Georg Winter and Noelia Urbán for their support in my thesis committee and in non-scientific matters.

Doing a PhD has required far more personal support then I had ever expected and I would not have made it without the support of Zozo and friends, my adopted Viennese family. Thank you Ize, for the food and the excellent travel guidance. Thank you Brenda and Miguel, for the food and the laughs. Thank you Matthias, for the food and your steadfast faith that you are right (even when you're not). Thank you Tala, for the food, your serenity and wisdom.

To Juju, my biggest cheerleader, thank you for your love and support over these years. Thank you for believing in me and for your unwavering moral compass (and also for the food). We're off on an adventure together and I can't wait to see what comes next.

Thank you to my friends at home, who I miss constantly, but who are always game for a cheeky adventure somewhere when it's been too long.

Lastly, thank you to my family, who have been my bedrock of support always, including during my PhD (despite having no idea what I'm doing).

Abstract

Congenital rare neurodevelopmental disorders (NDDs) facilitate great insight into the development and functioning of the central nervous system (CNS), as genes critical to the CNS can be identified. Through international collaborations, we identified variants of unknown significance in the gene *FIBCD1* in two unrelated patients with a severe, idiopathic NDD. *FIBCD1* had previously been demonstrated as a pattern recognition receptor of the innate immune system and had no known function in the CNS.

We first profiled the expression of *FIBCD1* in human and mouse tissues, finding high expression in the hippocampus of the brain, in line with the neurodevelopmental phenotypes observed in our patients. We next perturbed a putative *FIBCD1* orthologue (*dFIBCD1*) in *Drosophila melanogaster*, finding that shRNA-mediated neuronal knockdown of *dFIBCD1* resulted in developmental neurological disturbances in the larvae and neurological behavioural disturbances in adults. These findings suggested a previously unknown neuronal function of FIBCD1 and motivated us to further study its function in higher organisms. We obtained a *FIBCD1* KO mouse model, which we found to have impaired performance in hippocampal-dependent learning tasks compared to WT littermates.

Having confirmed an *in vivo* neurological role of *FIBCD1*, we next sought to determine its function. A previous study which reported a partial crystal structure for FIBCD1 identified a potential binding pocket for glycosaminoglycans (GAGs), which are polysaccharide structures found in extracellular matrices. We hypothesised FIBCD1 to be receptor of the brain extracellular matrix (ECM). To this end, we surveyed the hippocampal glycome content of KO and WT mice by HPLC. We observed a relative increase in a particular GAG, chondroitin sulphate 4S (CS-4S; CS-A), which we confirmed to be elevated by Western blot. Next, we determined FIBCD1 to facilitate the endocytosis of GAGs, preferentially CS-A, which is consistent with the hippocampal glycome disturbances in the KO mouse. We developed a cellular assay to experimentally test the patient variants' effects on FIBCD1 function and determined them all to be loss of function.

To understand FIBCD1's signalling function, we isolated mouse primary hippocampal neurons, stimulated FIBCD1, and performed RNA-sequencing. By comparing transcriptomes of stimulated and unstimulated WT vs KO conditions, we identify the transcriptional fingerprint of FIBCD1 stimulation, which includes a number of ECM structural components. Finally, we performed electrophysiological recordings in acute hippocampal slices and found impaired pre- and post-synaptic remodelling in the KO slices compared to WT, which reflects the deficient learning behaviours.

In summary, we report *FIBCD1* as a novel receptor for the brain ECM which, when disrupted, is associated to a complex NDD.

Zusammenfassung

Angeborene seltene neurologische Entwicklungsstörungen (NDD) ermöglichen einen umfassenden Einblick in die Entwicklung und Funktionsweise des zentralen Nervensystems (ZNS), da hierbei für das ZNS wichtige Gene identifiziert werden können. In internationaler Zusammenarbeit haben wir bei zwei nicht verwandten Patienten mit einer schweren, idiopathischen NDD, Varianten von unbekannter Bedeutung im Gen FIBCD1 identifiziert. FIBCD1 war zuvor als Mustererkennungsrezeptor des angeborenen Immunsystems nachgewiesen worden und hatte keine bekannte Funktion im ZNS.

Wir erstellten zunächst ein Profil der Ausprägung von FIBCD1 in menschlichem und Mausgewebe und stellten eine hohe Ausprägung im Hippokampus des Gehirns fest, die mit den bei unseren Patienten beobachteten neurologische Phänotypen übereinstimmt. Daraufhin haben wir ein mutmaßliches FIBCD1-Ortholog (dFIBCD1) in Drosophila melanogaster beeinträchtigt und festgestellt, dass die shRNA-vermittelte neuronale Ausschaltung von dFIBCD1 zu neurologischen Entwicklungsstörungen bei den Larven und zu neurologischen Verhaltensstörungen bei den Erwachsenen führte. Diese Ergebnisse ließen auf eine bisher unbekannte neuronale Funktion von FIBCD1 schließen und motivierten uns, seine Funktion in höheren Organismen weiter zu untersuchen. Wir erhielten ein FIBCD1-KO-Mausmodell, bei dem wir im Vergleich zu WT-Wurfgeschwistern Leistungseinbußen bei hippocampusabhängigen Lernaufgaben feststellten.

Nachdem wir die neurologische Rolle von FIBCD1 *in vivo* bestätigt hatten, versuchten wir als nächstes, seine Funktion zu bestimmen. In einer früheren Studie, in der eine partielle Kristallstruktur von FIBCD1 beschrieben wurde, wurde eine potenzielle Bindungstasche für Glykosaminoglykane (GAGs) identifiziert, bei denen es sich um Polysaccharidstrukturen handelt, die in extrazellulären Matrizen vorkommen. Wir stellten die Hypothese auf, dass FIBCD1 ein Rezeptor für die extrazelluläre Matrix (ECM) des Gehirns ist. Zu diesem Zweck untersuchten wir den Glykogengehalt im Hippokampus von KO- und WT-Mäusen mittels HPLC. Wir beobachteten einen relativen Anstieg eines bestimmten GAG, Chondroitinsulfat 4S (CS-4S; CS-A), dessen erhöhte Konzentration wir durch Western Blot nachweisen konnten. Als nächstes stellten wir fest, dass FIBCD1 die Endozytose von GAGs, vorzugsweise CS-A, erleichtert, was mit den Störungen des Glykogens im Hippokampus der KO-Maus übereinstimmt. Wir entwickelten einen Zellexperiment, um die Auswirkungen der Patientenvarianten auf die FIBCD1-Funktion experimentell zu testen, und stellten fest, dass sie alle einen Funktionsverlust aufweisen.

Um die Signalfunktion von FIBCD1 zu verstehen, isolierten wir primäre Hippokampus-Neuronen der Maus, stimulierten FIBCD1 und führten RNA-Sequenzierung durch. Durch den Vergleich der Transkriptome von stimulierten und nicht-stimulierten WT- und KO-Bedingungen konnten wir den transkriptionellen Fingerabdruck der FIBCD1-Stimulation identifizieren, der eine Reihe von ECM-

Strukturkomponenten umfasst. Schließlich führten wir elektrophysiologische Ableitungen in akuten Hippocampusschnitten durch und stellten fest, dass der prä- und postsynaptische Umbau in den KO-Scheiben im Vergleich zu den WT-Scheiben beeinträchtigt ist, was das mangelhafte Lernverhalten widerspiegelt.

Zusammenfassend stellen wir fest, dass FIBCD1 ein neuartiger Rezeptor für die ECM des Gehirns ist, der, bei einer gestörten Funktion, mit einer komplexen NDD verbunden ist.

List of Abbreviations

AD	Autosomal dominant
ADHD	Attention deficit hyperactivity disorder
AR	Autosomal recessive
ASD	Autism spectrum disorder
Aβ	Amyloid-β
BDNF	Brain derived neurotrophic factor
BSA	Bovine serum albumin
CAM	Cell adhesion molecule
ChABC	Chondroitinase ABC
CNS	Central nervous system
CS	Chondroitin sulphate
CSPG	Chondroitin sulphate proteoglycan
DEG	Differentially expressed gene
DMMB	Dimethylmethylene blue
DRG	Dorsal root ganglion
DS	Dermatan sulphate
ECM	Extracellular matrix
EPM	Elevated plus maze
ESC	Embryonic stem cell
FAK	Focal adhesion kinase
FReD	Fibrinogen recognition domain
FXS	Fragile-X syndrome
GAG	Glycosaminoglycan
GalNAc	N-acetylgalactosamine
GlcA	Glucoronic acid
GlcNAc	N-acetylglucosamine
GWAS	Genome-wide association study
HA	Hyaluronic acid
HPLC	High-performance liquid chromatography
HS	Heparan sulphate
HSPG	Heparan sulphate proteoglycan
IA	Inhibitory avoidance
ID	Intellectual disability
IdoA	Iduronic acid
iN	Induced neuron
iPSC	Induced pluripotent stem cell
KD	Knockdown
KS	Keratan sulphate
LTP	Long term potentiation
MD	Monocular deprivation
MEF	Mouse embryonic fibroblast
MK	Midkine
MMP	Matrix metalloproteinase
MPS	Mucopolysaccharidosis
MRI	Magnetic resonance imagery
MS	Mass spectrometry
MTLE	Mesial temporal lobe epilepsy

NCAM	Neural cell adhesion molecule
NDD	Neurodevelopmental disorder
NG2	Neuron-glial antigen 2
NGF	Nerve growth factor
NGS	Next generation sequencing
OD	Ocular dominance
OPC	Oligodendrocyte progenitor cell
Otx2	Orthodenticle homeobox protein 2
PBMC	Peripheral blood mononuclear cell
PFC	Prefrontal cortex
PKC	Protein kinase C
PNN	Perineuronal net
PSD	Post-synaptic density
PSD	Post-synaptic density
PV	Parvalbumin
UPD	Uniparental disomy
UTR	Untranslated region
WES	Whole exome sequencing
WFA	Wisteria floribunda agglutinin
WGS	Whole genome sequencing
XLD	X-linked dominant
XLR	X-linked recessive

List of Figures

1. Introduction

Human genetic diseases

The human genome consists of approximately 3 billion nucleotides (Lander *et al*, 2001; Venter *et al*, 2001) separated into 23 pairs of chromosomes, of which 22 pairs are autosomes and 1 pair are allosomes (or "sex chromosomes," X and Y). Only about 3% of the genome encodes proteins, consisting of approximately 21,000 genes (Dunham *et al*, 2012). Errors in the DNA code can cause disease which are heritable.

Genetic diseases caused by mutations in a single gene are referred to as "monogenic" and diseases caused by a combined effect of many genes are "polygenic." Monogenic diseases are usually rare. The European Union defines a rare disease as one that affects less than 1 in 2000 people, though 85% of the approximately 6000 identified rare diseases affect less than 1 in 1,000,000 people (Nguengang Wakap *et al*, 2020). Considering that rare diseases affect a collective 30,000,000 people in Europe, identifying, understanding and treating rare diseases is a public health issue (Valdez *et al*, 2016). Furthermore, identification of rare (monogenic) diseases highlight which of our 21,000 genes are particularly important to the development and function of the human body. The study of rare inherited diseases is therefore to the benefit of the wider public and not just those directly affected by such diseases.

Mendelian Modes of Inheritance

Humans are diploid, which means that the vast majority of our cells contain two sister copies of each autosome each inherited from either our mother or father. The corresponding genes between each sister autosome, which are called "alleles," code for the same proteins but can differ in genetic sequence.

Severe, monogenic disorders are often inherited in four basic modes: autosomal recessive (AR), autosomal dominant (AD), X-linked recessive (XLR) and X-linked dominant (XLD). A disease allele with a recessive mode of inheritance can be compensated for by a healthy sister allele. Therefore, patients with an AR disorder must harbour two diseased alleles each inherited from their mother and father, who are usually healthy and unaware that they each carry a single diseased allele. This is known as being a heterozygote, or "carrier". Diseases caused by mutation in genes on the X chromosome are referred to as "X-linked." XLR disorders primarily affect males (XY) as they do not have the possibility of a healthy sister X-linked allele to compensate for a diseased allele. XLR disorders are therefore usually transmitted from carrier mother to her son. For alleles that exhibit dominant modes of inheritance, only a single diseased allele is required for disease to manifest. For AD inheritance, usually

one of the parents is affected by the disease and passes on the diseased allele. XLD disorders are quite rare but can be transmitted from either parents with an equal chance of affecting sons or daughters.

Errors of chromosomal inheritance

While the majority of human cells are diploid, our gametes (the sperm and egg) are haploid, meaning they contain 1 copy of each chromosome. During fertilisation, a sperm and an egg fuse together to produce a diploid cell which is then able to divide, mature and form a foetus. However, there can be errors in the formation of the gametes which results in the gamete having an improper number of chromosomes, known as "aneuploidy". If one of the fertilising gametes is aneuploid, the resulting zygote will also be aneuploid. Aneuploidy of the autosomes is usually embryonically lethal, resulting in a spontaneous abortion, and accounts for over half of miscarriages during the first trimester (Ljunger *et al*, 2005). However, there are some occasions where foetal aneuploidy does not result in termination of the pregnancy. Gain of an autosome can be tolerated at chromosome 13 (causing Patau Syndrome), chromosome 18 (Edwards Syndrome) and chromosome 21 (Down's Syndrome) (Potapova & Gorbsky, 2017). Loss of any autosome is not viable. For the allosomes, aneuploidy is deleterious but is usually not lethal. The most common example is Turner Syndrome, caused by a missing X chromosome in females (45, XO). Another example is Kleinfelters Syndrome, where males have an extra X chromosome (47, XXY).

Uniparental disomy (UPD) is a phenomenon of inheritance of both copies of a paternal or maternal chromosome, with no contribution from the other parent. This can occur as a resolution of aneuploidy after fertilisation, where an extra chromosome is randomly eliminated (Fig. 1a) or duplication of a chromosome to replace a missing one (Fig. 1b). Alternatively, early mitotic crossing over can result in large arms of a chromosome being swapped, resulting in mosaic UPD (Fig. 1c). UPD is often not noticed throughout life, however, some chromosomes contain imprinted genes where it is critical to receive both maternal and paternally inherited alleles (del Gaudio *et al*, 2020), which can resort in imprinting disorders such as Prader-Willi Syndrome. Alternatively, UPD of a chromosome carrying a diseased AR allele can occur, which may lead to uncovering of the disorder in the offspring. This causes rare cases of a child inheriting an AR disorder despite only one of their parents being carrier.

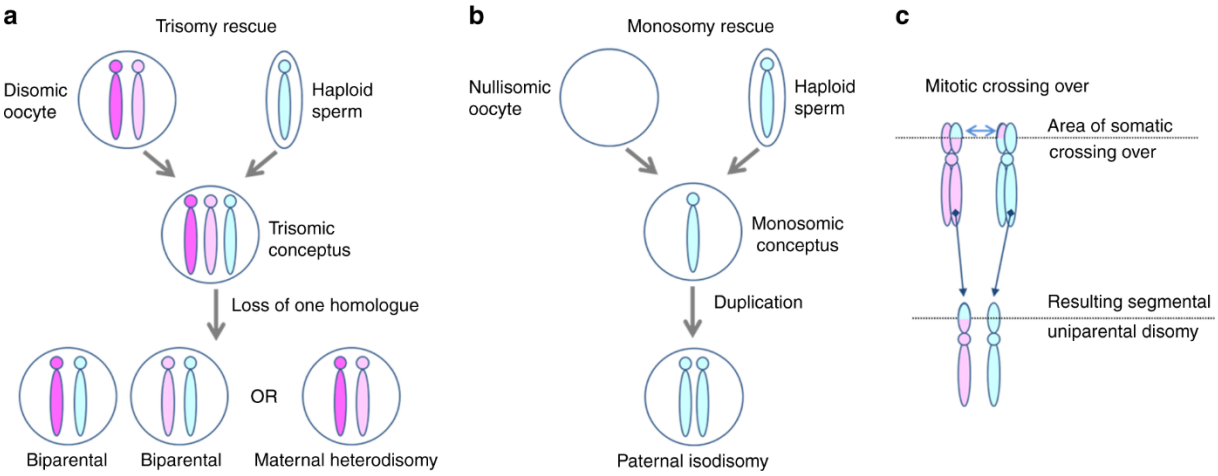

Figure 1: **Examples of common mechanisms by which uniparental disomy arises.** *Image reprinted with permission from del Gaudio et al., 2020.*

Genetics of neurodevelopmental disorders

Neurodevelopmental disorders (NDDs) are a group of disorders including intellectual disability (ID) and autism spectrum disorders (ASDs), characterised by early onset symptoms such as communication deficits, stereotypical and repetitive movements and impairments to communication and social interaction skills (Thapar *et al*, 2017). NDDs are often classified as syndromic, meaning there are associated co-morbidities other than the primary developmental symptom, or non-syndromic. NDDs can be caused by genetic or environmental factors (or a combination of both). Environmental risk factors include pre- or post-natal infection, maternal alcohol abuse and malnutrition. Many genetic NDDs are highly polygenic, meaning there are number of contributory genetic risk factors which have an individually small effect size. There are also a number of rare, monogenic NDDs caused by highly penetrant and deleterious genetic variants, usually AR inherited, which are the focus of the present thesis.

Identification of monogenic causes of NDDs reveals genes key to correct neurological development, thus facilitating a 'top-down' approach to studying CNS development. Thousands of genes have been identified thus far and the exponential rate of increase each year implies that NDD gene identification has not plateaued (Vissers *et al*, 2016; Kochinke *et al*, 2016). It has been estimated that there are over 1000 NDD genes still to be identified (Kaplanis *et al*, 2020). The most common monogenic NDD is Fragile-X Syndrome (FXS), an XLD disorder, which affects approximately 1 in 4000 males and 1 in 8000 females. FXS is characterised by developmental delay, autistic-like behaviours (e.g. avoidance of eye contact, flapping hand movements) and intellectual disability. Additionally, physical features such an elongated, narrow face, flexible fingers, large ears and macroorchidism are typical. FXS is caused by a CGG repeat expansion in the 5' untranslated region (5'-UTR) of the gene *FMR1*,

leading to hypermethylation and silencing of the gene. Symptoms occur on a spectrum of severity, with longer repeat expansions correlated with greater severity of symptoms (Garber *et al*, 2008). The *FMR1* protein product, FMRP, is involved in the regulation of protein synthesis at neuronal dendrites, regulating synaptic transmission and cognition (Garber *et al*, 2008). Another relatively common and well-studied monogenic NDD is Rett syndrome, which is XLD, caused by loss of function of the gene *MECP2*. Rett syndrome is a progressive disease primarily observed in females at a rate of 1 in 10,000, as males who inherit the deleterious allele are usually not viable. Clinically, patients with Rett disorder develop normally up to 6-18 months after birth, after which development stagnates and there is a rapid loss of language, motoric and cognitive skills (Chahrour & Zoghbi, 2007).

The brain extracellular matrix

The extracellular matrix (ECM) of the brain is a structurally dynamic microenvironment that has important roles in the development and function of the CNS. Human genetic disorders of ECM composition, synthesis, metabolism and signalling affect different systems, but most include the CNS, and can cause an NDD (Freeze et al, 2012).

The ECM is composed of glycans and glycoconjugates, including glycoproteins, proteoglycans and glycosphingolipids. The ECM of the brain shares many components with the ECM of other tissues. However, there are some features distinctive to the brain, including relatively low amounts of fibrous proteins (e.g. collagen) and high levels of glycosaminoglycans (GAGs) (Novak & Kaye, 2000). The ECM can be broadly classified by location into: 1) the pial basement membrane, which contains mostly fibrillary proteins and is located on the outer surface of the brain (Fig. 2A), 2) the interstitial neural ECM, which resides between cells and contains mostly GAGs, proteoglycans and hyaluronan (Fig. 2B) and 3) the cell-surface glycocalyx, which are membrane-localised glycoproteins, proteoglycans and glycolipids (Fig. 2C). Signalling from the interstitial and cell-surface ECM is essential for many neurodevelopmental processes including axon outgrowth, axon guidance, synaptogenesis, neuronal migration and remodelling of the synapse.

The brain ECM is composed of a vast array of different components. The present thesis will focus largely on a principal GAG, chondroitin sulphate (CS), and its conjugates, chondroitin sulphate proteoglycans (CSPGs).

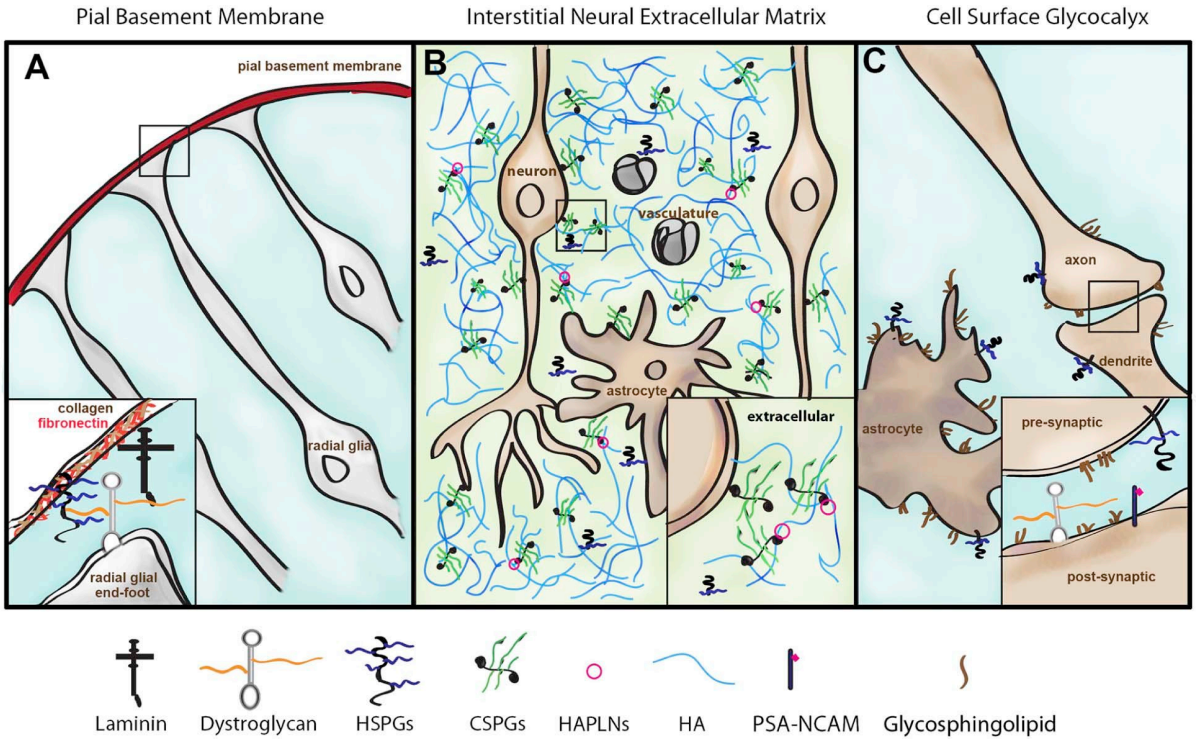

Figure 2: **Organisation of the brain extracellular matrix**. Brain extracellular structures are organised at (A) the pial basement membrane encapsulating the brain, (B) the interstitial space between brain cells and (C) the cell surface glycocalyx. *Reproduced with permission from Dwyer and Esko 2016.*

Components of the ECM: glycosaminoglycans

GAGs are polysaccharide structures consisting of variable repeating disaccharide subunits, which consist of an amino sugar and either a uronic acid or galactose. There are 5 types of GAGs: heparin, heparan sulphate (HS), chondroitin sulphate (CS), dermatan sulphate (DS), keratan sulphate (KS) and hyaluronic acid (HA). HS and HA both consist of N-acetylglucosamine (GlcNAc) and glucuronic acid (GlcA) but differ in that HS forms a proteoglycan and HA does not. CS consists of N-acetylgalactosamine (GalNAc) and GlcA, DS of GalNAc and iduronic acid (IdoA) and lastly KS of GalNAc and galactose. HS, CS, DS and KS all are conjugated to a core protein to form a proteoglycan, which are themselves classified based on the composition of their GAG side chains.

All GAGs are negatively charged, which is key to their function, and often associated with the presence of sulphate modifications. The exception is the unsulphated HA, where the negative charge arises from the GlcA subunits. Sulphation of the GAG chains is a complex and dynamic process regulated by sulfonyltransferases which catalyse the transfer of a sulfonyl group from an activated sulphate donor to the GAG amino group. In eukaryotic cells, the sulphate donor is the highly conserved 3'-phosphoadenosine-5'-phosphosulfate (PAPS). Sulphate modifications to the GAG chains is a tightly regulated process and contributes significantly to the functional diversity of the structures. For CS, sulfonyltransferases catalyse the 4-O- and 6-O- sulphation of the GalNAc units in variable degrees and

patterns. CS GalNAc units can be 4-sulphated (CS-4S, CS-A), 6-sulphated (CS-6S, CS-C) or both (CS-4,6S, CS-E). Additionally, the GlcA unit can be 2-O-sulphated by the enzyme uronosyl 2-O-sulfotransferase (2OST) (Kobayashi *et al*, 1999), in combination with 4-O-sulphated GalNAc (CS-B) or 6-O-sulphated GalNAc (CS-D) (Fig. 3).

Multiple lines of evidence suggest CS sulphation to be under tight spatiotemporal regulation during development. HPLC analysis of CS disaccharides showed CS-A to be expressed in the mouse cortex and cerebellum during prenatal development, which gradually increased during development (Miller & Hsieh-Wilson, 2015). Conversely, CS-C was also shown to be expressed in development but gradually decreases with time, though it still remained the second highest expressed CS in adulthood. CS-E was expressed highest in prenatal mouse cortex and decreased into adulthood, where it is expressed higher in the cortex than cerebellum; CS-D was seen highest in the cerebellum. The expression of the enzymes that catalyse the addition of the sulphate groups, which is also under tight regulation, generally correlates with the expression levels of the respective CS motifs (Purushothaman *et al*, 2007; Miller & Hsieh-Wilson, 2015).

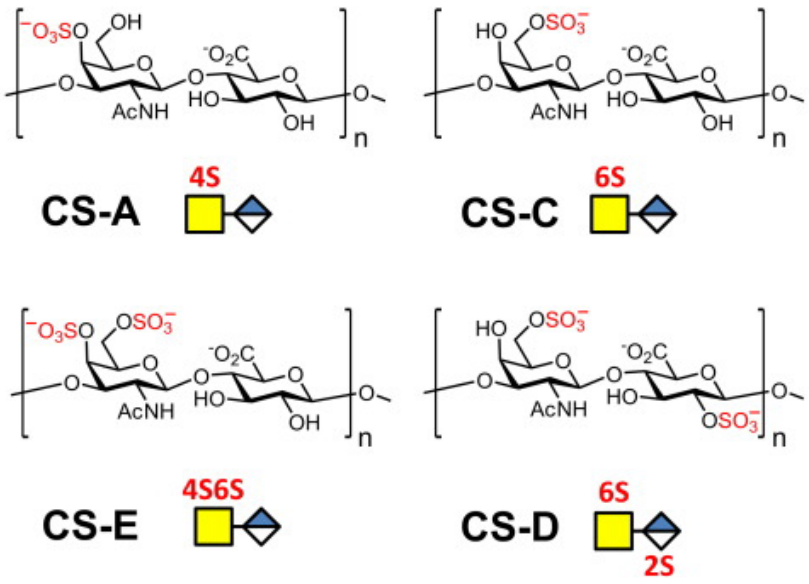

Figure 3: **The structure of common sulphated chondroitin sulphates**. Shown are the number and position of sulphate groups added to GalNAc (square) and/or GlcA (diamond) subunits of chondroitin sulphate. *Reproduced and modified with permission from Miller and Hsieh-Wilson 2015*.

Components of the ECM: chondroitin sulphate proteoglycans

GAGs are often conjugated to proteins to form proteoglycans. The core protein determines where a proteoglycan is localised (e.g. within a vesicle or extracellular); the GAGs normally mediate the function of a proteoglycan. CS chains conjugated to core proteins form chondroitin sulphate proteoglycans

(CSPGs), of which the most prominent are the lectican family (also known as hyalectans), which constitute the most abundant proteins in the brain ECM and the largest family of proteoglycan. In mammals there are four lectican genes coding for neurocan, brevican, versican and aggrecan (Smith *et al*, 2015). These CSPGs differ in the length of the core protein as well as the number, position and composition of the GAG side chains. Some lecticans (such as versican) can also be alternatively spliced, leading to structural isoforms. Structurally, lecticans contain globular C- and N-terminal domains interspersed by structurally heterogenous central domains, onto which the CS chains are covalently attached (Yamaguchi, 2000). The central domain is highly variable in length, sequence and the number of GAG binding sites. Versican has the longest central domain (c. 1700 amino acids); brevican the shortest (c. 300 amino acids). Aggrecan has the most potential CS binding sites in the central domain (c. 120); brevican the fewest (c. 3) (Yamaguchi, 2000). Lecticans associate with hyaluronan via their highly homologous N-terminal hyaluronan-binding domain, which is stabilised and strengthened by link-proteins. The lecticans also differ based on their localisation and cell type of origin. Brevican and neurocan expression is largely restricted to the nervous system; aggrecan and versican are found in other tissues as well (Yamaguchi, 2000). Neurocan is expressed by astrocytes and neurons, brevican mainly by neurons, versican by neurons and oligodendrocytes and aggrecan mainly by neurons (Zimmermann & Dours-Zimmermann, 2008). The expression of the lecticans is regulated during development. Neurocan and versican (splice variant GAGβ) comprise the 'immature ECM' and are highly expressed during development before a sharp reduction in expression shortly before birth. Aggrecan, brevican and versican (splice variant GAGα) make up the 'mature ECM,' as their expression gradually rises from development into adulthood, peaking at about P150 (Fig. 3) (Zimmermann & Dours-Zimmermann, 2008).

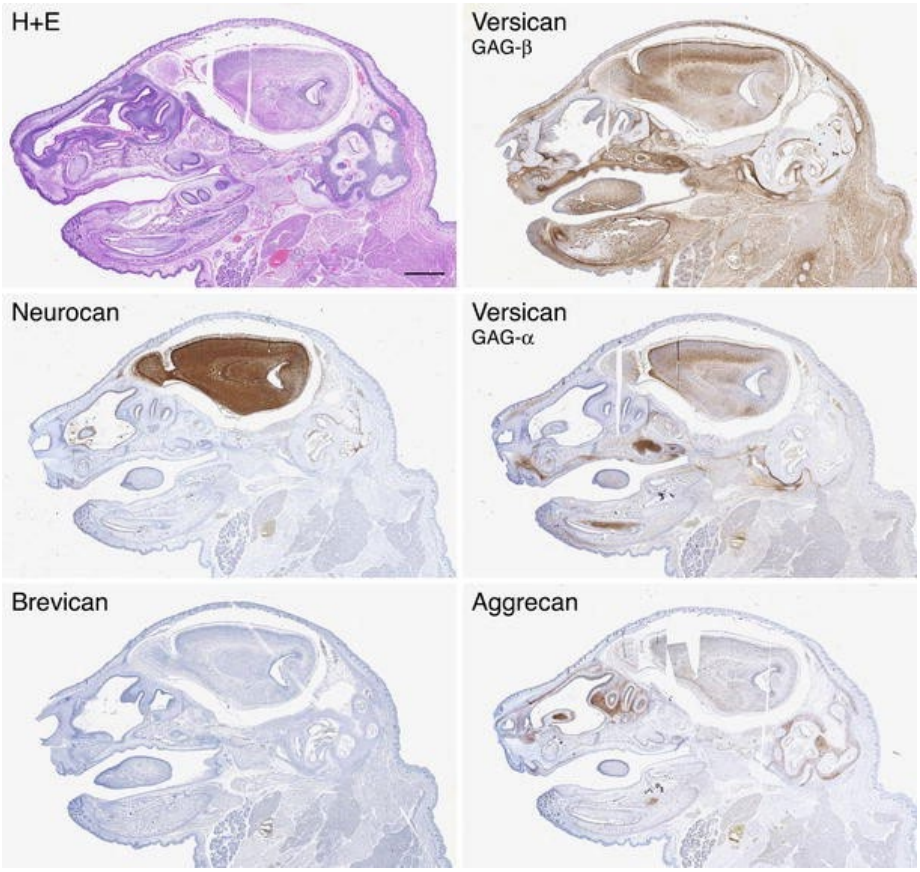

Figure 4: **Immunohistochemical staining of lectin family members in the head of E18.5 mice.** *Reproduced with permission from Zimmermann and Dours-Zimmermann 2008.*

In addition to the lectican family, prominent CSPGs in the CNS include neuron-glial antigen 2 (NG2), also called CSPG4, a cell-surface transmembrane protein expressed by non-neuronal cells such as microglia, macrophages and oligodendrocyte progenitor cells (OPCs) (Wang & He, 2009; Jones *et al*, 2002). NG2 inhibits neuronal attachment and neurite outgrowth *in vitro* (Dou & Levine, 1994) and congenital mutations have been associated with familial schizophrenia (de Vrij *et al*, 2019). Phosphacan is a proteoglycan that can contain either CS or KS side chains, expressed in the CNS, and derived by cleaving of receptor-type protein-tyrosine phosphatase (PTPζ/RPTPβ), a transmembrane receptor that is synthesised as a CSPG (Krishnaswamy *et al*, 2019). Phosphacan is expressed in regions of the brain including the hippocampus, cerebellum and olfactory bulb and, in the cerebellum, shown to localise around axonal parallel fibres but not synapses (Hayashi *et al*, 2005). *In vitro*, phosphacan inhibited adhesion and axonal outgrowth in cultured CGNs (Hayashi *et al*, 2005). Using a phosphacan KO mouse, researches demonstrated a disruption to the structure of perineuronal nets (PNNs) though the total number and distribution was unchanged (Eill *et al*, 2020). Decorin is a small proteoglycan sometimes associated with CS in the CNS and has been shown to be expressed by neurons and astrocytes in the postnatal rat neocortex, thalamus and hippocampus (Kappler *et al*, 1998). Decorin's function in the CNS is unknown and mice with knocked out *Dcn*, coding for decorin, were not reported to have neurological phenotypes (Danielson *et al*, 1997). Neuroglycan C (NGC) is a poorly studied

transmembrane CSPG that is expressed only in the CNS (Nakanishi *et al*, 2006). NGC is thought to have a role in promoting synaptogenesis and/or neurite outgrowth, as it was shown to be stimulatory to neurite outgrowth in primary rat cortical cultures, which was blocked by inhibitors of protein kinase C (PKC) and phosphoinositide 3-kinase (PI3K) (Nakanishi *et al*, 2006, 2010). Of note, studies in the mouse cerebellum showed that NGC was associated to CS chains in the developing but not the mature cerebellum, the reasons for which are unclear (Aono *et al*, 2000).

The role of CS and CSPGs in neuronal development and function

Perineuronal nets

PNNs are pericellular ECM condensates that encapsulate the soma, dendrites and often axons of neurons, mainly cortical parvalbumin (PV)-positive inhibitory interneurons. PNNs can also be observed in the amygdala and hippocampal CA2 region, where they encapsulate excitatory and inhibitory neurons (Fawcett *et al*, 2019). They are found also outside of the brain, such as at neurons in the dorsal horn. Most PNNs can be identified by staining with the lectin *Wisteria floribunda* agglutinin (WFA), which binds GalNAc residues of CSPGs within PNNs (Haji-Ghassemi *et al*, 2016) (Fig. 5). Many studies in the literature use WFA as a tool for PNN visualisation, however, it is often overlooked that there are also PNNs that are WFA-negative, such as those that encapsulate cortical output neurons.

PNNs are composed primarily of CSPGs of the lectican family joined to a hyaluronan backbone and stabilised by link proteins and tenascin-R (Fig. 5). Conditional knockout of *Acan*, coding for aggrecan, in a mouse model resulted in loss of PNN structures (Rowlands *et al*, 2018). This was not the case for brevican, versican or neurocan, suggesting that aggrecan is the only essential lectican for PNN formation or stability. KO of hyaluronan led to incomplete loss of PNNs and KO of the link proteins HAPLN1 and HAPLN4 led to loss of PNN without decreases in overall CSPG levels, suggesting a failure of the CSPGs to be incorporated into the PNNs. Formation of PNNs during development is also influenced by CS sulphation, the gene Otx2 (both discussed in more detail later) and synaptic activity.

PNNs have been classically studied in the context of visual cortex synaptic plasticity (discussed in more detail in a later section) but have also gained attention as regulators of learning and memory. PNNs have been shown to restrict synaptic plasticity and protect fear memories from erasure. While fear memories can be readily erased in juvenile rats by continued exposure to a non-reinforced conditioned stimulus, in adult rats, fear memories are more persistent. Gogolla and colleagues showed that the switch between juvenile and adult rats' fear extinction phenotypes correlates with the formation of PNNs. Destruction of PNNs by injection of the enzyme Chondroitinase ABC (ChABC) into the basolateral amygdala of adult rats re-enabled the extinction of fear memories compared to vehicle-injected control rats, indicating that PNNs function in the protection of memories from erasure

(Gogolla *et al*, 2009). However, it should be noted that ChABC acts by cleaving the GAG chain of CSPGs and HSPGs into soluble di- and tetra-saccharides. Therefore, ChABC action is not restricted to PNNs, which represent only 2% of the total CSPG content in the brain. A clearer association between PNNs and restricting synaptic plasticity was made by deletion of the link protein HAPLN1 in mouse CNS, which resulted in heightened plasticity into adulthood, normally restricted by PNNs during critical period closure (discussed in more detail later) (Carulli *et al*, 2010).

The mechanisms by which PNNs regulate synapse plasticity are not fully understood. Evidence suggests a complex relationship that appears to depend on neuronal type and brain region. Further, interrogation of PNN function through disruption of its constituents has largely relied on KO mouse models. Most PNN components also function outside of the PNNs, which makes observed phenotypes in the KO mouse difficult to assign solely to PNN disruption.

Tenascin-R KO mice, a more targeted model of PNN disruption, exhibit perturbed LTP in the hippocampus associated to alterations in GABAergic inhibition of pre-synaptic vesicle release and current flow through voltage-gated Ca^{2+} channels (Saghatelyan *et al*, 2000; Bukalo *et al*, 2001). Tenascin-R has also been shown to regulate action potential velocity through interactions with sodium channel subunits (Srinivasan *et al*, 1998). Brevican has been demonstrated to regulate AMPA channel motility, with KO mice exhibiting fewer innervations from excitatory neurons onto PV+ cells, reduced frequency of synaptic potentials and alterations in the function of K+ channels (Favuzzi *et al*, 2017). Brevican has also been shown to restrict AMPA receptor motility in primary hippocampal neuron dendritic spines, and alleviation of this restriction restored short-term synaptic plasticity (Frischknecht *et al*, 2009). Deletion of aggrecan in the mouse visual cortex resulted in loss of PNN structures and re-instated heightened synaptic plasticity reminiscent of juvenile stages of development, normally restricted by PNNs (Rowlands *et al*, 2018). Neurocan deletion did not have a significant effect on PNN formation but impairments in the maintenance of hippocampal LTP was observed (Zhou *et al*, 2001). Disruption of CS synthesis by knockout of key synthesis enzyme *CSGalNAcT1*, resulted in persistent cortical plasticity and immature PV+ cells, suggesting CS to be important to the maturation of inhibitory circuits (Hou *et al*, 2017). Some studies have suggested that the protein Semaphorin 3a (Sema3a) is an effector protein of PNNs, as it has been shown that Sema3a localises to PNNs, interacts with CS-4,6S (CS-E) of the ECM, and inhibits synaptic plasticity (Dick *et al*, 2013). Finally, CSPGs have been shown signal inhibitory cues through cell surface receptors, including PTPσ, which inhibits axonal outgrowth in injury models, LAR and Nogo receptors NgR1 and NgR3 (Dickendesher *et al*, 2012; Lee *et al*, 2008; Xu *et al*, 2015). However whether these receptors act on CSPGs in PNNs and have a role in synaptic plasticity has not been shown.

The late Roger Tsien proposed an additional function of PNNs as a stable means of storing very long-term memories (Tsien, 2013). The idea was that the holes in the lattice-like PNN structure, through which synapses form, are a metabolism-independent stable site for the return of synapses after withdrawal, even after a very long time or after a traumatic injury or prolonged state of unconsciousness (e.g. a coma). While an attractive idea, there is thus far little supportive evidence, in part due to the lack of tools to answer this question. As discussed, most studies have used ChABC or genetic means to perturb PNNs and it is often difficult to dissect the roles of PNNs on long term memory and other effects of PNN disruption (Fawcett *et al*, 2019).

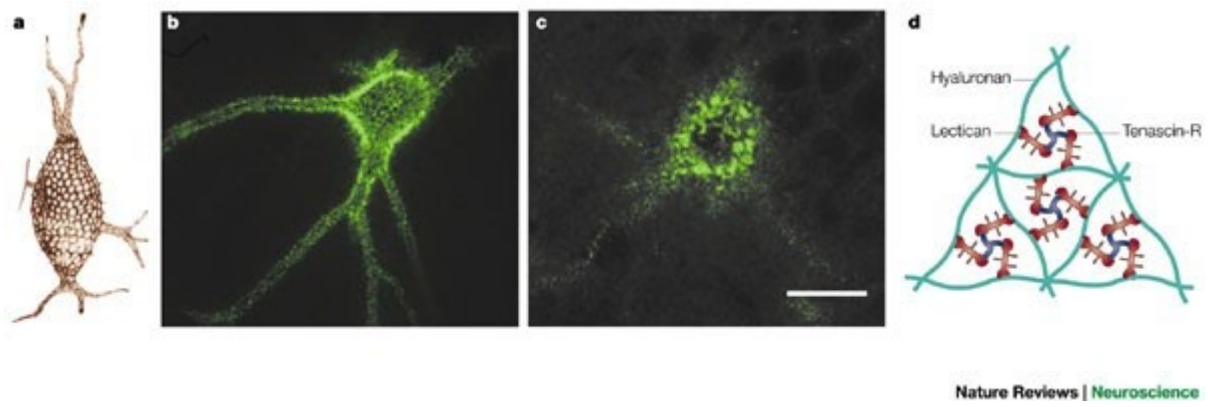

Figure 5: **Perineuronal nets**. (A) A drawing of a perineuronal net by Ramón y Cajal. (B) WFA staining of PNNs around an inhibitory interneuron. (C) WFA staining of a PNN after ChABC digestion. (D) Proposed structure of a PNN. *Reproduced with permission from Dityatev and Schachner, 2003.*

Axonal outgrowth inhibition and stimulation

A relatively well studied function of CSPGs is in the regulation of neurite outgrowth by stimulation or inhibition. The inhibitory effects of sulphated CSPGs on axonal outgrowth is perhaps best studied outside of the brain. After axonal injury in the spine, CSPG lesions rich in brevican, neurocan and versican (among others) are formed by reactive astrocytes, inhibiting the regeneration of the injured axon (Davies *et al*, 1999). Treatment of nerve-crushed mice/rats with ChABC to digest the GAG chains permits regeneration of the axon and recovery by the animal, presumably due to the alleviation of the inhibitory cues signalled by the CSPGs (Bradbury *et al*, 2002). Therefore, alleviation of CSPG inhibitory signalling represents a therapeutic avenue for nerve-crush injury (Bradbury & Burnside, 2019). In the brain, CSPGs often also signal inhibitory cues, defining growth non-permissive boundaries and thus aiding in neurite pathfinding (Katoh-Semba *et al*, 1995). Concordantly, areas thought to delineate boundaries to axonal outgrowth or cell migration often exhibit strong immunostaining for CS, such as at the glomerulus of the olfactory bulb (Gonzalez & Silver, 1994). CSPG binding to neuronal receptors leads to an intracellular signalling through RhoA and Rho kinase (ROCK) that inhibit cytoskeletal

polymerisation, causing growth cone collapse and inhibition of neurite outgrowth (Fujita & Yamashita, 2014). Inhibition of ROCK signalling in the mouse visual cortex has been shown to abrogate CSPG-dependent phenotypes (Ribot *et al*, 2021).

While CSPGs are usually considered as inhibitory, growth-blocking structures, they also play a role in shaping and stimulating neurite outgrowth. Axonal outgrowths *in vivo* have been observed to cross CSPG-rich regions, such as in the developing neocortical subplate (Bicknese *et al*, 1994). It is thought that the different effects of CSPGs on axonal growth is due to differential sulphate patterning on the GAG chains. *In vitro,* CS-D and CS-E have been shown to promote outgrowth of neural extensions in primary hippocampal neurons. Plating of primary hippocampal neurons on primary CS-D (sourced from shark cartilage) stimulated the outgrowth of multiple dendritic protrusions, whereas CS-E (from squid cartilage) promoted the outgrowth of a single axon (Hikino *et al*, 2003). The morphological differences induced by CS-D and CS-E stimulation imply distinct signalling mechanisms, which are not understood. The mouse variant of phosphacan, DSD-1-PG, is expressed by glia cells and has also been shown to be stimulatory to neurite outgrowth of primary mesencephalic and hippocampal rat neurons *in vitro* (Garwood *et al*, 1999). This affect appears to be mediated by the CS-D-rich GAG side chains of DSD-1-PG, as removal of these chains or blockage with an antibody (473HD) attenuated their stimulatory affect (Clement *et al*, 1998; Faissner *et al*, 1994). Therefore, pathfinding by neurites is regulated in part by the expression of certain GAG sulfonyltransferases which, through GAG sulphation, delineate boundaries or growth permissive regions.

Mechanistically, it is likely that the stimulatory effects of CSs on neurite outgrowth arises from their affinities to neuronal growth factors (Miller & Hsieh-Wilson, 2015). Midkine (MK) and brain derived neurotrophic factor (BDNF) have been demonstrated to more strongly associate with synthetic CS-E compared to CS-A and CS-C (Gama *et al*, 2006), and other studies have shown preferential association of nerve growth factor (NGF), BDNF and neurotrophin-3 (NT-3) to CS-D and CS-E compared to CS-A and CS-C (Gama *et al*, 2006; Rogers *et al*, 2011). It is thought that these CSs stimulate neuronal growth by recruiting such growth factors and facilitating binding to their neuronal membrane receptors (Rogers *et al*, 2011). Additionally, neuronal receptors for these specifically sulphated CSs could mediate their effects on neuronal growth, such as contactin-1 (CNTN-1).

Some sulphated CSs can have opposite effects on neurite outgrowth of different types of neurons (Miller & Hsieh-Wilson, 2015). CS-E, for example, has been shown to be stimulatory to primary hippocampal and mesencephalic neurons *in vitro*, but is inhibitory to dorsal root ganglia (DRG) and cerebellar granule neurons (CGN), suggesting that the role of CS-E *in vivo* is context specific. The mechanisms underlying this seemingly contradictory function are not well understood but may be due

cell type specific differences in CS surface receptors, which confer opposing effects on neurite outgrowth by differing intracellular signalling pathways.

Critical period regulation

The most severe forms of amblyopia (also known as "lazy eye"), where the brain favours one eye over the other, can be caused by monocular deprivation (MD) during development. This can be caused, for example, by a dense cataract in one eye. Early experiments with cats and rhesus macaques showed that MD during development lead to changes in the visual cortex that would persist into adulthood. After prolonged MD, the visual cortex was shown to become less responsive to ocular stimulation of the deprived eye, resulting in a stronger influence of one eye over the other. This is known as ocular dominance (OD). Significantly, it was shown that changes in the visual cortex's response to the deprived eye would reverse if MD was alleviated during development but not if alleviated in adulthood. Furthermore, induction of MD in adulthood rather than during development did not lead to changes in the visual cortex's responses. These findings suggested a window of postnatal plasticity, known as the "critical period," where the visual cortex could adjust based on optical stimulation. After closure of the critical period, the visual cortex is 'locked-in,' and would have much reduced responses to changes in ocular stimulation. These findings informed clinical practice of postnatal MD in children and was the part of the work that won the 1981 Nobel Prize in Medicine (Wiesel, 1982).

Today, OD plasticity by MD is still used as a model to study the mechanisms of critical period signalling, often in mice. While the visual cortex is often used to explain and contextualise the critical period, this process occurs across regions of the brain (Hensch, 2004). A critical period of synaptic plasticity has been observed in several species, including zebrafish, mouse and human (Hensch, 2004). We now know that the critical period is characterised by heightened synaptic plasticity and experience-driven formation and modification of functional microcircuits in the brain. The closure of the critical period, at around 7 years of age in humans, stabilises and maintains the functional microcircuits formed during this period, restricting the formation of new or modifications to existing microcircuits.

The changes during critical period closure are associated with a number of structural and molecular alterations (Hensch, 2005). The ECM has a significant role in regulating the critical period. The closure of the critical period is correlated with the formation of PNNs (Pizzorusso *et al*, 2002), whose inhibitory function is thought to contribute to the restricted synaptic plasticity after critical period closure. The injection of ChABC into the visual cortex to degrade CSPGs, such as those found in PNNs, was shown to reactivate ocular dominance plasticity in adult rats (Pizzorusso *et al*, 2002) and, to a lesser degree, in cats (Vorobyov *et al*, 2013). Further, PNNs were shown to protect fear memories from erasure, which was ablated by ChABC injection (Gogolla *et al*, 2009). A recent study showed that

astrocytes regulate closure of the critical period and formation of PNNs in the mouse visual cortex through Connexin-30 (Cx30) signalling, which inhibits RhoA/ROCK signalling and expression of matrix metalloproteinase-9 (MMP9) and is required for formation of mature PNNs (Ribot *et al*, 2021).

While CSPGs were thought to largely present as a physical barrier to synaptic plasticity, later work showed that the sulphation pattern of CS side chains was key to critical period closure, suggesting a signalling mechanism in addition to (or instead of) a physical barrier (Bradbury *et al*, 2002; Miyata *et al*, 2012). Critical period closure was shown to correlate with a switch in CS sulphation from CS-C^{high}/CS-A^{low} to CS-C^{low}/CS-A^{high} in chickens (Kitagawa *et al*, 1997). Overexpression of the enzyme that catalyses the -6S modification, C6ST-1, in the mouse brain led to the maintenance of CS-C^{high}/CS-A^{low} into adulthood, resulting in persistent OD plasticity and prevention of the formation of PNNs, directly linking the ratio of CS-C to CS-A in the closure of the critical period (Miyata *et al*, 2012). The seeming importance of CS-C and -A to brain development suggests the existence of receptors specific for CS-A and -C, but none have been reported.

ECM receptors

Integrins

Integrins are the principal receptors for ECM substrates throughout the body. The integrin family is very large with diverse functions, many of which are largely not relevant to the CNS, such as cell invasion, metastasis, cytokine activation and cytokine release. The following section will focus on the role of integrins as they relate to ECM signalling through integrins and CNS development and function.

Integrins are transmembrane, heterodimeric receptors and are one of the principal receptors for ECM molecules throughout the body. Integrins are composed of an α and a β unit and 18x α and 8x β units and 24x unique combinations have been identified in mammals (Hynes, 2002). Different subunit combinations are found throughout the body and the different combinations confer functionality. The α-subunit confers specificity to the ligand; the β-subunit links the receptor to the cytoskeleton and intracellular signalling mechanisms (Wu & Reddy, 2012). Integrins undergo bidirectional allosteric conformational changes reflective of their functional state (Park & Goda, 2016). When inactive, integrins have a closed conformation in both their extra- and intra-cellular domains. Binding of an intracellular ligand to an integrin opens up the extracellular clasp domain to promote binding to the ECM and, conversely, binding of a ligand of the ECM to the extracellular domain of an integrin opens up the intracellular domain to facilitate intracellular ligand binding and signalling.

Integrins bind a wide range of extracellular ligands. Integrins containing α5, α8 and αV subunits belong to the RGD family of integrins, as they recognise ECM molecules containing the peptide

sequence Arg-Gly-Asp (R-G-D) such as fibronectin and thrombospondins. Collagen-binding integrins contain α1 and α2 subunits. Of the β units, integrins containing β1 and β3 are the best studied in the brain, though others are also expressed (Pinkstaff *et al*, 1999). β1 subunits promiscuously binds with α subunits, including the aforementioned α5, α8, αV as well as α3 subunits; the β3 subunit is exclusive to the αV subunit.

Integrins have roles in both the development and functioning of the CNS (Park & Goda, 2016). During development, integrins have been demonstrated to be key to the migration and differentiation of neural stem cells in the ventricular and subventricular zones and, in differentiating neurons, integrins containing β1 subunits promote axon growth by binding to the axon guidance cues semaphorin 7a (Sema7a). Sema3a has been shown to signal dendritic guide cues in hippocampal neurons via integrin-dependent focal adhesion kinase (FAK) phosphorylation. Mice KO for Sema3a exhibited defective dendritic arborisation *in vivo* and *in vitro* primary neurons (Schlomann *et al*, 2009). Integrin-ECM interactions are also crucial to synaptogenesis. Various integrin heterodimers localise at the synapse, particularly at the post-synaptic density (PSD). Glutamatergic synaptogenesis in the hippocampus has been demonstrated to be dependent on α3/β1 and α5/β1 integrins. Inhibition of β1 integrins by antagonists and blocking antibodies were shown to lead to decreases in synaptogenesis in CA1 pyramidal neurons (Nikonenko *et al*, 2003). Integrins are also key to the highly dynamic morphological alterations observed in synapse. Activation of β1 and β3-containing integrins with RGD-containing peptides was demonstrated to induce dendritic spine elongation in cultured primary hippocampal neurons (Shi & Ethell, 2006). Addition of RGD peptide to acute hippocampal slices was shown to disrupt LTP. Though initial potentiation was normal, it decayed over time faster in slices treated with RGD peptides, suggesting a role of integrins in stabilising LTP (Staubli *et al*, 1990). Subsequent studies using integrin blocking antibodies and KO mouse models have largely corroborated these findings and shown that subunits β1, α3, α5 and α8 to be the key effectors (McGeachie *et al*, 2011). The consolidation of LTP by integrin signalling is thought to be through regulation of actin polymerisation and AMPA channel insertion into the post-synaptic membrane (Kramár *et al*, 2006).

Integrins are also involved in the transition of synapses from an immature to a mature state through Abl2/Arg nonreceptor tyrosine kinase (Arg) signalling, characterised by a reduction in pre-synaptic release probability and switch in post-synaptic NMDARs rich in GluN2B subunits to GluN2A (Xiao *et al*, 2016). Loss of integrin-Arg signalling resulted in persisting levels of immature synapses during postnatal development, dendritic spine loss, increase in NMDAR-dependent currents and perturbed long term synaptic plasticity (Xiao *et al*, 2016). Reelin has also been demonstrated to modulate NMDAR activity via integrin binding through a mechanism that converges on Src-dependent phosphorylation of NMDARs. Integrins function in consolidating long-term synaptic plasticity by

regulating actin polymerisation and stabilisation of actin neo-filaments through RhoA-ROCK and RAC1 signalling, respectively, as shown by antibody-mediated blockage of β1 integrin signalling, which prevented filamentous actin polymerisation in hippocampal dendritic spines and perturbed LTP (Kramár *et al*, 2006; Rex *et al*, 2009).

LAR and PTPσ

Two members of the LAR subfamily of PTP receptors have been demonstrated as CSPG receptors: LAR and PTPσ. While studies of LAR and PTPσ have been mostly related to the spinal cord and peripheral neurons, they have been linked to a role in development of the brain also. LAR is expressed in the adult rat cortex, hippocampus, striatum, midbrain and cerebellum (Dunah *et al*, 2005). Mice that are knockout for LAR are viable but exhibit reduced cholinergic innervation in the dentate gyrus and smaller cholinergic neurons in the basal forebrain (Yeo *et al*, 1997) as well as deficiencies in spatial learning tasks and hyperactivity (Kolkman *et al*, 2004). LAR has been demonstrated to bind CSPGs with high affinity and to mediate transduction of CSPG signals within the cell in transfected cell lines, abrogated by GAG digestion with ChABC (Fisher *et al*, 2011). Further, LAR has been shown to mediate CSPG inhibitory signals to dorsal root ganglia (DRG) cells (Fisher *et al*, 2011). PTPσ is expressed during mouse development, declining after birth, and restricted to the olfactory bulb, cerebellum and hippocampus (Meathrel *et al*, 2002). PTPσ knockout mice exhibit high degrees of neonatal mortality, with 60% of knockout mice dying within the first 48 hours after birth. The surviving knockout mice exhibit neurological defects such as spastic movements, impaired proprioception, ataxia and a reduction in forebrain cholinergic neurons (Wallace *et al*, 1999). PTPσ was demonstrated to bind neurocan and aggrecan CSPGs with high affinity, partially abrogated by pre-treatment with ChABC. The residual activity suggested that PTPσ may bind to other regions of CSPGs than the CS GAG chains. DRGs deficient in PTPσ expression were resistant to CSPG-induced inhibition of neurite outgrowth. PTPσ knockout mice showed improved regeneration of axons after spinal cord injury, likely due to the neurons being resistant to the inhibitory signal of the glial CSPG lesion and identifying PTPσ as a therapeutic target in spinal cord injury (Shen *et al*, 2009). This was followed up by identification of a membrane-permeable PTPσ inhibitor that likewise improved axonal regeneration after injury (Lang *et al*, 2015). While the regenerative capacities were improved by PTPσ perturbation, the regeneration through the glial scar was incompletely rescued, possibly due to the presence of other CSPG receptors signalling inhibitory cues (Lang *et al*, 2015; Shen *et al*, 2009). However, this improved but limited regenerative capacity was consistent with data showing improved but incomplete axonal regeneration after destruction of the CSPG scar by ChABC (Bradbury *et al*, 2002), suggesting that the presence of other CSPG receptors does not fully explain the incomplete axonal regeneration in PTPσ knockout

neurons. Intracellular mechanisms of CSPG inhibition on neurite outgrowth are incompletely understood, but there have been studies implicating signalling by RhoA, Akt/protein kinase B (PKB), protein kinase C (PKC), and glycogen synthase kinase 3β (GSK-3β) in neurons (Sharma *et al*, 2012). LAR activation by CSPGs was shown to transduced intracellularly by reducing Akt phosphorylation and activating RhoA in CGNs (Fisher *et al*, 2011).

NgR1 and NgR3

The Nogo receptors NgR1 and NgR3 are membrane-anchored proteins that were demonstrated as receptors for CSPGs and myelin-associated inhibitors (MAIs) and mediate inhibitory cues to neurite outgrowth *in vitro* (Dickendesher *et al*, 2012). NgR1 is expressed in multiple regions of the mouse brain including the hippocampus, cortex and cerebellum and participates in synaptic plasticity in the visual cortex, including closure of the critical period (McGee *et al*, 2005). NgR1 has been shown to participate in hippocampal synaptic plasticity and to regulate dendritic spine morphology (Delekate *et al*, 2011; Lee *et al*, 2008). NgR3 expression largely overlaps with NgR1, however its functional role is less understood. A conditional double NgR1 and NgR3 knockout mouse had improved axonal regenerative capacity through glial CSPG lesions, which was further enhanced by ablation of PTPσ, demonstrating a NgR1 and NgR3 as function CSPG receptors and corroborating previous studies of a functional redundancy with PTPσ. There is some evidence that intracellular signalling by the Nogo receptors converges on similar mechanisms as PTPσ and LAR, namely RhoA and Akt, but these mechanisms remain poorly understood (Sharma *et al*, 2012).

CNTN-1

Contactin-1 (*CNTN-1*) is a membrane-localised member of the immunoglobulin superfamily that has been demonstrated as a receptor for CS-E (Mikami *et al*, 2009). The contactin family is known to be expressed in the nervous system and to be involved in neural cell adhesion and neuritogenesis (Karagogeos, 2003; Falk *et al*, 2002), but CNTN-1 is poorly understood. CNTN-1 has been shown to bind CS-E and mediate neuritogenesis in primary hippocampal neurons (Mikami *et al*, 2009). Further, CNTN-1 binds to neural growth factors such as MK and BDNF (Deepa *et al*, 2002). Taken together, CNTN-1 is a receptor for CS-E and has a role in neurodevelopment *in vitro*, but the function of CS-E in neurodevelopment *in vivo* is unclear.

Additional binding partners of CSPGs

Semaphorins

The semaphorins are a family of guidance molecules that can be secreted or anchored to the membrane. Semaphorins can have chemoattractive or chemorepulsive properties and there is some evidence of interactions with CSPGs (Bagnard *et al*, 1998). Sema3a is a class III member of the semaphorin family. Also known as Collapsin-1, it is a secreted protein that signals at synapses via the receptors Neuropilin-1 (Nrp-1) and Plexin (Plxn) (Winberg *et al*, 1998; Bouzioukh *et al*, 2006). Sema3a is expressed in cortical layers during development and acts to guide radial migration of cortical neurons and, in addition, Sema3A is expressed in PNNs with a role in modulation of synapse morphology and function (Bouzioukh *et al*, 2006; Vo *et al*, 2013), suggesting an interaction with CSPGs. Sema3a and CS are further linked by the observation that Nrp-1 can be post-translationally modified with CS chains, affecting its function, albeit in a non-neuronal setting (Shintani *et al*, 2006). Immunofluorescent studies identified Sema3a localisation at PNNs of the mouse cortex and to co-localise with aggrecan, versican and phosphacan and Sema3a localisation was abolished after ChABC treatment (Vo *et al*, 2013). A follow up study showed that Sema3a binds specifically to CS-E in PNNs and that this interaction is potent inhibitor of axonal outgrowth (Dick *et al*, 2013). Immunofluorescent staining of Sema3a revealed a 'honeycomb' distribution of the protein at PNNs, with the gaps in staining localising around presynaptic terminals, suggesting a role of Sema3a in synaptic plasticity (de Winter *et al*, 2016). In support of this, mice reared in an enriched environment (an experimental model to promote synapse plasticity) (Nithianantharajah & Hannan, 2006) exhibited lower PNN levels and reduced Sema3a staining within PNNs (de Winter *et al*, 2016). Exogenous application of recombinant Sema3a to cultured primary hippocampal neurons reduced the density of mature synapses, supporting a role of secreted Sema3a in modulation of synapse formation and function (Bouzioukh *et al*, 2006).

Sema5a is expressed during development under tight regulation, including in developing somites and limb buds of the mouse embryo (Adams *et al*, 1996) and in the telencephalon of developing chick embryos (Pineda *et al*, 2005). Sema5a contains two thrombospondin repeats through which it interacts with CSPGs and heparan sulphate proteoglycans (HSPGs) and through these interactions Sema5a can act as growth permissive (HSPG-bound) or inhibitive (CSPG-bound) (Kantor *et al*, 2004). Studies using a knockout mouse supported a role for Sema5a as a negative regulator of synaptic density in neonatal and adult mouse ganglionic cells and the KO mice showed impaired social interaction with stranger mice, a phenotype usually associated with ASD (Duan *et al*, 2014). Interestingly, a GWAS identified reduced expression of *SEMA5A* as a risk factor in ASD (Weiss *et al*, 2009) and an ASD patient was identified with a *de novo* microdeletion in *SEMA5A* (Mosca-Boidron *et al*, 2016).

Cell adhesion molecules

Cell adhesion molecules (CAMs) are glycoproteins involved in cell-ECM and cell-cell interactions, important to tissue integrity, cell migration and intercellular signalling (Djerbal *et al*, 2017). In the CNS, neural cell adhesion molecule (NCAM) interacts with β1-containing integrins to regulate neurite outgrowth and neuronal adhesion *in vitro* through interactions with phosphacan (Milev *et al*, 1994). Similarly, neurocan has been demonstrated to bind NCAM and inhibit neurite outgrowth (Friedlander *et al*, 1994). Pre-treatment with ChABC abolished NCAM-neurocan but not NCAM-phosphacan interaction, suggesting the latter interaction is mediated by GAGs containing CS (Djerbal *et al*, 2017). Taken together, it has been suggested that NCAM is the cell surface receptor for phosphacan and neurocan (Djerbal *et al*, 2017).

Intracellular molecules

While CSPGs are largely considered as components of the ECM, an emerging body of evidence suggests specific binding of CS-containing GAGs to molecules expressed within the cell. Collapsin response mediator protein 4 (CRMP4) is one such molecule, which is expressed in the CNS throughout life. CRMP4 KO mice exhibit abnormal orientation of pyramidal neurons in layer V of the cerebral cortex which was suggested to be due to impaired CSPG signalling (Takaya *et al*, 2017). CRMP4 has been shown to localise at hippocampal growth cones and to promote growth cone formation and spreading as well as dendritic outgrowth through regulation of the actin cytoskeleton (Khazaei *et al*, 2014). Finally, deletion of CRMP4 was shown to abrogate CSPG inhibitory signals after axonal injury (Nagai *et al*, 2015). Surprisingly, despite being an intracellular molecule, CRMP4 was demonstrated to bind CS with high affinity *in vitro* (Franken *et al*, 2003), though the functional consequences of this is not understood.

Orthodenticle homeobox protein 2 (Otx2) is a homeoprotein demonstrated to bind CS-D and CS-E moieties of PNNs through a GAG binding motif (Beurdeley *et al*, 2012) and to function in the mouse critical period. During the critical period, Otx2 is transferred between cells from the choroid plexus to the visual cortex, where it is accumulated in PV-positive interneurons (Sugiyama *et al*, 2008). Otx2 transfer regulates both the initiation and termination of the cortical critical period (Sugiyama *et al*, 2008; Miyata *et al*, 2012) and Otx2's function in the critical period was disrupted by mutating its GAG recognition motif (RK-peptide) (Lee *et al*, 2017). It is thought that PNNs at PV-positive interneurons act to capture Otx2 for internalisation as injection of a synthetic peptide containing the RK GAG binding motif competed with Otx2 for PNN binding and prevented Otx2 accumulation in PV-positive interneurons (Beurdeley *et al*, 2012). In addition, Otx2 is involved in assembly of PNNs during

the critical period and in adult. Injection of Otx2 into the visual cortex was shown to induce premature formation of PNNs and closure of the critical period and, conversely, Otx2 KO mice show delays in PNN formation and critical period closure (Sugiyama *et al*, 2008). The Otx2-PNN interaction is considered a positive feedforward loop, in which PNNs attract Otx2 for internalisation, which in turn promotes the assembly of PNNs, attracting more Otx2 and so on, which serves to maintain PNNs in adult life and inhibition of synapse plasticity (Bernard & Prochiantz, 2016).

The ECM and human disease

Autism

A link between dysregulated GAGs and ASD has been made. Immunofluorescent staining of post-mortem brain tissues showed a reduction in HS signal in samples from young autistic individuals in the subventricular zone of the lateral ventricles compared to healthy donor controls (Pearson *et al*, 2013). These findings were consistent with immunofluorescent analysis of sections from an inbred mouse strain used to model autism, known as the BTBR mouse, which displays several phenotypes often associated to autistic features in humans (Meyza *et al*, 2012). Importantly, the antibody used in these studies recognises N-sulphated HS, therefore, the reduction in IF staining described here may indicate altered post-translational modifications of HS rather than a reduction in HS *per se*. Conditional knockout of an enzyme critical to HS synthesis, *Ext1*, in excitatory neurons at 3 weeks after birth in a mouse model resulted in phenotypes considered as autistic features, such as impaired social interactions and impaired vocalisations (Irie *et al*, 2012). Additionally, patch-clamp experiments of pyramidal cells in the amygdala indicated a reduction in postsynaptic AMPAR-mediated synaptic strength which was attributed to a reduction in postsynaptic AMPAR surface expression (Irie *et al*, 2012). No morphological disturbances were noted, both in gross architecture of the brain and in cellular morphologies, which suggests that HS has a role in the maintenance of the brain after development, which is consistent with the phenotypes observed after postnatal ablation of HS synthesis. Finally, alterations in urinary GAG levels has been noted in ASD patients, but the reasons for this and whether changes in GAG levels relate to the brain are unknown (Endreffy *et al*, 2016). In summary, alterations in HS has been noted in post-mortem samples of autistic brains and in two mouse models exhibiting autistic features, though the exact mechanism linking HS to autism remains to be elucidated.

Epilepsy

Dysregulation of proteoglycans and GAGs has been associated to epileptic seizures. Epilepsy is observed in approximately 30% of mucopolysaccharidosis (MPS) cases, particularly MPS I, II and III,

which are caused by defects in GAG metabolism (molecular details described below). The observed seizures are mostly tonic-clonic, but other types of seizure such as focal, absence and myoclonic have been described (Scarpa *et al*, 2017). Mesial temporal lobe epilepsy (MTLE), the most common form of epilepsy, affects the amygdala and hippocampus. In post-mortem samples, patients with MTLE were observed to have elevated HA and CS and unchanged HS compared to healthy controls (Perosa *et al*, 2002). Increased expression of RPTPβ was also noted in astrocytes within the hippocampus of epileptic samples (Perosa *et al*, 2002). Mouse models in which epilepsy was induced have also described alterations in CS content and brevican cleavage (Yuan *et al*, 2002) and changes in phosphacan and neurocan expression (Okamoto *et al*, 2003).

Schizophrenia

Schizophrenia is a chronic condition characterised by positive symptoms (hallucinations, delusions) and negative symptoms (thought decay, social withdrawal). There is a reasonably well-studied link between disruptions to the ECM and schizophrenia. GWAS have made links between schizophrenia and variants in several ECM components including the CSPGs neurocan and NGC, as well as several MMPs and ADAMTS enzymes (Mühleisen *et al*, 2012; Pantazopoulos *et al*, 2021; Ripke *et al*, 2014). Studies have investigated PNNs in the prefrontal cortex (PFC), an area of the brain associated with higher order functions such as orchestration of thoughts relating to personality, sociability and decision making, many of which are disrupted in schizophrenia. WFA-reactive PNNs have been shown to arise in the PFC during postnatal development and continue until adolescence (Mauney *et al*, 2013), which is often when schizophrenic symptoms arise. In post-mortem samples from aged schizophrenic patients, a reduction (~75%) in PNNs were observed in the PFC. This appeared to be specific to the brain region and to schizophrenia; alterations in PNNs were not observed in the visual cortex of schizophrenic patients nor in the PFC of patients with bipolar disorder (Mauney *et al*, 2013). Another study found no change in the number of PFC PNNs of schizophrenic patients, but a reduction in the WFA-intensity and intensity off PNN-localised aggrecan (Enwright *et al*, 2016). Reductions in PNNs in the entorhinal cortex and amygdala of schizophrenic patients have also been reported (Pantazopoulos *et al*, 2010). Various studies have associated schizophrenia to gene expression dysregulation of aggrecan, versican and neurocan (Pietersen *et al*, 2014), the ECM glycoprotein Reelin (Impagnatiello *et al*, 1998), of which the KO mouse displays Schizophrenic phenotypes (Fang *et al*, 2019), HAPLN1, MMPs 9, 16, 24 and 25 (Pietersen *et al*, 2014), integrins (Walsh *et al*, 2002), PTPβ/ζ (Takahashi *et al*, 2011) and Sema3a (Eastwood *et al*, 2003). Since most of these studies have used post-mortem tissue samples, it is difficult to know whether these observations directly relate to the schizophrenic

phenotypes or whether they are corollary changes to the ECM during schizophrenic dysfunction in the brain.

Alzheimer's disease

Alzheimer's disease (AD) is a neurodegenerative disease characterised by progressive neuronal loss with associated cognitive decline and loss of motor skills. While the mechanisms of AD remain poorly understood, neuronal and synaptic loss occur in the hippocampus, entorhinal cortex, cerebellum and motor and sensory cortices. Classic pathologies include plaques of aggregated amyloid-β protein (Aβ) and hyperphosphorylation of tau protein and neurofibrillary tangles. Components of the ECM, including CSPGs and HSPGs, have been linked to the pathology of AD. CSPGs and HSPGs have been found within Aβ plaques (DeWitt *et al*, 1993) and AD progression was associated with loss of PNNs at PV^{+}-interneurons, though the interneurons themselves were unaffected (Baig *et al*, 2005). Further, it was shown that cortical regions with high densities of PNNs were less likely to co-stain with hyperphosphorylated tau and had reduced neurofibrillary bundles, suggesting a neuroprotective role of PNNs (Brückner *et al*, 1999). CSPGs and HSPGs accumulate around the cores of fibrillated Aβ, stabilising them and shielding them from proteolysis, thereby enhancing the fibrillization process (van Horssen *et al*, 2003; Soares Da Costa *et al*, 2017). Aβ binds to HS at the same site as HS associates with FGF-2, which may disrupt HS's function (Lindahl *et al*, 1999). Treatment of AD with glycomimetics – which mimic the action of polysaccharides such as GAGs – has been explored. The most studied of the GAG mimetics is 3-aminopropylsulfonic acid (trade name Alzhemed™) which was shown to bind to soluble Aβ and prevent fibrilization. However Alzhemed failed Phase III clinical trials as it was not shown to have any clinical benefit, possibly associated with other underlying pathologies of AD such as Tau (Aisen *et al*, 2006; Santa-Maria *et al*, 2007).

Spinal cord injury and stroke

Injuries to the CNS are followed by the proliferation and localisation of astrocytes, glial precursors, microglia and fibroblasts to the injury site and formation of CSPG-rich scar tissue. This is known as reactive astrogliosis and is thought to have evolved as a defence mechanism upon CNS injury, as the reactive astrocytes help to preserve existing tissue by maintaining a favourable microenvironment for surviving neurons, restricting the spread of inflammation and preventing infection (Sofroniew, 2009). Glial scars have been observed at sites of ischemic stroke, repeatedly demyelinated neurons in multiple sclerosis, sites of traumatic brain injury and sites of axonal severance in spinal cord injury. Glial scars are a double-edged sword. While initially beneficial to maintaining surviving neurons, the CSPG-rich glial scars are inhibitory to neuronal outgrowth, precluding the neurons' ability to regenerate and heal

after the traumatic injury. For this reason, recovery rates after spinal cord injury are poor, and injury after stroke is often permanent (James *et al*, 2019). The ablation of glial scars has received quite a lot of attention as a potential therapeutic avenue for inducing axonal regeneration and healing, as local administration of ChABC was shown to promote functional recovery after spinal cord injury in rats (Bradbury *et al*, 2002; Sharma *et al*, 2012; Alilain *et al*, 2011). While ChABC injection alone does not appear to be a viable therapeutic option for human patients, in part due to its poor enzymatic longevity at 37^{o}C, research into alternative methods of glial scar ablation is ongoing (Bradbury & Burnside, 2019).

Defects In glycosaminoglycan metabolism

MPS is a group of autosomal recessive inherited lysosomal storage disorders caused by deficiencies in the enzymatic catalysis of GAGs including HS, CS and DS singly or in combination. MPS falls into seven types: MPS I (Hurler syndrome, Scheie syndrome, Hurler-Scheie syndrome), MPS II (Hunter syndrome), MPS III (Sanfilippo syndrome), MPS IV (Morquio syndrome), MPS VI (Maroteaux-Lamy syndrome), MPS VII (Sly syndrome), MPS IX (Natowicz syndrome). MPS type V and VIII are no longer used as categories of MPS, as they were re-classified as subtypes of other MPS once it was discovered they share deficiencies in common enzymes. Depending on the MPS type, the breakdown of different GAGs fail and accumulates into lesions affecting the functionality of various tissues and organs, including the brain. Symptoms vary between the different forms of MPS, but common symptoms include distinctive facial features described as “coarse,” heart abnormalities, hepatosplenomegaly, breathing problems and neurological abnormalities. In most MPS cases, patients appear phenotypically normal at birth but symptoms appear around the age of two years old.

Hurler syndrome (MPS I-H) is the most severe MPS caused by deficiencies of the enzyme α-L-iduronidase (IDUA) which catalyses the breakdown of heparin and dermatan sulphates. Symptoms can become apparent as early as 6 months after birth, and include developmental delay, macrocephaly, delayed growth, recurrent infections of the urinary and upper respiratory tracts, cloudy corneas and severe spinal deformities as well as regression in mental development at about two years old. Scheie syndrome (MPS I-S) is also caused by deficient IDUA function, but symptoms are far less severe. Patients typically have normal intelligence and life expectancy, but experience stiff joints, carpal tunnel syndrome, aortic regurgitation and cloudy corneas. Hurler-Scheie syndrome (MPS I-H/S) is an intermediate between Hurler and Scheie syndromes and is extremely rare.

Hunter syndrome (MPS II) is an X-linked recessive disorder caused by dysfunctional iduronate 2-sulphatase (IDS) which catalyses heparan and dermatan sulphates catabolism. Symptoms usually appear between two and four years old and include progressive growth delay, stiff joints, coarse facial

features, macrocephaly, hepatosplenomegaly and craniofacial dysmorphias. Intellectual disability can occur in more severe forms.

Sanfilippo syndrome (MPS III) falls into four subclasses depending on the deficient enzyme: type A (heparan-N-sulphatase), B (α-N-acetylglucosaminidase), C (heparan-α-glucosaminide N-acetyltransferase) and D (N-acetylglucosamine 6-sulphatase). All four enzymes are involved in the catalysis of heparan sulphate. Sanfilippo syndrome primary affects the CNS, with symptoms including intellectual disability, delayed developmental milestones, sleep disorder, seizures, loss of language skills and seizures.

Morquio syndrome (MPS IV) exists in two subclasses depending on the deficient enzyme: type A (N-acetyl-galactosamine-6-sulphatase) and B (β-galactosidase) which catalyse keratan sulphate and CS-A, respectively. Symptoms include skeletal developmental defects, delayed growth and scoliosis. The CNS is generally not affected.

Maroteaux-Lamy syndrome (MPS VI) is caused by deficient N-acetylgalactosamine-4-sulphatase, which catalyses dermatan sulphate. Symptom severity can vary dramatically, but include coarse facial features, cloudy corneas and hepatosplenomegaly. The CNS is generally not affected.

Sly syndrome (MPS VII) is caused by deficient β-glucoronidase and accumulation of dermatan, heparan and CS-E. Symptom severity is also variable, but include intellectual disability, skeletal abnormalities, cloudy corneas, hernias, short stature and coarse facial features.

Finally, Natowicz syndrome (MPS IX) is caused by deficient hyaluronidase and is very rare. Symptoms include short stature, cysts and craniofacial dysmorphias.

The testing for accumulated GAGs is a useful biomarker in the diagnosis of MPS. GAG accumulation can be tested for in the urine, blood, cerebrospinal fluid, amniotic fluid and serum/plasma, but urine has been the most common due to the non-invasive sample collection. A common analytical technique uses the dye dimethylmethylene blue (DMMB) which binds to sulphated GAGs and precipitates, allowing quantification of GAG in a sample by spectrophotometric absorbance. The advantage of DMMB is that is cheap and easy to run, however it does not distinguish between different types of sulphated GAGs (e.g. heparan vs chondroitin sulphate) and cannot be used for blood or tissue samples (Kubaski *et al*, 2017). A more common technique in the present day is to use mass spectrometry (MS) to separate an ionized sample by mass/charge ratio, with the resulting spectra used to infer the identity of the original compound. Multiple iterations of the technique have been described, such as coupling with liquid chromatography and the use of differential isotope tagging, to facilitate sensitive, quantitate analysis of the composition of GAG chains (Kubaski *et al*, 2017; Lawrence *et al*, 2008). While relatively expensive, MS-based methods offer superiority in precision and sensitivity

over other techniques including DMMB. If the biomarker test returns positive, test for catalytic enzyme activity can be performed, which are the gold-standard for diagnosing MPS (Kubaski *et al*, 2020).

Technological advances

Sequencing

Advances in sequencing technologies, particularly the development of next generation sequencing (NGS), has propelled forward the rate of NDD genetic diagnosis and identification of genes key to CNS development. NGS facilitates high-throughput genomic assessment of a patient with suspected genetic disease. There are three major classes of NGS used by diagnostic centres: panel sequencing, whole exome sequencing (WES) and whole genome sequencing (WGS). Panel sequencing uses hybrid-capture methodologies to target a pre-selected set of genes for sequencing. The screened gene set is chosen is normally a set of known disease-causing genes based on the patients' symptoms. This has been a successful approach for diagnosing patients for which there is a large collection of potentially causative genes and has the additional advantage that the data generated is relatively small and easy to parse. However, a drawback is the highly targeted nature of this method, therefore the chance of incidental finding is low. WES uses hybrid capture to isolate and sequence almost all exons of the genome (about 2-3% of the total), within which the majority of genetic disease variants are located. This approach requires the researcher to comb through many detected variants, of which the vast majority are inconsequential. The researcher will search for variants within genes known to cause disease matching the patient's phenotype. If none are identified, the researcher may identify variants within genes not yet reported to cause disease but are a promising candidate. This may lead to a research project where patient's variant(s) are characterised and the function of the gene elucidated. WGS is an unbiased sequencing of the entire genome, with the subsequent workflow being similar to WES. In addition to variants located in exons, WGS identifies potentially disease-causing variants in non-exonic regions of the genome, such as splice donor/acceptor sites, promoter and enhancer sequences and non-coding RNAs (Zhang & Lupski, 2015). WGS generates a massive dataset and is also the costliest, as each genome costs approximately 1000$ to sequence and generates approximately 100Gb of data. WGS is not yet widely adopted in diagnostic centres due to the analytical burden, cost, storage resources, and limited increase in diagnostic success compared to WES. A common strategy for diagnostic centres is to begin with panel sequencing and potential follow-up with WES, which usually represents the highest cost/benefit ratio (Warr *et al*, 2015).

2. Aim of the thesis

The aim of this thesis was to identify novel neurodevelopmental disorders associated with congenital variants and to characterise the pathologies and underlying mechanisms of the disorder.

3. Results

The following section contains a submitted manuscript titled ‘FIBCD1 is an endocytic GAG receptor associated to a novel neurodevelopmental disorder’ intended for publication. The author of this thesis is co-first author.

FIBCD1 is an endocytic GAG receptor associated to a novel neurodevelopmental disorder

Christopher W Fell[1,2,3]†, Astrid Hagelkruys[4]†, Ana Cicvaric[5,6], Marion Horrer[4], Lucy Liu[7], Joshua Shing Shun Li[7], Johannes Stadlmann[4,8], Anton A Polyansky[9] , Stefan Mereiter[4], Miguel Angel Tejada[4,10], Tomislav Kokotović[1,2,3], Venkat Swaroop Achuta[1,3], Angelica Scaramuzza[1,3], Kimberly A Twyman[11], Michelle M Morrow[12], Jane Juusola[12], Huifang Yan[13,14], Jingmin Wang[13,14], Margit Burmeister[15,16], Biswa Choudhury[17], Thomas Levin Andersen[18,19], Gerald Wirnsberger[4,20], Uffe Holmskov[21], Norbert Perrimon[7], Bojan Zagrović[9], Francisco J Monje[5], Jesper Bonnet Moeller[21,22], Josef M Penninger[4,23*] and Vanja Nagy[1,2,3*]

[1]Ludwig Boltzmann Institute for Rare and Undiagnosed Diseases, Vienna, Austria. [2]CeMM, Research Center for Molecular Medicine of the Austrian Academy of Sciences, Vienna, Austria. [3]Department of Neurology, Medical University of Vienna, Vienna, Austria. [4]IMBA, Institute of Molecular Biotechnology of the Austrian Academy of Sciences, VBC – Vienna BioCenter Campus, Vienna, Austria. [5]Centre for Physiology and Pharmacology, Department of Neurophysiology and Neuropharmacology, Medical University of Vienna, Vienna, Austria. [6]Department of Psychiatry and Behavioral Sciences, Feinberg School of Medicine, Northwestern University, Chicago, IL, USA. [7]Department of Genetics, Harvard Medical School, Howard Hughes Medical Institute, Boston, USA. [8]Institute of Biochemistry, University of Natural Resource and Life Sciences, Vienna, Austria. [9]Department of Structural and Computational Biology, Max Perutz Labs, University of Vienna, Campus Vienna BioCenter 5, A-1030 Vienna, Austria. [10]Research Unit on Women's Health-Institute of Health Research INCLIVA, Valencia, Spain. [11]Mercy Kids Autism Center, Saint Louis, MO, USA. [12]GeneDx, Gaithersburg, MD, USA. [13]Department of Pediatrics, Peking University First Hospital, Beijing, China. [14]Joint International Research Center of Translational and Clinical Research, Beijing, China. [15]Michigan Neuroscience Institute, University of Michigan, Ann Arbor, MI, USA. [16]Departments of Computational Medicine & Bioinformatics, Psychiatry and Human Genetics, University of Michigan, Ann Arbor, MI, USA. [17]Department of Cellular and Molecular Medicine, UCSD, La Jolla, CA, USA. [18]Clinical Cell Biology, Department of Pathology, Odense University Hospital, Odense, Denmark. [19]Pathology Research Unit, Department of Clinical Research and Department of Molecular Medicine, University of Southern Denmark, Odense, Denmark. [20]Apeiron Biologics AG, Vienna BioCenter Campus, Vienna, Austria. [21]Cancer and Inflammation Research, Department of Molecular Medicine, University of Southern Denmark, Odense, Denmark. [22]Danish Institute for Advanced Study, University of Southern Denmark, Odense, Denmark. [23]Department of Medical Genetics, Life Science Institute, University of British Columbia, Vancouver, Canada.

† * Equal contribution

FIBCD1 is an endocytic GAG receptor associated to a novel neurodevelopmental disorder

Christopher W Fell[1,2,3]†, Astrid Hagelkruys[4]†, Ana Cicvaric[5,6], Marion Horrer[4], Lucy Liu[7], Joshua Shing Shun Li[7], Johannes Stadlmann[4,8], Anton A Polyansky[9] , Stefan Mereiter[4], Miguel Angel Tejada[4,10], Tomislav Kokotović[1,2,3], Venkat Swaroop Achuta[1,3], Angelica Scaramuzza[1,3], Kimberly A Twyman[11], Michelle M Morrow[12], Jane Juusola[12], Huifang Yan[13,14], Jingmin Wang[13,14], Margit Burmeister[15,16], Biswa Choudhury[17], Thomas Levin Andersen[18,19], Gerald Wirnsberger[4,20], Uffe Holmskov[21], Norbert Perrimon[7], Bojan Zagrović[9], Francisco J Monje[5], Jesper Bonnet Moeller[21,22], Josef M Penninger[4,23*] and Vanja Nagy[1,2,3*]

[1] Ludwig Boltzmann Institute for Rare and Undiagnosed Diseases, Vienna, Austria.
[2] CeMM, Research Center for Molecular Medicine of the Austrian Academy of Sciences, Vienna, Austria.
[3] Department of Neurology, Medical University of Vienna, Vienna, Austria.
[4] IMBA, Institute of Molecular Biotechnology of the Austrian Academy of Sciences, VBC – Vienna BioCenter Campus, Vienna, Austria.
[5] Centre for Physiology and Pharmacology, Department of Neurophysiology and Neuropharmacology, Medical University of Vienna, Vienna, Austria.
[6] Department of Psychiatry and Behavioral Sciences, Feinberg School of Medicine, Northwestern University, Chicago, IL, USA.
[7] Department of Genetics, Harvard Medical School, Howard Hughes Medical Institute, Boston, USA.
[8] Institute of Biochemistry, University of Natural Resource and Life Sciences, Vienna, Austria.
[9] Department of Structural and Computational Biology, Max Perutz Labs, University of Vienna, Campus Vienna BioCenter 5, A-1030 Vienna, Austria.
[10] Research Unit on Women's Health-Institute of Health Research INCLIVA, Valencia, Spain
[11] Mercy Kids Autism Center, Saint Louis, MO, USA.
[12] GeneDx, Gaithersburg, MD, USA.
[13] Department of Pediatrics, Peking University First Hospital, Beijing, China.
[14] Joint International Research Center of Translational and Clinical Research, Beijing, China.
[15] Michigan Neuroscience Institute, University of Michigan, Ann Arbor, MI, USA.
[16] Departments of Computational Medicine & Bioinformatics, Psychiatry and Human Genetics, University of Michigan, Ann Arbor, MI, USA.
[17] Department of Cellular and Molecular Medicine, UCSD, La Jolla, CA, USA.
[18] Clinical Cell Biology, Department of Pathology, Odense University Hospital, Odense, Denmark.
[19] Pathology Research Unit, Department of Clinical Research and Department of Molecular Medicine, University of Southern Denmark, Odense, Denmark.
[20]Apeiron Biologics AG, Vienna BioCenter Campus, Vienna, Austria.
[21] Cancer and Inflammation Research, Department of Molecular Medicine, University of Southern Denmark, Odense, Denmark.
[22] Danish Institute for Advanced Study, University of Southern Denmark, Odense, Denmark.
[23] Department of Medical Genetics, Life Science Institute, University of British Columbia, Vancouver, Canada.

†Authors contributed equally

*Corresponding authors:

Vanja Nagy, vanja.nagy@rud.lbg.ac.at c/o CeMM, Lazarettgasse 14, AKH, BT 25.3, 1090, Vienna, Austria.
Josef M. Penninger, josef.penninger@ubc.ca. Life Sciences Institute, Vancouver Campus, 2350 Health Sciences Mall, Vancouver, BC Canada V6T 1Z3.

ABSTRACT

Disruptions to brain extracellular matrix (ECM) composition and signalling have been implicated in neurodevelopmental disorders (NDD), but pathophysiologies are poorly understood. Through sequencing of two patients with idiopathic NDD, we identified biallelic variants of unknown significance within *FIBCD1* (p.G29S;R406C and p.P456L), which has no known function in the central nervous system. We showed that *FIBCD1* is expressed in discrete brain regions of humans and mice. Behavioural studies in flies knocked-down for a putative *Fibcd1* orthologue, *CG10359,* and knock-out (KO) mice showed *FIBCD1* is critical for nervous system development and mouse hippocampal-dependent learning tasks. We found KO mice hippocampi to have an accumulated glycosaminoglycan (GAG), chondroitin sulphate-4S, which we determined FIBCD1 to bind and endocytose. We next demonstrated that patient *FIBCD1* variants disrupt FIBCD1-CS-4S association, therefore are loss-of-function. KO acute hippocampal slices exhibited deficient synaptic remodelling that could be restored upon enzymatic digestion of CSPGs. In summary, we identified FIBCD1 as an endocytic receptor for the brain glycome and a novel gene associated to an NDD, revealing its critical, evolutionary conserved function in the nervous system.

INTRODUCTION

Neurodevelopmental disorders (NDDs) are a heterogeneous group of nervous system diseases that include autism spectrum disorder (ASD), attention deficit hyperactivity disorder (ADHD), intellectual disability (ID) and have shared molecular aetiology with psychiatric disorders such as schizophrenia[1]. NDDs often manifest in association with neurological symptoms such as structural brain anomalies, seizures, global developmental delays and/or muscular impairments[2]. Large portions of NDDs have genetic origins, affecting various developmental events such as neurogenesis, axon outgrowth and guidance, synaptogenesis, migration and synapse function/plasticity[2-5].

The brain extracellular matrix (ECM) is a dynamic microenvironment that plays a critical role in developmental events as well as in the maintenance of CNS function in adults[6,7]. The ECM is structurally heterogeneous and is composed primarily of glycans and glycoconjugates (proteoglycans, glycoproteins and glycolipids). A seminal proteoglycan in the brain is chondroitin sulphate proteoglycan (CSPG) which consists of chondroitin sulphate (CS) glycosaminoglycan (GAG) chains conjugated to a core protein. Links between CSPGs and psychiatric disorders such as schizophrenia has been made by GWAS and variants in *CSPG4* were recently linked to schizophrenia[8,9]. Additionally, dysregulation of the glycoprotein Reelin has been implicated in schizophrenia and modelled in various Reeler mice[10,11].

Different spatiotemporal distribution of CSPGs with variable GAG sulphate modifications correlate with specific and discrete developmental stages as part of the dramatic ECM reorganisation that accompanies and regulates brain maturation[7,12,13]. CSPGs participate in axonal outgrowth, synaptic remodelling, cellular migration and closure of the critical period of development, where they condense into peri-neuronal nets (PNNs) which restrict synaptic plasticity and participate in memory formation, retention and extinction[6,14,15]. Furthermore, the

formation of astroglial CSPG scars after nervous tissue injury, including stroke or spinal cord injury, are inhibitory to axonal regeneration[16]. Modulation of cellular responses to CSPG inhibitory signals, for example through cellular CSPG receptors, are a potential therapeutic avenue for these adverse events[17 18].

To date, few CSPG receptors have been identified. Receptor Protein Tyrosine Phosphatase sigma (PTPσ) and its subfamily member Leukocyte Common Antigen-Related (LAR), as well as the Nogo receptor family members, Nogo66 receptor–1 and 3 (NgR1 and 3) were demonstrated to bind to andmediate CSPG inhibition of axonal regeneration[19-21]. Interestingly, modulation of PTPσ by a small peptide mimetic was shown to alleviate CSPG-inhibition and promote axonal regeneration after injury[17], highlighting the therapeutic potential of targeting CSPG receptors. Less is known regarding recognition of specifically sulphated GAGs on CSPGs. CS-4,6S (or CS-E) recognition was reported for Contactin-1 (CNTN1), though its role in the brain is poorly understood, and in the lungs for Receptor for Advanced Glycation End Products (RAGE)[22,23]. Variants in CSPG receptors have thus far not been implicated in NDDs or psychiatric disorders.

Here, we report deleterious variants in *Fibrinogen C Domain Containing 1* (*FIBCD1*) identified by whole exome sequencing (WES) of two unrelated patients diagnosed with severe ASD and NDD. Symptoms noted in the patients include delayed social and cognitive abilities, poor eye contact, attention deficit hyperactivity disorder (ADHD), anxiety, facial dysmorphias and structural brain anomalies. FIBCD1 is a type 2 receptor with high homology to ficolins and has been shown to act as a pattern recognition receptor for chitin. FIBCD1 is expressed in mucosal epithelial tissues, with highest expression in the human respiratory and gastrointestinal tracts, testes, placenta and brain. FIBCD1 consists of a short N-terminal cytoplasmic tail, transmembrane domain, coiled-coil region through which FIBCD1 forms homotetramers, poly-cationic region and a C-terminal extracellular fibrinogen-related domain (FReD) which participates in ligand interactions[24]. It was shown to limit fungal

outgrowth, regulate the gut fungal mycobiome and dampen intestinal inflammation[25,26]. Molecularly, FIBCD1 was demonstrated to have an endocytic function with potential binding sites for GAGs such as CS[24,27]. Despite its high expression in the brain, no function for FIBCD1 in the CNS has been reported thus far.

We show that FIBCD1 is expressed in discrete human and mouse brain regions and that it is critical for various nervous system functions in genetic mouse and fly models. We show that FIBCD1 is a receptor that binds and endocytoses GAGs of the brain ECM and mediates neuronal responses to CSPG signalling. We then show that identified patient variants are deleterious to FIBCD1 function by abrogating the affinity of the receptor to its ligand. Taken together, our data characterise an evolutionarily conserved novel receptor for GAG chains conjugated to CSPGs in the brain and identify a new complex NDD caused by loss-of-function variants in the *FIBCD1* gene, advancing our understanding of the interplay of neural cells and the ECM.

MATERIALS AND METHODS

Patients and Whole Exome Sequencing

All procedures were performed following informed consent and approval from patients and relatives and obtained in accordance with the Declaration of Helsinki. The cohort was curated in a collaborative effort and with the aid of GeneMatcher[28].

Patient 1

gDNA from the proband and parents were captured using the IDT xGen Exome Research Panel v1.0. NGS using an Illumina system with 100bp or greater paired-end reads. Aligned reads (GRCh37) were analysed for sequence variants using a custom-developed analysis tool. Additional details have been previously described[29]. The general assertion criteria for variant classification are publicly available on the GeneDx ClinVar submission page (http://www.ncbi.nlm.nih.gov/clinvar/submitters/26957/).

Patient 2

Procedures were in accordance with the ethical standards and approval of the Medical Ethics Committee of Peking University First Hospital. The IRB number is No. [2005]004. Patients were sequenced and analysed as described previously[30], with sequencing performed by Joy Oriental Co. (Beijing, China).

Animals

Mus musculus

All mice were housed at the Comparative Medicine Mousehouse Vienna BioCenter, Vienna, Austria. Fibcd1tm1Lex mice (MGI: 5007144)[31] were bred on a C57BL/6J genetic background. Only age- and sex-matched littermates from respective crosses were used. All mice were housed at IMBA (Vienna, AT), in a 12-h light/dark cycle, food and water *ad libitum*. Experiments were

approved by the Bundesministerium für Wissenschaft, Forschung und Wirtschaft (BMWFW-66.009/0048-WF/V/3b/2018) and carried out according to EU-directive 2010/63/EU. Only age- and sex-matched littermates from respective crosses were used for experiments.

Drosophila melanogaster

Flies were age, light, sex and temperature matched. All crosses were raised at 25°C on standard molasses food.

In situ hybridisation

Brains were dissected from two 8-10 weeks old C57B6J mice, fixed in 4% paraformaldehyde, dehydrated and paraffin-embedded. 3.5-µm-thick frontal sections were *in situ* hybridised with an enhanced RNAScope 2.5 high-definition procedure (310035, ACD Bioscience), described previously[32].

RT-qPCR

Mouse tissues/cells were collected into TRIzol (Invitrogen), reverse transcribed with iScript cDNA synthesis kit (Bio-Rad) and amplified with GoTaq qPCR master mix (Promega) on a CFX384 system (Bio-Rad). Data were normalised to *Gapdh.* Human cDNA panels were obtained from Origene: TissueScan, Human Brain cDNA Array (#HBRT101), Human Normal cDNA Array (#HMRT304).

In Silico Modelling of FIBCD1

Docking

In silico docking was performed using GOLD version 5.2.2[33] and the FReD X-ray structure (PDB: 4M7F; aa 239-458)[27]. The post-rescoring of docking solutions (100 in total) was done

as described previously[34]. The binding free energy of CS-4S and CS-6S to FReD was estimated using PRODIGY-LIGAND[35] after complex refinement using HADDOCK2.2 web-server[36].

Patient Variants

The initial protein configuration was taken from the FReD X-ray structure with R406C and P456L variants introduced using PyMol[37]. The structures were subjected to all-atom molecular dynamics (MD) simulations in the microsecond range using GROMACS 5.1.4[38] and Amber99SB-ILDN force field[39] as described previously[40], with the following differences: box-size=6x6x6 nm^3, TIP3P water[41], no position restraints during production run. Root-mean-squared deviations (RMSD) from the starting configuration were calculated over backbone atoms (GROMACS *rms* utility). Conformational clustering (GROMACS *cluster* utility) was performed with the backbone RMSD cut-off for neighbouring structures of 0.9 Å – a minimum value at which only a single dominant state was identified for WT. Electrostatic potential was calculated and mapped onto the protein solvent.

Binding assays

Characterisation of FIBCD1 binding specificity to CS-4S and CS-6S was performed through ELISA-based inhibition experiments as described previously[24].

MRI

Anaesthetised male mice (12 months) were imaged in the Preclinical Imaging Facility at VBC Facilities (pcPHENO, VBCF) as described previously[42].

Behaviour assays

Drosophila negative geotaxis assay

Female *Nsyb-Gal4* animals were crossed with *UAS-RNAi* lines targeting *CG10359*. Female offspring were tested at 10d after eclosion. Flies were knocked-out with CO_2, sorted into batches of 3-7, recovered for 25h, flipped into empty vials and given 10-15m to recover. The climbing index is the percentage of flies that pass the 5cm mark in 5s after gently tapping to the bottom of a vial.

Mouse

Elevated Plus Maze were performed as described previously using an automated activity system (TSE-Systems). Morris Water Maze, Y-Maze, Inhibitory Avoidance and foot shock scoring was performed as described previously[42] [43] at pcPHENO, VBCF. Hot plate assay was performed by placing the animal on a hot plate (Ugo Basile) at 50°C and next day at 52°C, and manually observed for first reaction for a maximum of 60s. Counted reactions included: jumping, licking, shaking or lifting of the hind paws. For reaction to capsaicin, 1 µg of capsaicin (Sigma; M2028) diluted in 15 µl PBS was injected intraplantar in the hind paw and animal was observed for 5 min and timed for duration of the reactions described above. Reaction to acetone was recorded as duration of cumulative licking or biting of the hind paw following acetone application three times at intervals of 30s.

<u>HPLC</u>

CS was extracted from defatted, pronase digested microdissected hippocampi (CA1) and digested using ChABC (Sigma-Aldrich #C3667). The resulting GAGs were labelled with 2-aminobenzamide by reductive amination and analysed as described previously[44]. Identity of glycosaminoglycan-derived disaccharides was inferred from retention time alignment with the major constituents of CS sodium salt from shark cartilage (Sigma-Aldrich, C4384), and bovine trachea (Sigma-Aldrich #C9819).

Tissue Culture

Primary Neurons

E18.5 pups were sacrificed and hippocampi dissected into Hank's Buffered Saline Solution (HBSS, Gibco #14185045). The tissue was minced, trypsinised (0.025%) and triturated with heat-polished glass pipettes. Plating was in Neurobasal medium (ThermoFisher #21103049) with 10% FCS, 2mM L-glutamine (Gibco #25030149), B27 (Gibco #17504001), 10mM Hepes (Gibco #15630056), penicillin/streptomycin. 50% of media was exchanged to FCS-free medium after 24 hours and then every 36 hours. CSPG (Merck #CC117) coatings were performed as described previously[20,45].

FIBCD1 overexpression

mFibcd1 cDNA with 3' V5 tag G-blocks (IDT) was cloned with ΔFReD construct using XhoI-EcoRI restriction enzymes into a custom pMSCV-IRES-mCherry plasmid. N2a cells were lentivirus transduced and FACS-sorted for mCherry+ cells. *hFIBCD1* cDNA (Origene #RC206180) was sub-cloned by Gateway cloning into a custom plasmid (via pDONR201) with 3' 3xFLAG tags and blasticidine resistance. Q5 site-directed mutagenesis kit (NEB #E0554) was used to introduce point variants. HEK 293T cells were lentivirus transduced and selected with 14µg/ml blasticidine.

Western blot

Hippocampi were homogenised in ChABC buffer (40 mM Tris-HCl pH 8.0, 40 mM sodium acetate) containing Benzonase and Halt protease/phosphatase inhibitors (ThermoScientific), pelleted and supernatant containing soluble protein fraction was separated from the pellet (insoluble fraction), which was resuspended in ChABC buffer. One aliquot of each fraction was incubated with ChABC for 12h at 37°C, then heated for 5 mins at 95ºC, separated by SDS-PAGE and transferred onto PVDF membranes. Blocking was for 1h with 5% milk in TBST

overnight at 4°C with primary antibodies (1:100, anti CS-0S, 1B5; anti CS-4S, 2B6, antiCs-6S, 3B3; Amsbio). Blots were washed 3x 5mins in TBST and incubated with HRP-conjugated secondary anti-mouse-IgG-H&L chain or anti-rabbit-IgG-F(ab')2 (GE Healthcare) antibody for 1h at RT, washed 3x 5mins in TBST and visualised.

Immunoprecipitation

N2a cells expressing mFIBCD1, FIBCD1ΔFReD or empty vector were washed twice with PBS and lysed in Hunt buffer (20 mM Tris-HCl pH 8.0, 100 mM sodium chloride, 1 mM EDTA, 0.5% NP-40) with Halt protease/phosphatase inhibitors (Thermo) in 3 consecutive freeze and thaw steps, pelleted, and the supernatant collected. Lysates were precleared for 1h with magnetic Protein G Dynabeads (Invitrogen) and immunopurified with anti-V5 agarose beads (Sigma) overnight at 4C. After 5 washing steps in Hunt buffer, input and immunoprecipitation samples were separated by SDS-PAGE, blotted and stained with anti-V5 antibody (ab15828, 1:2000 dilution), and Western blotting was performed as described above.

Microscopy

At DIV2 and DIV14, primary neurons were PBS washed, fixed in 4% PFA (+4% glucose) for 10 minutes at RT, then quenched with 10mM glycine/PBS for 10 minutes at RT. After 2x 0.01% Triton-X/PBS (PBST) washes, permeabilisation was with 0.25% Triton-X/PBS for 3 minutes and blocked in 5% goat serum for 1h. Primary antibodies were incubated overnight at 4°C and washed 3x in PBST. Secondary antibodies were incubated for 1h at RT and washed 3x with PBST before mounting. Semi-random fields of the coverslips were acquired (Leica) and quantified in ImageJ, experimenters blinded to condition and genotype.

HEK 293T were PBS rinsed and fixed in 4% PFA (4% glucose) for 10 minutes at RT, then 10 minutes with PBS (10mM glycine). The cells were washed 2x with PBS, permeabalised with 0.25% Triton-X/PBS, blocked for 1h with 5% goat serum and incubated with primary

antibodies (anti-FLAG, 1:1000) overnight at 4°C, washed 2x, then secondary antibodies added (Alexa-Fluor 1:500) and DAPI (1:2000) for 1h at RT, washed again 2x then mounted and imaged on a Zeiss LSM980.

HEK 293T cells – CS-4S internalisation

Cells were seeded in black CellCarrier-96 Ultra Microplates (Perkin Elmer) and, next day, incubated with 100ug/ml tagged 4-O-sulfated CS (Amsbio #AMS.CSR-FACS-A1), diluted in PBS (0.8mM $CaCl_2$) and incubated at 37°C for 45 minutes. The cells were then fixed in 4% PFA for 10 minutes, washed, and further stained with CellMask Orange Plasma Membrane Stain (Invitrogen #C10045, 1:3000) and Hoechst (Invitrogen #H3570, 1:2000) for 10 minutes at 37°C. The cells were washed again and imaged on an Opera Phenix (Perkin Elmer). Images were analysed with a custom pipeline in Harmony analysis software (Perkin Elmer).

Flow cytometry

N2a cells expressing mFIBCD1-V5, mFIBCD1-V5$^{\Delta FReD}$ or empty vector were washed once with PBS and incubated for 4h with 100µg/ml labelled GAGs: 4-O-sulfated CS (AMS.CSR-FACS-A1, AMSBIO), poly-sulphated CS (AMS.CSR-FACS-P1) or dermatan sulphate (AMS.CSR-FADS-B1) in DMEM. Cells were collected and acquired on FACS LSR Fortessa (BD). The experiment was performed in three independent replicates. HEK 293Ts expressing 3xFLAG-tagged hFIBCD1, hFIBCD1_W6*, hFIBCD1_G29S, hFIBCD1_R406C, hFIBCD1_P456L were seeded and, next day, washed with PBS, trypsinised, pelleted and resuspended in 10µg/ml 4-O-sulfated chondroitin sulphate (Amsbio) in fresh PBS (0.8mM $CaCl_2$) and incubated at 37°C for 45 minutes. Samples were washed in ice-cold PBS (0.8mM $CaCl_2$) and acquired on LSRFortessa Cell Analyzer (BD). The experiment was performed in two independent replicates and analysed by FlowJo v10.6.1 (FlowJo LLC).

RNA-sequencing

RNA was isolated using RNeasy Mini kit (Qiagen #74104). Library prep, sequencing and alignment were done at the VBC NGS Facility (Austria), with poly-a enrichment and sequencing on an Illumina HiSeq 3000/4000, 50bp single-read. DESeq2 package[46] was used to identify DEGs, excluding pseudogenes and allosome-located DEGs. Galaxy web platform[47] and WebGestalt[48], over-representation analysis method, were used for data analysis.

Acute hippocampal slice preparation and electrophysiological recordings

Memory-related synaptic plasticity and electrophysiological recordings were studied *ex vivo* in hippocampal slices as previously described[49-54].

RESULTS

Identification of potentially deleterious human germline *FIBCD1* variants

Two unrelated patients presented to the clinics with severe complex NDD of suspected genetic origin. Patient 1 (P1) is a 12 year old nonverbal male from a Caucasian non-consanguineous family, diagnosed with severe ASD, delayed verbal cognition, anxiety and ADHD. He has high pain tolerance, fine motor coordination deficits and mild facial dysmorphia. Additionally, he experiences frequent allergic rhinitis and sinusitis (Table 1). There is no history of neurological disease in the family, however, several members of the maternal family have learning disabilities. As part of his clinical diagnostic evaluation, WES was performed at GeneDx, USA (www.genedx.com) and the following rare variants (with minimal allele frequency of <0.01) were prioritised: compound heterozygous *FIBCD1* Chr9:133805421 C>T; c.85 G>A; p.(G29S) and Chr9:133779621 G>A; c.1216C>T; p.(R406C) (Fig. 1A), with CADD scores of 6.832 and 25.1, respectively, and a *de novo* variant in *CSMD3* Chr8: 113933925 T>C; c.1564 A>G; p.(K522E) with a CADD score of 24.7. While *CSMD3* variants have been reported in association with NDDs, most published missense variants have population data in gnomAD[55] or internal data at GeneDx, reducing the likelihood that this variant is related to the phenotype ([56]; GeneDx, Inc. personal communication). Therefore, the *FIBCD1* variants were prioritised for further analysis. Sanger sequencing determined one *FIBCD1* variant was inherited from each of the parents (Fig. 1A). There were no other variants with confirmed association to human disease identified that would match the phenotype or inheritance pattern in the patient. Patient 2 (P2) is a nonverbal 3 year old Chinese female from a non-consanguineous family with no history of genetic neurological disease, that presented with severe NDD, delayed social and cognitive abilities and delayed sitting and walking. Magnetic resonance imaging (MRI) revealed thickened cortex, decreased white/grey matter ratio, bilateral enlarged frontal gyri and ventriculomegaly (Fig. 1B). The patient also has microcephaly and dysmorphic facial features

(Table 1). Additionally, recurrent pneumonia was noted. Clinical genetic testing was performed and revealed inheritance by uniparental disomy (UPD) with mosaicism. Homozygous variants of unknown significance were found in: *FIBCD1* Chr9:133779470 G>A; c.1367C>T; p.(P456L) (Fig. 1A) with a CADD score of 29, *UNC13B* Chr9:35376187; c.1531T>C; p.(C511R) with a CADD score of 28.4, and *RIC1* Chr9:5765523; c.2951C>T; p.(A984V) with a CADD score of 28.6. Variants within *UNC13B* and *RIC1* were dismissed from consideration due to a lack of clinical similarities with published cases[57-59] and *FIBCD1* variants were prioritised for further functional validation. All the *FIBCD1* variants named above are located in highly conserved regions (Fig. 1C).

FIBCD1 is expressed in neurons of human and mouse brain

As the function of *FIBCD1* in the CNS has not been explored, we first examined its expression pattern in the brain. We profiled human *FIBCD1* expression using a cDNA array from 48 different tissues and determined the brain to be the third highest *FIBCD1* expressing tissue (Fig. 1D). The Human Protein Atlas[60], reports *FIBCD1* expression to be largely restricted to the hippocampus. Indeed, a further *FIBCD1* gene expression analysis with a cDNA array of 24 human brain regions determined that *FIBCD1* expression is highest in the hippocampus, followed by the hypothalamus and cortex (Fig. 1D, inset). In mice, *in situ* hybridisation (ISH) using complementary DNA probe pairs against mouse *Fibcd1* mRNA in adult coronal brain sections revealed strong localisation of *Fibcd1* in the pyramidal cell layer of the hippocampus, granule cells of the dentate gyrus, dispersed cells of the cortex, the medial habenula and hypothalamus (Fig. 1E). While RT-qPCR of 6 different mouse brain regions determined that some *Fibcd1* transcripts can be observed in the olfactory bulb as well, again expression was highest in the hippocampus (Fig. 1F and Fig. S1A-B). In a publicly available dataset of bulk RNA seq of sorted mouse brain cell populations, brainrnaseq.org[61], we noted *Fibcd1* expression

to be highest in neurons and virtually absent from all other cell types sequenced (Fig. S1C). *Fibcd1* transcript levels were high in embryonic mouse brain and dropped to their lowest levels at postnatal day (P) 7 and again increased during postnatal brain development to return to their high embryonic levels at P25 (Fig. 1G and Fig. S1A, D).

FIBCD1-deficiency leads to neurological defects in mice and flies

To investigate the physiological role of FIBCD1 *in vivo*, we studied phenotypic outcomes of FIBCD1-deficiency in *D. melanogaster* and *M. musculus*. *CG10359*, with no assigned function, is a putative *FIBCD1* orthologue in *D. melanogaster*, with a high degree of FReD amino acid sequence homology with human and mouse Fibcd1, hereafter referred to as *dFibcd1* (Fig. S2A). To assess the function of *dFibcd1*, we performed RNA interference (RNAi)-mediated *dFibcd1* knock-down. We crossed three independent RNAi constructs targeting *dFibcd1* (downstream of *UAS* promoter sequence, hereafter as lines #1, #2 and #3) with lines expressing *GAL4* under the control of either the tubulin (tub) promoter for whole body RNAi expression or the *neuronal Synaptobrevin* promoter (*Nsyb*) for neuronal expression of RNAi. As full body knockdown of *dFibcd1* was lethal or semi-lethal in 2 of 3 lines (Fig. S2B), we proceeded only with neuronal knock-down of *dFibcd1* flies. Neuronal (Nsyb) knock-down of *dFibcd1* affected neuronal development, visualised by abnormal morphology at the larva neuromuscular junction (NMJ) (Fig. 2A). All 3 Nsyb>RNAi lines exhibited reduced number of pre-synaptic boutons (Fig. 2B) and line #3 further exhibited reduced degree of neuronal branching (Fig. 2C). To assess if these developmental defects led to neurological phenotypes in adults, we assessed fly climbing behaviour by negative geotaxis assay. We found that Nsyb>RNAi line knockdown of *dFibcd1* resulted in reduced climbing ability when compared to flies expressing control RNAi targeting luciferase (Fig. 2D and Fig. S2C).

To investigate FIBCD1's function in mammals, we obtained *Fibcd1* KO mice (MGI:5007144[31]), which were healthy, viable and exhibited no obvious abnormalities (Fig. S3A-C). We validated the absence of *Fibcd1* expression in KO hippocampi (Fig. S3A). 15T MRI volumetric analysis revealed no significant differences in total brain volume or 11 isolated brain regions as compared to control littermates, determining no overt structural abnormalities in the brains of mice with FIBCD1-deficiency (Fig. S3D). We then subjected *Fibcd1* WT and KO adult mice to a series of hippocampal-dependent learning tasks. We first established that there is no difference in baseline anxiety levels between the two cohorts of mice as assessed by the Elevated Plus Maze (EPM) (Fig. S3E). Morris Water Maze (MWM) revealed no difference in the acquisition and retention of spatial learning between *Fibcd1* WT and KO mice (Fig. S3F-G). Nociceptive responses to noxious chemicals, heat stimulation or mild foot shock in sensory nervous system processing of acute pain were indistinguishable between KOs and control littermates (Fig. S3H-I). However, we found that *Fibcd1* KO mice were significantly impaired in spatial working memory as assessed by spontaneous alternation in the Y-Maze (Fig. 2E). Further, we found that in comparison to WT and heterozygous controls, *Fibcd1* KO animals were significantly impaired in fear-associated learning in the inhibitory avoidance (IA) task (Fig. 2F). Taken together, these data establish FIBCD1 as an evolutionary conserved component of different aspects of neuronal development and adult function.

FIBCD1 binds to glycosaminoglycans

A previous study that determined the crystal structure of FIBCD1 extracellular, ligand-binding FReD, hypothesised that FIBCD1 could also bind GAGs such as chondroitin and dermatan sulphate in addition to its known ligand, chitin[27]. Further, FIBCD1 has been shown to bind and endocytose acetylated structures such as acetylated BSA[24]. CS, a major component of the brain

385 ECM, consists of subunits N-acetylgalactosamine (GalNAc) and a glucuronic acid (GlcA)
386 which can be modified by the addition of sulphate groups. Sulphation of CS is catalysed by
387 sulfonyl transferases and designated according to the position of the sulphate group on the
388 GalNAc unit, such as unsulphated (CS-0S), 4-O-sulphated (CS-4S, CS-A) and/or 6-O-
389 sulphated (CS-6S, CS-C or CS-4,6S, CS-E), comprising an instructive signature for various
390 cellular and developmental functions referred to as the 'sulphation code'[62]. Therefore, we
391 posited FIBCD1 to be an endocytic receptor for GAGs, such as CS, and investigated whether
392 FIBCD1 preferentially binds to certain sulphated GAGs over others.

393 To determine if FIBCD1 interacts with components of the ECM *in vivo*, we analysed
394 the composition of the ECM in the absence of FIBCD1. We surveyed the hippocampal glycome
395 by high performance liquid chromatography (HPLC) of WT and KO mice and noted alterations
396 in various GAG moieties in the KO hippocampi, most notably a relative increase of CS-4S and
397 decrease of CS-6S compared to controls (Fig. 3A). As HPLC determines relative rather than
398 quantitative differences, we next treated hippocampal protein lysates with ChABC, which
399 reveals CS 'stub' epitopes to be detectable by antibodies raised against CSs and immunoblotted
400 for differently sulphated CS GAGs. We observed an increase in CS-4S stub abundance, whereas
401 the CS-0S and -6S stubs were unchanged (Fig. 3B). To further investigate the relationship of
402 FIBCD1 to CS-4S and CS-6S, top binding poses for GAGs including CS-4S and CS-6S were
403 identified using *in silico* molecular docking and an X-ray structure of the extracellular FReD
404 (PDB 4M7F), followed by post-rescoring of docking solutions as described previously[34].
405 According to the scoring function, CS-4S exhibits a better fit to the FReD as compared to CS-
406 6S (45.3 vs 43.3), with the orientations of the two ligands on the FReD surface being nearly
407 orthogonal to each other (Fig. 3C and Fig. S4A). Importantly, the orientation of CS-4S, with its
408 sulphate group packing tightly into a pocket formed by Y405, H415, and Y431 residues of the
409 FReD, leads to a more favourable electrostatic interaction and subsequently lower binding free
410 energy ($\Delta\Delta G$ value of -1.3 kJ mol^{-1}) as predicted by a linear model, published elsewhere[35]. To

characterise binding affinities of FIBCD1 to CS-4S and CS-6S we performed competitive ELISA experiments as described previously[24]. Using a previously reported FIBCD1 ligand, acetylated BSA, and increasing concentrations of CS-4S or CS-6S, we determined a preference of FIBCD1 to bind CS-4S over CS-6S, with an approximately 10-fold lower IC_{50} concentration of CS-4S compared to CS-6S (Fig. 3D).

To assess FIBCD1 binding to GAGs in a cellular context, we cloned V5-tagged full-length mouse WT *Fibcd1* cDNA and a truncated version without the FReD (*Fibcd1*$^{\Delta FReD}$) (Fig. S4B). We overexpressed the two mFIBCD1 constructs in the mouse N2a cell line and by RT-qPCR and immunoblot analyses confirmed overexpression of FIBCD1 and V5-reactive bands at predicted molecular weights (Fig. S4C-E). We then incubated the cells with fluoresceinamine (FITC)-tagged CS-4S, polysulphated CS (CS-PS) and dermatan sulphate (DS) and acquired the cells by flow cytometry. We determined that cells expressing full length WT *Fibcd1* showed increased $V5^+/FITC^+$ fluorescence intensity in comparison to cells expressing empty vector or *Fibcd1*$^{\Delta FReD}$, but this was not the case for cells incubated with CS-PS or DS, confirming preferred binding of FIBCD1-expressing cells to CS-4S, dependent on the FReD (Fig. 3E). To investigate if FIBCD1 facilitates internalisation of GAGs, we incubated HEK 293T cells stably overexpressing full length human FIBCD1 with FITC-tagged CS-4S and observed an increased uptake of CS-4S in FIBCD1-expressing cells compared to untransduced controls (Fig. 3F and S4F), confirming that FIBCD1 facilitates endocytosis of GAGs such as CS-4S. In summary, we conclude that FIBCD1 is a neuronally expressed receptor for GAGs of the ECM, with a preference for CS-4S, and that the absence of FIBCD1 leads to hippocampal ECM composition dysregulation.

Identified patient *FIBCD1* variants are loss-of-function

To determine whether the germline *FIBCD1* variants identified in P1 and P2 affect protein folding or function we performed all-atom MD simulations in the microsecond range of the two *FIBCD1* variants contained within the FReD (p.R406C and p.P456L) and the WT as control. Both WT and patient variant conformations stayed relatively close to the initial structure, with the backbone root-mean-square deviation (RMSD) being the highest for R406C, intermediate for P456L and the lowest for WT (Fig. S5A), but never exceeding 2.5 Å. In order to compare WT and the two mutant structures, the dominant MD conformations were identified using structural clustering. The dominant P456L and R406C structures deviated from the dominant WT structure by 1.6 Å and 1.5 Å backbone RMSD, respectively, while being relatively more similar to each other (1.2 Å). The largest structural rearrangements induced by the variants took place in the 389-399 and 423-448 loop regions, which surround the ligand binding site (Fig. 3G). Here, the R406C variant had a direct effect due to a disruption of the salt bridge between R406 and D433, which in the WT likely stabilised the mutual arrangement of the two loop regions. In the case of the P456L variant, the effect was allosteric, whereby perturbation of the conformational dynamics of the C-terminus, likely due to the removal of the sterically restricted P456, was transmitted towards the upstream 423-448 loop region. Importantly, a similar structural effect of both variants was connected to a similar perturbation of the electrostatic properties on the protein surface in the vicinity of the ligand binding site. In particular, both variants significantly increased the negative charge density of the surface patch surrounding the ligand binding site (especially R406C), in contrast with the WT where the corresponding surface was positively charged (Fig. 3G). We expect that this perturbation significantly weakens the binding of negatively charged ligands such as GAGs by the mutated FReDs.

To substantiate these observations, we generated human HEK293T cell lines stably overexpressing FLAG-tagged human WT FIBCD1 cDNA and each of the variants G29S, R406C and P456L, as well as a W6* variant located in gnomAD database (Fig. S5B) which generates a premature STOP codon at the 6th amino acid residue of FIBCD1. This truncated

isoform is presumably loss-of-function and served as a negative control. We confirmed expression in each overexpressing cell line, barring W6*, by immunofluorescence (Fig. S5C). We asked if the variants identified in our patients functionally perturbed FIBCD1:GAG binding, as indicated by the MD study. We incubated the FIBCD1 overexpressing cells with FITC-tagged CS-4S and acquired by flow cytometry. As with mouse WT FIBCD1 (Fig. 3E), we determined that cells expressing full length human WT FIBCD1 showed increased percentage of $FITC^+$ cells relative to unstained controls or cells expressing FIBCD1_W6* (Fig. 3H). This was not the case for cells expressing any of the patient variants, which exhibited a similar percentage of $FITC^+$ cells as the untransduced control and cells expressing FIBCD1_W6* (Fig. 3H). Together these data suggest that while the *FIBCD1* variants identified in patients did not affect protein expression, they disrupted the binding of FIBCD1 to GAGs such as CS-4S. Further, the molecular docking experiments suggest that the disturbed binding of the R406C and P456L variants may be due to a disruption of the surface electrostatic charge of the CS binding pocket of FIBCD1's FReD. Taken together, we conclude that P1 and P2 harbour variants deleterious to FIBCD1 function.

FIBCD1 mediates GAG signalling in neurons

In vivo, GAG chains, including CSs, are often conjugated to a proteoglycan (CSPG) in variable sulphated forms. *In vitro* studies have demonstrated primary CSPGs to be inhibitory to neuronal adhesion, neurite outgrown, growth cone formation, axonal regeneration and neurogenesis, mediated by CSPG receptors[45]. Based on our findings that FIBCD1 binds GAGs, we hypothesised FIBCD1 to be a receptor for proteoglycans such as CSPGs.

To test this, we harvested and cultured primary neurons from embryonic (E)18.5 WT and KO mouse hippocampi plated on a coating of primary CSPGs, which contains a mixture of sulphated GAGs. We assessed neuronal morphologies after 2 and 14 days *in vitro* (DIV) by

analysing cells that stain positive for the neuronal-specific marker Microtubule-associated protein 2 (MAP2). At DIV2, we found the adherence of *Fibcd1* WT neurons was partially abrogated by the presence of CSPG coating but not in cultures plated on CSPGs after treatment with the enzyme ChABC, which cleaves the GAG chains into soluble disaccharides and tetrasaccharides, leaving the core protein intact (Fig. 4A)[45,63]. At DIV14, we found a dramatic increase in neuronal somata aggregation in cultures plated on CSPGs, also prevented by ChABC pre-digestion, again in agreement with previous literature (Fig. 4B)[45]. In contrast, neurons cultured from *Fibcd1* KO hippocampi showed slight, but not significant, DIV2 adherence impairment and slight, but also not significant, DIV14 somata aggregations, indicating that *Fibcd1* KO neurons are resistant to CSPG coating-induced phenotypes (Fig. 4A-B). Likely, the residual detection of CSPGs in *Fibcd1* KOs was due to the presence of other CSPG receptors, such as PTPσ[20]. These data confirm FIBCD1 as a CSPG hippocampal receptor, mediating neuronal responses to CSPG signalling, dependent on the GAG chains.

To investigate neuronal, FIBCD1-dependent transcriptional responses to CSPGs, we isolated RNA from primary hippocampal neurons plated on coverslips coated with CSPGs (*Fibcd1* WT^{CSPG}, *Fibcd1* KO^{CSPG}) and without (*Fibcd1* WT, *Fibcd1* KO) at DIV3. We performed bulk RNA-sequencing with poly-A enrichment using 4 to 5 biological replicates per condition. We reasoned an early time point after plating transcriptional changes would more likely reflect cellular developmental effects of FIBCD1-CSPG binding as opposed to secondary effects such as increased cell stress, soma aggregation or dendritic fasciculation. Hierarchical clustering showed small intra-group differences and distinct separation between groups by genotype (WT or KO) and treatment (+/- CSPG) (Fig. S6A). Comparison of differentially expressed genes (DEGs, FDR<0.05) between *Fibcd1* KO and WT cells (without CSPG) revealed 462 significant DEGs with *Fibcd1* being the most downregulated DEG, as expected (Fig. S6B). We noted that a number of the top enriched DEGs in the *Fibcd1* KO vs. WT condition to be genes specifically expressed in non-neuronal cells (e.g. *Pdgfra*, *Olig2*),

514 suggesting that DEGs may be reflecting differences between WT and KO cultures in glia
515 numbers, which are technically challenging to control for. We therefore explored our data
516 further comparing only between conditions within the same genotype, i.e. *Fibcd1* WT^{CSPG} vs
517 WT and *Fibcd1* KO^{CSPG} vs KO, which allowed us to isolate the DEGs dependent on FIBCD1
518 activity.

519 Comparison between WT^{CSPG} vs WT revealed 462 significant DEGs, of which the
520 majority (396) were downregulated. Comparison between KO^{CSPG} vs KO revealed 345
521 significant DEGs, of which again the majority (301) were downregulated (Fig. 4C). We cross-
522 referenced DEGs identified in the WT and KO datasets to reveal a set of genes that are
523 responding to CSPGs in both genotypes and those that are dependent on *Fibcd1* expression
524 (Fig. 4D). Among the top dysregulated genes common to both genotypes, independent of
525 *Fibcd1* expression, was *Thbs1*, recently shown to be necessary and sufficient for axon
526 regeneration after injury[64], normally inhibited by the formation of glial CSPG scars[20],
527 suggesting that the effects of CSPGs may be mediated by *Thbs1* gene regulation in hippocampal
528 neurons. Many of the remaining genes are involved in binding or remodelling of the actin
529 cytoskeleton (*Acta2, Tagln, Shroom3, Nes, Actin, Palld, Ajuba, Flnb*) which reflect the
530 morphological perturbations induced by plating the cells on CSPGs. Gene ontology (GO) term
531 enrichment analysis for downregulated genes revealed terms such as “extracellular matrix
532 binding” and “extracellular matrix structural component” in *Fibcd1* WT cells upon CSPG
533 treatment (Fig. 4E), which suggests that FIBCD1 engages with the components of the ECM and
534 also facilitates transcriptional regulation of genes known to play a role in the ECM. Intriguingly,
535 the third-most enriched term was “integrin binding”, reflecting a number of integrin subunits
536 and integrin-related genes that are significantly downregulated in WT cells upon CSPG
537 treatment (Fig. S6C). We next analysed the DEGs unique to the WT cellular response to CSPGs
538 which are dependent on *Fibcd1* expression (Fig. 4D). Among the genes dysregulated in
539 response to CSPGs only in the WT cultures are genes coding for integrin subunits (*Itga1*,

Itgam), integrin binding and/or modulation (*Adamts8, Tln1*)[65,66], genes involved in the synthesis or degradation of ECM components (*Adamts8, Hspg2, Cemip, Col12a1*)[67] and, finally, genes involved in binding to the ECM and adhesion of cells to each other and to the ECM (*Flnc, Wisp1, Tln1*)[66,68-71]. Therefore, these genes represent the transcriptional fingerprint of primary hippocampal neurons mediated by FIBCD1 binding to CSPG. Together, these data demonstrate FIBCD1 to be a novel receptor for CSPGs that mediates transcriptional responses of neurons to components enriched in the brain ECM.

FIBCD1-deficiency impacts synaptic remodelling that is rescuable by CSPG digestion

To validate our behavioural findings, ascertain FIBCD1's role at the synapse and to investigate the potential pathology of accumulated GAGs such as CS-4S in the hippocampus (Fig. 3A-B), we next performed field recordings of acute hippocampal slices from adult *Fibcd1* WT and KO mice pre-incubated with ChABC (to digest CSPGs) or penicillinase (Pen, a negative control). We hypothesised that behavioural deficiencies likely caused by the dysregulation of the GAG content in the *Fibcd1* KO mice could be rescued by digestion with ChABC, as is the case with other neuropathies associated with altered ECM composition (e.g. Alzheimer's disease[72,73]).

Therefore, we examined the electrical properties of the CA3 Schaffer-collateral to CA1 circuit, a key pathway implicated in the formation and maintenance of spatial memories[74]. We first analysed basal properties of synaptic transmission using standard input/output protocols and found no significant differences between all conditions (Fig. S7A-B), indicating the ChABC treatment does not alter the properties of basal synaptic transmission in agreement with previous literature[75]. We next examined paired-pulse-induced facilitation, a form of short-term pre-synaptic plasticity directly related to neurotransmitter release[76]. We observed no differences

between Pen or ChABC treated WT slices, in agreement with previous literature[75]. However, slices obtained from KO mice and treated with Pen showed reduced paired-pulse-facilitation compared to Pen-treated WT slices (Fig. 5A-B). Remarkably, this reduction was restored to WT levels in the ChABC-treated KO slices (Fig. 5A-B). Finally, we examined the effects of theta-burst stimulation (TBS) induced synaptic long-term potentiation (LTP) such as the kind recorded during learning events in mice. Consistent with previous literature[75,77], ChABC treatment reduced, but did not abolish, potentiation in WT slices, starting at the first recorded pulse (Fig. 5C, light blue vs dark blue traces). We found slices from KO mice pre-treated with Pen to exhibit reduced potentiation compared to Pen-treated WT slices (i.e. baseline differences) (Fig. 5C, dark blue vs dark red traces), similar to ChABC-treated WT slices (light blue trace), but, remarkably, this deficit was again rescued in KO slices pre-treated with ChABC (Fig. 5C, pink trace and Fig. S7C-D). Together, these defects in synaptic plasticity in the KO hippocampus reflects and explains the learning deficits previously observed (Fig 2E-F), and the complete rescue of remodelling deficiencies by ChABC treatment supports our hypothesis that GAG accumulation lies at the centre of the FIBCD1 related pathology. Furthermore, our findings here confirm FIBCD1 to be essential to hippocampal function in adult mice.

DISCUSSION

Here we report *FIBCD1* loss-of-function variants in a previously unknown neurodevelopmental disorder, demonstrate high expression of FIBCD1 in the mammalian brain and characterise its conserved role in the nervous system.

We show that knock-down of a putative *FIBCD1* orthologue in flies, *CG10359*, results in defects at the neuromuscular junction and deficiencies in behaviours associated to neurological function. Furthermore, FIBCD1-deficient mice exhibited impaired performance in hippocampal-dependent learning tasks. We identify FIBCD1 as a neuronal receptor for GAGs found in the brain ECM, with an accumulation of CS-4S noted in hippocampi of *Fibcd1* KO mice. Importantly, the variants identified in the patients reported here disrupt the association of FIBCD1 to CS-4S demonstrating they are deleterious to protein function. FIBCD1 mediates neuronal responses to CSPGs and a transcriptional programme associated with cell-cell and cell-matrix interactions. Finally, we found FIBCD1-deficiency to be associated with synaptic dysfunction that could be fully rescued by modulating the ECM with enzymatic digestion.

It is widely recognised that brain ECM composition is critical for CNS development and function and disruptions to synthesis, post-translation modulation or degradation of ECM components are associated with neurodevelopmental disorders, such as ASD and mucopolysaccharidosis[78]. Identification and functional characterisation of CSPG receptors is of interest to the fields of neurodevelopment, learning and memory and regenerative biology[6,15,17,79]. However, few receptors for CSPGs of the ECM have been reported or characterised and, of those identified, none have been found to harbour germline genetic variants associated with disease.

We have presented evidence of two patients with loss-of-function variants in *FIBCD1* that exhibit symptoms of severe neurodevelopmental dysfunctions, including delayed social, cognitive and verbal abilities, ASD, ADHD, facial dysmorphias and structural brain anomalies.

P2 was too young at last examination to be fully evaluated for ASD or ID, however, while exhibiting similar symptoms as P1, was more affected. Intriguingly, signs of immune system symptoms such as recurring allergic rhinitis, sinusitis and pneumonia in both patients is in line with the literature describing FIBCD1 in immune responses[80]. In addition to *FIBCD1* variants, P2's exome sequencing revealed additional variants of unknown significance (VUS) in *UNC13B* and *RIC1*. *UNC13B* encodes a pre-synaptic protein highly expressed in the brain, MUNC13-2, that has recently been associated with partial focal epilepsy[59], not found in P2, and was therefore dismissed as potentially causative in this case. Variants in *RIC1* gene have recently been associated with autosomal recessive CATIFA Syndrome (cleft lip, cataract, tooth abnormality, intellectual disability, facial dysmorphism, attention-deficit hyperactivity disorder, OMIM: 618761)[57,58]. With the exception of P2's micrognathia, she exhibits none of the hallmark symptoms of CATIFA syndrome. However, the contribution of the RIC1 variant to the overall clinical pathology of the patient cannot be ruled out, even if unlikely. We have established a conserved but variable role for FIBCD1 in nervous system function in two animal models with some notable differences to the patient symptomatology. Unlike in flies, FIBCD1 is not required for survival in mice, however, it is important for certain types of hippocampal-dependent learning. We performed a battery of behavioural assays and did not detect nociceptive or sensory deficiencies nor increased anxiety in the KO mice, unlike the features noted in P1. A recent preprint, however, reports elevated amygdala levels of *Fibcd1* mRNA in response to fear conditioning in mice[81]. We also did not detect any structural abnormalities in the brains of the *Fibcd1* KO mice as was noted in P2, however, was also not a shared feature in the two patients. As additional cases with deleterious *FIBCD1* variants are reported, it will be of great interest to characterise the extent of the clinical variability.

Molecular modelling analysis has suggested R406C (P1) and P456L (P2) lead to FIBCD1 loss-of-function by disrupting the binding pocket's electrostatic charge, diminishing the affinity to its GAG ligand, which is consistent with our cellular assay for

635 FIBCD1:CS-4S binding. However, it is less clear how the other P1 variant, G29S, disrupts
636 binding of FIBCD1 to CS-4S. While we find the glycine at this residue is largely
637 conserved among other species, the mouse orthologue contains the same substitution of glycine
638 to serine as in P1. How the function of G29 residue diverges from mouse to human, whether it
639 is important for structural conformation of FIBCD1, targeting, or downstream signalling
640 remains to be elucidated. Nevertheless, we demonstrated all three FIBCD1 variants to be
641 deleterious to protein function of FIBCD1 and in view of the data in the model organisms and
642 cell culture, is likely to be causative of the patients' symptoms. Full understanding of the
643 neuropathology caused by deleterious *FIBCD1* variants awaits more clinical cases for
644 comparison of their clinical symptoms.

645 FIBCD1 is an endocytic lectin, reported to bind chitin on cellular walls of pathogens
646 and to regulate the innate immune response to Candida infections[24,25]. We provide
647 computational, biochemical, cellular and *in vivo* evidence that FIBCD1 also has endogenous
648 ligands in the brain and intimately participates in the regulation of ECM composition through
649 endocytosis or receptor-mediated signalling, or both. Indeed, transcriptomic changes upon
650 CSPG stimulation of *FIBCD1* WT and KO primary hippocampal cultures reveal a novel ligand-
651 dependent signalling function for FIBCD1, primarily encompassing genes involved in ECM
652 binding and structure. Interestingly, a number of DEGs were integrin subunits or integrin-
653 related genes, molecules well known for interacting with the ECM and signalling during
654 neuronal development and synaptic activity[6,79]. Considering that closely related proteins
655 containing FReDs have been shown to directly interact with integrins[82], it is tempting to
656 speculate a physical FIBCD1:integrin interaction, the mechanism of which remains to be
657 uncovered. We cross-referenced the DEGs present in both the WT^{CSPG} vs WT and KO^{CSPG} vs
658 KO datasets to identify the genes specifically regulated by FIBCD1 binding to CSPGs. We
659 identified a number of genes coding for integrin subunits or integrin binding and/or modulation
660 as well as genes involved in the synthesis or degradation of ECM components and, finally,

genes involved in binding to the ECM and adhesion of cells to the ECM. While the functions of many of these genes have been elucidated in a non-neuronal context, it's likely that their function is largely conserved in neurons and, therefore, these genes make up the transcriptional fingerprint regulated by FIBCD1's interaction with CSPGs in primary hippocampal neurons.

The LTP deficits noted in the hippocampal circuit validates the behavioural deficiencies in the mice and could potentially be generalised to synapse function of other brain regions, contributing to some of the clinical symptoms of the patients. The complete rescue of LTP deficits by ChABC digestion of CSPGs suggests that the mouse hippocampus develops normally in the absence of FIBCD1 and it is the pathological accumulation of GAGs containing CS-4S over time that is responsible for the observed behavioural and synaptic phenotypes. This is in contrast to the dependence of *dFibcd1* expression in *D.melanogaster* survival and neuronal development as exhibited by the lethality of the full body *dFibcd1* knock-down flies, suggesting that *Fibcd1* may have developed a more specialised role in mammals. Nevertheless, it will be of great interest to delineate the role of CS-4S during activity-driven synaptic plasticity, in what context it is released from the ECM and how it contributes to hippocampal function.

To conclude, FIBCD1 is a receptor for GAGs of the ECM and mediator of ECM signalling, disruptions to which are associated with a complex NDD and aberrant synaptic function.

ACKNOWLEDGMENTS

We are grateful to the patients and their clinicians for their trust and collaboration. We would like to thank Drs. William Gahl (NIH), Jeffrey Esko (UCSD) and Hudson Freeze (Sanford Burnham Prebys Medical Discovery Institute) for their insightful comments and discussions. We further thank Malene Hyggelbjerg Nielsen for technical assistance with the ISH data. We are thankful to all members of the IMP-IMBA Bio-optics Core Facility for assistance in cell sorting and imaging as well as the Molecular Biology Service. We thank the Preclinical Phenotyping Facility, the Preclinical Imaging Facility and the Next Generation Sequencing Facility at the Vienna BioCenter Core Facilities GmbH (VBCF), member of Vienna BioCenter (VBC), Austria.

C.W.F. is funded by a DOC fellowship of the Austrian Academy of Sciences (OeAW): 25525; L.L. is a fellow of the Damon Runyon Cancer Research Foundation (DRG-2319-18); S.M. is funded by the European Union's Horizon 2020 research and innovation programme under the Marie Sklodowska-Curie grant agreement No. 841319; T.K. is funded by a DOC fellowship of the Austrian Academy of Sciences (OeAW): 25408; A.S is funded by the Austrian Science Fund (FWF): P 32924; J.B.M. is funded by the Novo Nordisk foundation; J.M.P. is supported by the Austrian Federal Ministry of Education, Science and Research, the Austrian Academy of Sciences and the City of Vienna and grants from the Austrian Science Fund (FWF) Wittgenstein award (Z 271-B19), the T. von Zastrow foundation, and a Canada 150 Research Chairs Program (F18-01336); V.N. is funded by Ludwig Boltzmann Gesellschaft core funding, the Austrian Science Fund (FWF): P 32924 and TAI 202 1000 Ideas Project.

AUTHOR CONTRIBUTIONS

Conceptualisation: V.N., C.W.F. Formal Analysis: C.W.F., A.H., A.C., L.L., J.S.S.L., M.A.T., T.K., S.M., J.S., A.A.P., A.S., M.M.M., J.J., J.B.M., V.N. Funding Acquisition: J.P., V.N. Investigation: C.W.F., A.H., A.C., L.L., J.S.S.L, M.A.T., M.H., S.M., J.S., A.A.P., A.S., K.A.T., H.Y., J.W., T.L.A., G.W., J.B.M., V.N. Resources: N.P., B.Z., F.Q.M., J.B.M., J.M.P., V.N. Supervision: U.H., N.P., B.Z., F.Q.M., J.B.M., J.M.P., V.N. Visualisation: C.W.F., A.H., A.C., M.H., L.L., J.S.S.L., S.M., M.A.T., J.S., A.A.P., J.B.M., V.N. Writing – original draft: C.W.F., V.N., with contribution from all authors.

DECLARATIONS OF INTEREST

J.J. and M.M.M. are employees of GeneDx, Inc.

REFERENCES

1 Rees, E. *et al.* Schizophrenia, autism spectrum disorders and developmental disorders share specific disruptive coding mutations. *Nat Commun* **12**, 5353, doi:10.1038/s41467-021-25532-4 (2021).

2 Parenti, I., Rabaneda, L. G., Schoen, H. & Novarino, G. Neurodevelopmental Disorders: From Genetics to Functional Pathways. *Trends Neurosci* **43**, 608-621, doi:10.1016/j.tins.2020.05.004 (2020).

3 Vissers, L. E., Gilissen, C. & Veltman, J. A. Genetic studies in intellectual disability and related disorders. *Nat Rev Genet* **17**, 9-18, doi:10.1038/nrg3999 (2016).

4 van Bokhoven, H. Genetic and epigenetic networks in intellectual disabilities. *Annu Rev Genet* **45**, 81-104, doi:10.1146/annurev-genet-110410-132512 (2011).

5 Fell, C. W. & Nagy, V. Cellular Models and High-Throughput Screening for Genetic Causality of Intellectual Disability. *Trends Mol Med*, doi:10.1016/j.molmed.2020.12.003 (2021).

6 Dityatev, A., Schachner, M. & Sonderegger, P. The dual role of the extracellular matrix in synaptic plasticity and homeostasis. *Nat Rev Neurosci* **11**, 735-746, doi:10.1038/nrn2898 (2010).

7 Smith, P. D., Coulson-Thomas, V. J., Foscarin, S., Kwok, J. C. & Fawcett, J. W. "GAG-ing with the neuron": The role of glycosaminoglycan patterning in the central nervous system. *Exp Neurol* **274**, 100-114, doi:10.1016/j.expneurol.2015.08.004 (2015).

8 Muhleisen, T. W. *et al.* Association between schizophrenia and common variation in neurocan (NCAN), a genetic risk factor for bipolar disorder. *Schizophr Res* **138**, 69-73, doi:10.1016/j.schres.2012.03.007 (2012).

9 de Vrij, F. M. *et al.* Candidate CSPG4 mutations and induced pluripotent stem cell modeling implicate oligodendrocyte progenitor cell dysfunction in familial schizophrenia. *Mol Psychiatry* **24**, 757-771, doi:10.1038/s41380-017-0004-2 (2019).

10 Impagnatiello, F. *et al.* A decrease of reelin expression as a putative vulnerability factor in schizophrenia. *Proc Natl Acad Sci U S A* **95**, 15718-15723, doi:10.1073/pnas.95.26.15718 (1998).

11 Fatemi, S. H. Reelin mutations in mouse and man: from reeler mouse to schizophrenia, mood disorders, autism and lissencephaly. *Mol Psychiatry* **6**, 129-133, doi:10.1038/sj.mp.4000129 (2001).

12 Kitagawa, H., Tsutsumi, K., Tone, Y. & Sugahara, K. Developmental regulation of the sulfation profile of chondroitin sulfate chains in the chicken embryo brain. *J Biol Chem* **272**, 31377-31381, doi:10.1074/jbc.272.50.31377 (1997).

13 Miller, G. M. & Hsieh-Wilson, L. C. Sugar-dependent modulation of neuronal development, regeneration, and plasticity by chondroitin sulfate proteoglycans. *Exp Neurol* **274**, 115-125, doi:10.1016/j.expneurol.2015.08.015 (2015).

14 Sorg, B. A. *et al.* Casting a Wide Net: Role of Perineuronal Nets in Neural Plasticity. *J Neurosci* **36**, 11459-11468, doi:10.1523/JNEUROSCI.2351-16.2016 (2016).

15 Gogolla, N., Caroni, P., Luthi, A. & Herry, C. Perineuronal nets protect fear memories from erasure. *Science* **325**, 1258-1261, doi:10.1126/science.1174146 (2009).

16 Pekny, M. & Nilsson, M. Astrocyte activation and reactive gliosis. *Glia* **50**, 427-434, doi:10.1002/glia.20207 (2005).

17 Lang, B. T. *et al.* Modulation of the proteoglycan receptor PTPsigma promotes recovery after spinal cord injury. *Nature* **518**, 404-408, doi:10.1038/nature13974 (2015).

18 Muir, E., De Winter, F., Verhaagen, J. & Fawcett, J. Recent advances in the therapeutic uses of chondroitinase ABC. *Exp Neurol* **321**, 113032, doi:10.1016/j.expneurol.2019.113032 (2019).

19 Dickendesher, T. L. *et al.* NgR1 and NgR3 are receptors for chondroitin sulfate proteoglycans. *Nat Neurosci* **15**, 703-712, doi:10.1038/nn.3070 (2012).

20 Shen, Y. *et al.* PTPsigma is a receptor for chondroitin sulfate proteoglycan, an inhibitor of neural regeneration. *Science* **326**, 592-596, doi:10.1126/science.1178310 (2009).

21 Xu, B. *et al.* Role of CSPG receptor LAR phosphatase in restricting axon regeneration after CNS injury. *Neurobiol Dis* **73**, 36-48, doi:10.1016/j.nbd.2014.08.030 (2015).

22 Mikami, T., Yasunaga, D. & Kitagawa, H. Contactin-1 is a functional receptor for neuroregulatory chondroitin sulfate-E. *J Biol Chem* **284**, 4494-4499, doi:10.1074/jbc.M809227200 (2009).

23 Mizumoto, S., Takahashi, J. & Sugahara, K. Receptor for advanced glycation end products (RAGE) functions as receptor for specific sulfated glycosaminoglycans, and anti-RAGE antibody or sulfated glycosaminoglycans delivered in vivo inhibit pulmonary metastasis of tumor cells. *J Biol Chem* **287**, 18985-18994, doi:10.1074/jbc.M111.313437 (2012).

24 Schlosser, A. *et al.* Characterization of FIBCD1 as an acetyl group-binding receptor that binds chitin. *J Immunol* **183**, 3800-3809, doi:10.4049/jimmunol.0901526 (2009).

25 Moeller, J. B. *et al.* Modulation of the fungal mycobiome is regulated by the chitin-binding receptor FIBCD1. *J Exp Med* **216**, 2689-2700, doi:10.1084/jem.20182244 (2019).

26 Thomsen, T. *et al.* The recognition unit of FIBCD1 organizes into a noncovalently linked tetrameric structure and uses a hydrophobic funnel (S1) for acetyl group recognition. *J Biol Chem* **285**, 1229-1238, doi:10.1074/jbc.M109.061523 (2010).

27 Shrive, A. K. *et al.* Crystal structure of the tetrameric fibrinogen-like recognition domain of fibrinogen C domain containing 1 (FIBCD1) protein. *J Biol Chem* **289**, 2880-2887, doi:10.1074/jbc.M113.520577 (2014).

28 Sobreira, N., Schiettecatte, F., Valle, D. & Hamosh, A. GeneMatcher: a matching tool for connecting investigators with an interest in the same gene. *Hum Mutat* **36**, 928-930, doi:10.1002/humu.22844 (2015).

29 Retterer, K. *et al.* Clinical application of whole-exome sequencing across clinical indications. *Genet Med* **18**, 696-704, doi:10.1038/gim.2015.148 (2016).

30 Yan, H. *et al.* Genetic analysis of 20 patients with hypomyelinating leukodystrophy by trio-based whole-exome sequencing. *J Hum Genet* **66**, 761-768, doi:10.1038/s10038-020-00896-5 (2021).

31 Tang, T. *et al.* A mouse knockout library for secreted and transmembrane proteins. *Nat Biotechnol* **28**, 749-755, doi:10.1038/nbt.1644 (2010).

32 Lassen, N. E. *et al.* Coupling of Bone Resorption and Formation in Real Time: New Knowledge Gained From Human Haversian BMUs. *J Bone Miner Res* **32**, 1395-1405, doi:10.1002/jbmr.3091 (2017).

33 Jones, G., Willett, P., Glen, R. C., Leach, A. R. & Taylor, R. Development and validation of a genetic algorithm for flexible docking. *J Mol Biol* **267**, 727-748, doi:10.1006/jmbi.1996.0897 (1997).

34 Ribeiro Ede, A., Jr. *et al.* The structure and regulation of human muscle alpha-actinin. *Cell* **159**, 1447-1460, doi:10.1016/j.cell.2014.10.056 (2014).

35 Kurkcuoglu, Z. *et al.* Performance of HADDOCK and a simple contact-based protein-ligand binding affinity predictor in the D3R Grand Challenge 2. *J Comput Aided Mol Des* **32**, 175-185, doi:10.1007/s10822-017-0049-y (2018).

36 van Zundert, G. C. P. *et al.* The HADDOCK2.2 Web Server: User-Friendly Integrative Modeling of Biomolecular Complexes. *J Mol Biol* **428**, 720-725, doi:10.1016/j.jmb.2015.09.014 (2016).

37 Schrodinger, LLC. *The PyMOL Molecular Graphics System, Version 1.8* (2015).

38 Abraham, M. J. *et al.* GROMACS: High performance molecular simulations through multi-level parallelism from laptops to supercomputers. *SoftwareX* **1-2**, 19-25, doi:https://doi.org/10.1016/j.softx.2015.06.001 (2015).

39 Lindorff-Larsen, K. *et al.* Improved side-chain torsion potentials for the Amber ff99SB protein force field. *Proteins* **78**, 1950-1958, doi:10.1002/prot.22711 (2010).

40 Sponga, A. *et al.* Order from disorder in the sarcomere: FATZ forms a fuzzy but tight complex and phase-separated condensates with alpha-actinin. *Sci Adv* **7**, doi:10.1126/sciadv.abg7653 (2021).

41 Jorgensen, W. L. Quantum and statistical mechanical studies of liquids. 10. Transferable intermolecular potential functions for water, alcohols, and ethers. Application to liquid water. *Journal of the American Chemical Society* **103**, 335-340, doi:10.1021/ja00392a016 (1981).

42 Nagy, V. *et al.* HACE1 deficiency leads to structural and functional neurodevelopmental defects. *Neurol Genet* **5**, e330, doi:10.1212/NXG.0000000000000330 NG2018008979 [pii] (2019).

43 Nielsen, D. M. & Crnic, L. S. Automated analysis of foot-shock sensitivity and concurrent freezing behavior in mice. *J Neurosci Methods* **115**, 199-209, doi:10.1016/s0165-0270(02)00020-1 (2002).

44 Takegawa, Y. *et al.* Simultaneous analysis of heparan sulfate, chondroitin/dermatan sulfates, and hyaluronan disaccharides by glycoblotting-assisted sample preparation followed by single-step zwitter-ionic-hydrophilic interaction chromatography. *Anal Chem* **83**, 9443-9449, doi:10.1021/ac2021079 (2011).

45 Jin, J. *et al.* Effect of chondroitin sulfate proteoglycans on neuronal cell adhesion, spreading and neurite growth in culture. *Neural Regen Res* **13**, 289-297, doi:10.4103/1673-5374.226398 (2018).

46 Love, M. I., Huber, W. & Anders, S. Moderated estimation of fold change and dispersion for RNA-seq data with DESeq2. *Genome Biol* **15**, 550, doi:10.1186/s13059-014-0550-8 (2014).

47 Jalili, V. *et al.* The Galaxy platform for accessible, reproducible and collaborative biomedical analyses: 2020 update. *Nucleic Acids Res* **48**, W395-W402, doi:10.1093/nar/gkaa434 (2020).

48 Liao, Y., Wang, J., Jaehnig, E. J., Shi, Z. & Zhang, B. WebGestalt 2019: gene set analysis toolkit with revamped UIs and APIs. *Nucleic Acids Res* **47**, W199-W205, doi:10.1093/nar/gkz401 (2019).

49 Cicvaric, A. *et al.* Enhanced synaptic plasticity and spatial memory in female but not male FLRT2-haplodeficient mice. *Sci Rep* **8**, 3703, doi:10.1038/s41598-018-22030-4 (2018).

50 Cicvaric, A. *et al.* The brain-tumor related protein podoplanin regulates synaptic plasticity and hippocampus-dependent learning and memory. *Ann Med* **48**, 652-668, doi:10.1080/07853890.2016.1219455 (2016).

51 Rammes, G. *et al.* Isoflurane anaesthesia reversibly improves cognitive function and long-term potentiation (LTP) via an up-regulation in NMDA receptor 2B subunit expression. *Neuropharmacology* **56**, 626-636 (2009).

52 Simon, W., Hapfelmeier, G., Kochs, E., Zieglgansberger, W. & Rammes, G. Isoflurane blocks synaptic plasticity in the mouse hippocampus. *Anesthesiology* **94**, 1058-1065 (2001).

53 Monje, F. J. *et al.* Focal adhesion kinase regulates neuronal growth, synaptic plasticity and hippocampus-dependent spatial learning and memory. *Neuro-Signals* **20**, 1-14 (2012).

54 Kim, E. J. *et al.* Alzheimer's disease risk factor lymphocyte-specific protein tyrosine kinase regulates long-term synaptic strengthening, spatial learning and memory. *Cell Mol Life Sci* (2012).

55 Karczewski, K. J. *et al.* The mutational constraint spectrum quantified from variation in 141,456 humans. *Nature* **581**, 434-443, doi:10.1038/s41586-020-2308-7 (2020).

56 Wu, J. *et al.* Genomic landscapes of Chinese sporadic autism spectrum disorders revealed by whole-genome sequencing. *J Genet Genomics* **45**, 527-538, doi:10.1016/j.jgg.2018.09.002 (2018).

57 Unlu, G. *et al.* Phenome-based approach identifies RIC1-linked Mendelian syndrome through zebrafish models, biobank associations and clinical studies. *Nat Med* **26**, 98-109, doi:10.1038/s41591-019-0705-y (2020).

58 Patel, N. *et al.* Novel phenotypes and loci identified through clinical genomics approaches to pediatric cataract. *Hum Genet* **136**, 205-225, doi:10.1007/s00439-016-1747-6 (2017).

59 Wang, J. *et al.* UNC13B variants associated with partial epilepsy with favourable outcome. *Brain*, doi:10.1093/brain/awab164 (2021).

60 Uhlen, M. *et al.* Proteomics. Tissue-based map of the human proteome. *Science* **347**, 1260419, doi:10.1126/science.1260419 (2015).

61 Zhang, Y. *et al.* Purification and Characterization of Progenitor and Mature Human Astrocytes Reveals Transcriptional and Functional Differences with Mouse. *Neuron* **89**, 37-53, doi:10.1016/j.neuron.2015.11.013 (2016).

62 Soares da Costa, D., Reis, R. L. & Pashkuleva, I. Sulfation of Glycosaminoglycans and Its Implications in Human Health and Disorders. *Annu Rev Biomed Eng* **19**, 1-26, doi:10.1146/annurev-bioeng-071516-044610 (2017).

63 Zhao, R. R. & Fawcett, J. W. Combination treatment with chondroitinase ABC in spinal cord injury--breaking the barrier. *Neurosci Bull* **29**, 477-483, doi:10.1007/s12264-013-1359-2 (2013).

64 Bray, E. R. *et al.* Thrombospondin-1 Mediates Axon Regeneration in Retinal Ganglion Cells. *Neuron* **103**, 642-657 e647, doi:10.1016/j.neuron.2019.05.044 (2019).

65 Collins-Racie, L. A. *et al.* ADAMTS-8 exhibits aggrecanase activity and is expressed in human articular cartilage. *Matrix Biol* **23**, 219-230, doi:10.1016/j.matbio.2004.05.004 (2004).

66 Nieswandt, B. *et al.* Loss of talin1 in platelets abrogates integrin activation, platelet aggregation, and thrombus formation in vitro and in vivo. *J Exp Med* **204**, 3113-3118, doi:10.1084/jem.20071827 (2007).

67 Yoshino, Y. *et al.* Targeted deletion of HYBID (hyaluronan binding protein involved in hyaluronan depolymerization/ KIAA1199/CEMIP) decreases dendritic spine density in the dentate gyrus through hyaluronan accumulation. *Biochem Biophys Res Commun* **503**, 1934-1940, doi:10.1016/j.bbrc.2018.07.138 (2018).

68 Begay, R. L. *et al.* Filamin C Truncation Mutations Are Associated With Arrhythmogenic Dilated Cardiomyopathy and Changes in the Cell-Cell Adhesion Structures. *JACC Clin Electrophysiol* **4**, 504-514, doi:10.1016/j.jacep.2017.12.003 (2018).

69 Desnoyers, L., Arnott, D. & Pennica, D. WISP-1 binds to decorin and biglycan. *J Biol Chem* **276**, 47599-47607, doi:10.1074/jbc.M108339200 (2001).

70 Manso, A. M. *et al.* Loss of mouse cardiomyocyte talin-1 and talin-2 leads to beta-1 integrin reduction, costameric instability, and dilated cardiomyopathy. *Proc Natl Acad Sci U S A* **114**, E6250-E6259, doi:10.1073/pnas.1701416114 (2017).

71 Haage, A. *et al.* Talin Autoinhibition Regulates Cell-ECM Adhesion Dynamics and Wound Healing In Vivo. *Cell Rep* **25**, 2401-2416 e2405, doi:10.1016/j.celrep.2018.10.098 (2018).

72 Vegh, M. J. *et al.* Hippocampal extracellular matrix levels and stochasticity in synaptic protein expression increase with age and are associated with age-dependent cognitive decline. *Mol Cell Proteomics* **13**, 2975-2985, doi:10.1074/mcp.M113.032086 (2014).

73 Yang, S. *et al.* Perineuronal net digestion with chondroitinase restores memory in mice with tau pathology. *Exp Neurol* **265**, 48-58, doi:10.1016/j.expneurol.2014.11.013 (2015).

74 Wilson, M. A. & Tonegawa, S. Synaptic plasticity, place cells and spatial memory: study with second generation knockouts. *Trends Neurosci* **20**, 102-106, doi:10.1016/s0166-2236(96)01023-5 (1997).

75 Bukalo, O., Schachner, M. & Dityatev, A. Modification of extracellular matrix by enzymatic removal of chondroitin sulfate and by lack of tenascin-R differentially affects several forms of synaptic plasticity in the hippocampus. *Neuroscience* **104**, 359-369, doi:10.1016/s0306-4522(01)00082-3 (2001).

76 Nicoll, R. A. & Malenka, R. C. Expression mechanisms underlying NMDA receptor-dependent long-term potentiation. *Ann N Y Acad Sci* **868**, 515-525, doi:10.1111/j.1749-6632.1999.tb11320.x (1999).

77 Kochlamazashvili, G. *et al.* The extracellular matrix molecule hyaluronic acid regulates hippocampal synaptic plasticity by modulating postsynaptic L-type Ca(2+) channels. *Neuron* **67**, 116-128, doi:10.1016/j.neuron.2010.05.030 (2010).

78 Dwyer, C. A. & Esko, J. D. Glycan susceptibility factors in autism spectrum disorders. *Mol Aspects Med* **51**, 104-114, doi:10.1016/j.mam.2016.07.001 (2016).
79 Dityatev, A. & Schachner, M. Extracellular matrix molecules and synaptic plasticity. *Nat Rev Neurosci* **4**, 456-468, doi:10.1038/nrn1115 (2003).
80 Jepsen, C. S. *et al.* FIBCD1 Binds Aspergillus fumigatus and Regulates Lung Epithelial Response to Cell Wall Components. *Front Immunol* **9**, 1967, doi:10.3389/fimmu.2018.01967 (2018).
81 Reis, A. M. *et al.* Sex-specific transcriptomic and epitranscriptomic signatures of PTSD-like fear acquisition. *bioRxiv*, 2021.2011.2025.468910, doi:10.1101/2021.11.25.468910 (2021).
82 Thomsen, T., Schlosser, A., Holmskov, U. & Sorensen, G. L. Ficolins and FIBCD1: soluble and membrane bound pattern recognition molecules with acetyl group selectivity. *Mol Immunol* **48**, 369-381, doi:10.1016/j.molimm.2010.09.019 (2011).

TABLE TITLES AND LEGENDS

Table 1: **Comparison of clinical findings and genetics of reported patients**.

		P1	P2
Background	Sex	M	F
	Current Age	12 y.o.	3 y.o.
	Ethnicity	Caucasian	Chinese
	FIBCD1	Compound Het.	UPD with mosaicism
		c.85G>A ; c.1216C>T	c.1367C>T
		p.G29S ; p.R406C	p.P456L
Neurology			
	Diagnosis	Severe ASD	Severe NDD
	Psychological Evaluation	Borderline delayed cognition	Delayed social and cognitive abilities
		Anxiety	
		ADHD combined type	
	Sitting and Walking	Normal	Delayed
	Language	Nonverbal	Nonverbal
	Epilepsy	-	-
	Intellectual Disability	-	Too young to be evaluated
	Sensory	High pain tolerance, sensitive touch	n/a
	Motoric	Fine motor coordination deficits	n/a
Neuroradiology			
	MRI	n/a	Slightly thickened cortex
			Decreased white matter volume
			Ventriculomegaly
			Bilateral enlarged frontal gyri
Dysmorphias			
	Craniofacial	Triangular shaped head	Microcephaly
		Hypertelorism	Micrognathia
		Almond-shaped eyes	Low set ears
		Posteriorly rotated and low set ears	
		Epicanthal folds	
Other systems			
	Cardiovascular	-	Patent ductus arteriosus, resolved at 6 months
	Respiratory	-	Recurrent pneumonia
	Immune	Allergic rhinitis, sinusitis	-

Abbreviations: UPD = Uniparental Disomy; ASD = Autism Spectrum Disorder; ADHD = Attention Deficit Hyperactivity Disorder; NDD = Neurodevelopmental Disorder; Het = Heterozygous

923 Table 2: **Materials used in this study.**

Genotyping primers:	
Fibcd1 WT	CGCTGGTCTTGCTGGAAG TCTTCTCTTCCCTCTGCACA
Fibcd1 KO	GCAGCGCATCGCCTTCTATC TGGCACAGGTTAAGGAATT
Primers for qPCR:	
Gapdh	GTCGGTGTGAACGGATTTGG GACTCCACGACATACTCAGC
mFibcd1(ex1-2)	CTGGAAGATGGTCCACGAG CCGTGCACAGGACATAACTG
mFibcd1(ex3-4)	TCAAGGCTGACCTTCAGAGG GAAGCCAGCTGGGTAGTGAG
mFibcd1(ex4-5)	CAGCTGGCTTCCAGGTCTAC CCAACCTCGGAAAAAGTTCA
hFibcd1	CAGGACGATGGCGTCTACTC
	GATCCTCTTGAGCCCTAGCC
Antibodies for immunoblots:	
b-Actin	A5316 (Sigma)
CS-0S (1B5)	270431-CS (Amsbio)
CS-4S (2B6)	270432-CS (Amsbio)
CS-6S (3B3)	270433-CS (Amsbio)
Anti-V5 tag	Ab15828 (Abcam)
Fluorescent Sugars for Flow Cytometry:	
Fluoresceinamine Labeled Sodium Chondroitin Sulfate A (A1)	AMS.CSR-FACS-A1 (Amsbio)
Fluoresceinamine Labeled Sodium Chondroitin Poly-Sulfate (P1)	AMS.CSR-FACS-P1 (Amsbio)
Fluoresceinamine Labeled Sodium Dermatan Sulfate (B1)	AMS.CSR-FADS-B1 (Amsbio)
Antibodies/dyes for immunofluorescence:	
MAP2	Millipore 05-346
FLAG (M2)	Sigma F1804
Alexa Fluor® 546 anti-mouse	Thermo A-11003
Goat F(ab) anti mouse (IgG)	Abcam (ab6668)
Alexa Fluor® 647 AffiniPure Goat Anti-Horseradish Peroxidase	Jackson Immunoresearch
Mouse anti-nc82 (Bruchpilot)	Developmental Hybridoma Studies Bank
DAPI	Carl Roth
WFA-488	Vector Laboratories (FL-1351)
Drosophila reagents	
Stock	RRID/source
y[1] w[*]; P{w [+mC]=r4-GAL4}3	BDSC_33832
y[1] v[1]; P{y[+t7.7] v[+t1.8]=TRiP.HMJ30271}attP40	BDSC_63703

w1118; P{GD2280}v4128/TM3	FlyBase_FBst0464025
P{KK105143}VIE-260B	FlyBase_FBst0474536
y[1] w[*]; P{w[+m*]=nSyb-GAL4.S}3	BDSC_51635
y[1] w[*]; P{w[+mC]=tubP-GAL4}LL7/TM3, Sb[1] Ser[1]	BDSC_5138
PBac{UAS-empty}VK00037	Yoon et al., Cell Metabolism, 2017
y[1] v[1]; P{TRiP.JF01355}attP2	BDSC_31603

924

925

926

927

928

929

Figure 1

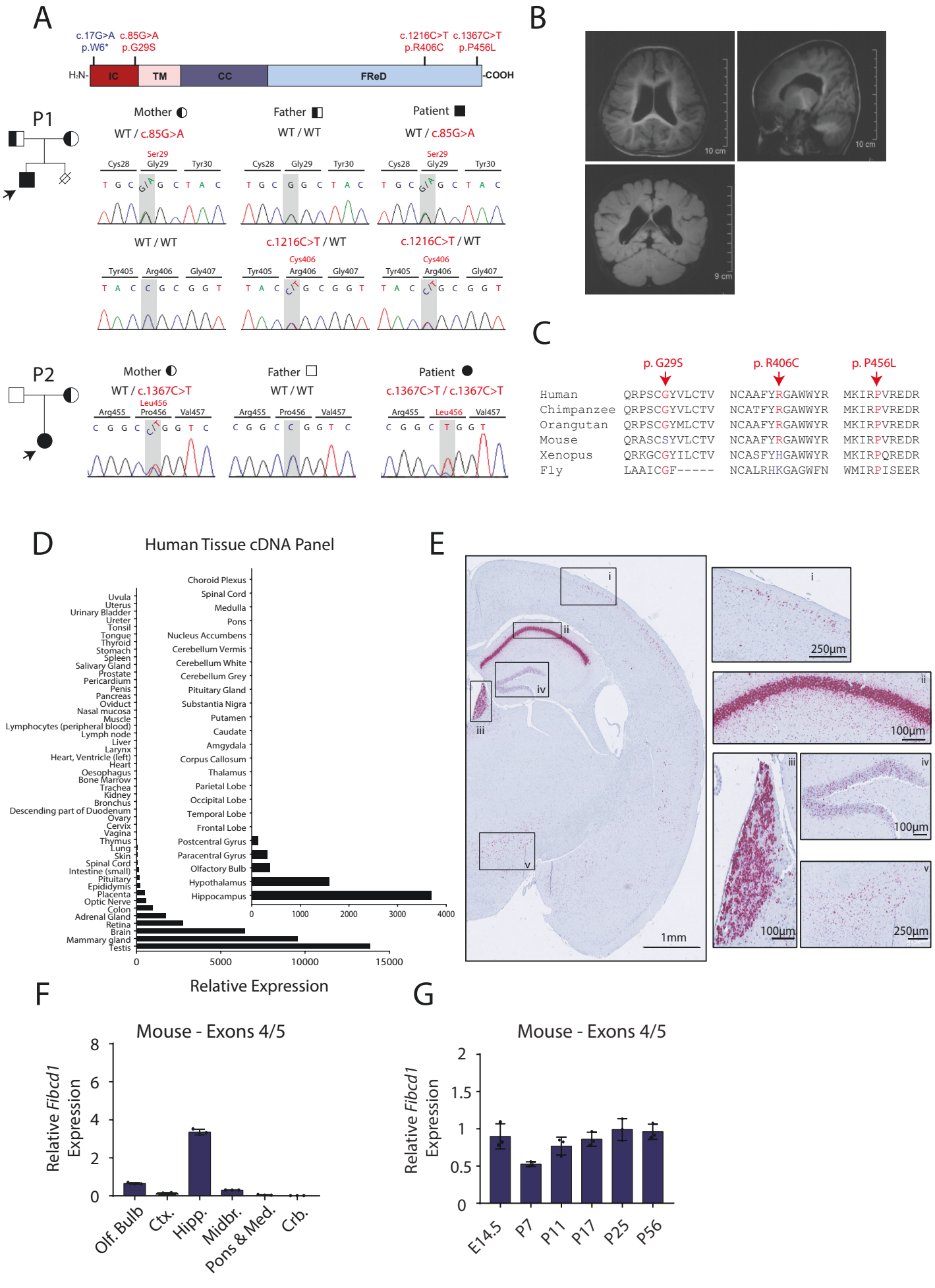
A
c.17G>A p.W6*
c.85G>A p.G29S
c.1216C>T p.R406C
c.1367C>T p.P456L
H2N-
iC
TM
CC
FReD
-COOH
P1
Mother
WT / c.85G>A
Father
WT / WT
Patient
WT / c.85G>A
Ser29
Cys28 Gly29 Tyr30
T G C G/A G C T A C
WT / WT
c.1216C>T / WT
c.1216C>T / WT
Cys406
Tyr405 Arg406 Gly407
T A C C/T G C G G T
P2
Mother
WT / c.1367C>T
Father
WT / WT
Patient
c.1367C>T / c.1367C>T
Leu456
Arg455 Pro456 Val457
C G G C C/T G G T C
B
10 cm
10 cm
9 cm
C
p. G29S
p. R406C
p. P456L
Human QRPSCGYVLCTV NCAAFYRGAWWYR MKIRPVREDR
Chimpanzee QRPSCGYVLCTV NCATFYRGAWWYR MKIRPVREDR
Orangutan QRPSCGYMLCTV NCAAFYRGAWWYR MKIRPVREDR
Mouse QRASCSYVLCTV NCAAFYRGAWWYR MKIRPVREDR
Xenopus QRKGCGYILCTV NCASFYHGAWWYR MKIRPQREDR
Fly LAAICGF----- NCALRHKGAGWFN WMIRPISEER
D
Human Tissue cDNA Panel
Uvula
Uterus
Urinary Bladder
Ureter
Tonsil
Tongue
Thyroid
Stomach
Spleen
Salivary Gland
Prostate
Pericardium
Penis
Pancreas
Oviduct
Nasal mucosa
Muscle
Lymphocytes (peripheral blood)
Lymph node
Liver
Larynx
Heart, Ventricle (left)
Heart
Oesophagus
Bone Marrow
Trachea
Kidney
Bronchus
Descending part of Duodenum
Ovary
Cervix
Vagina
Thymus
Lung
Skin
Spinal Cord
Intestine (small)
Pituitary
Epididymis
Placenta
Optic Nerve
Colon
Adrenal Gland
Retina
Brain
Mammary gland
Testis
0 5000 10000 15000
Choroid Plexus
Spinal Cord
Medulla
Pons
Nucleus Accumbens
Cerebellum Vermis
Cerebellum White
Cerebellum Grey
Pituitary Gland
Substantia Nigra
Putamen
Caudate
Amygdala
Corpus Callosum
Thalamus
Parietal Lobe
Occipital Lobe
Temporal Lobe
Frontal Lobe
Postcentral Gyrus
Paracentral Gyrus
Olfactory Bulb
Hypothalamus
Hippocampus
0 1000 2000 3000 4000
Relative Expression
E
i
ii
iii
iv
v
1mm
250µm
100µm
100µm
100µm
250µm
F
Mouse - Exons 4/5
Relative Fibcd1 Expression
0 2 4 6 8
Olf. Bulb
Ctx.
Hipp.
Midbr.
Pons & Med.
Crb.
G
Mouse - Exons 4/5
Relative Fibcd1 Expression
0 0.5 1 1.5 2
E14.5
P7
P11
P17
P25
P56

Figure 1: **Expression of *FIBCD1* in human tissues and properties of *FIBCD1* variants identified in 2 cases of undiagnosed neurodevelopmental disorders.**

(A) Top, schematic of FIBCD1 protein, with labelled intracellular domain (IC, red), transmembrane domain (TM, pink), coiled coil (CC, dark blue) and FReD (light blue). Location of patient variants denoted in red, blue variant denotes the control used in later experiments. Left, family pedigrees of P1 (top) and P2 (bottom) showing affected proband (filled, arrow) and carriers (half-filled). Right, representative traces of Sanger sequencing to confirm segregation within the family. P1 variants are inherited in autosomal recessive manner; P2 exhibits inheritance by uniparental disomy. (B) P2 MRI images (axial, sagittal and coronal plane) showing ventriculomegaly, slightly thickened cortex and bilateral enlarged gyri. (C) Amino acid sequence conservation sites of patient variants Gly29Ser, Arg406Cys and Pro456Leu in different species, as labelled. (D) *FIBCD1* expression in various human visceral tissues and brain regions (inset). Expression is plotted relative to the tissue with lowest detectable expression (trachea; inset, choroid plexus). N represents technical replicates; N = 2. (E) In-situ hybridisation with probe pairs specific to *Fibcd1* mRNA (purple) in mouse whole-brain coronal section, left hemisphere shown. Insets of high *Fibcd1* expressing regions are (i) cortex, (ii) pyramidal cell layer of hippocampus, (iii) medial habenula, (iv) granule cell layer of the dentate gyrus and (v) hypothalamus. Scale bar sizes are as indicated. Representative of 3 independent experiments. (F) Relative mRNA expression levels of mouse *Fibcd1* (primers binding to exon 4 and 5) normalised to *Gapdh,* in the indicated adult brain regions, analysed by RT-qPCR (n = 3). Olf.Bulb = olfactory bulb; Ctx. = cortex; Hipp. = hippocampus; Midbr. = midbrain; Pons & Med = pons and medulla; Crb. = cerebellum. (G) Relative mRNA expression levels of mouse *Fibcd1* (primers binding to exon 4 and 5) normalised to *Gapdh* in the hippocampus of the indicated developmental time points, analysed by RT-qPCR. N represents biological replicates; N = 3. Data is represented as mean and error bars represent SD.

Figure 2

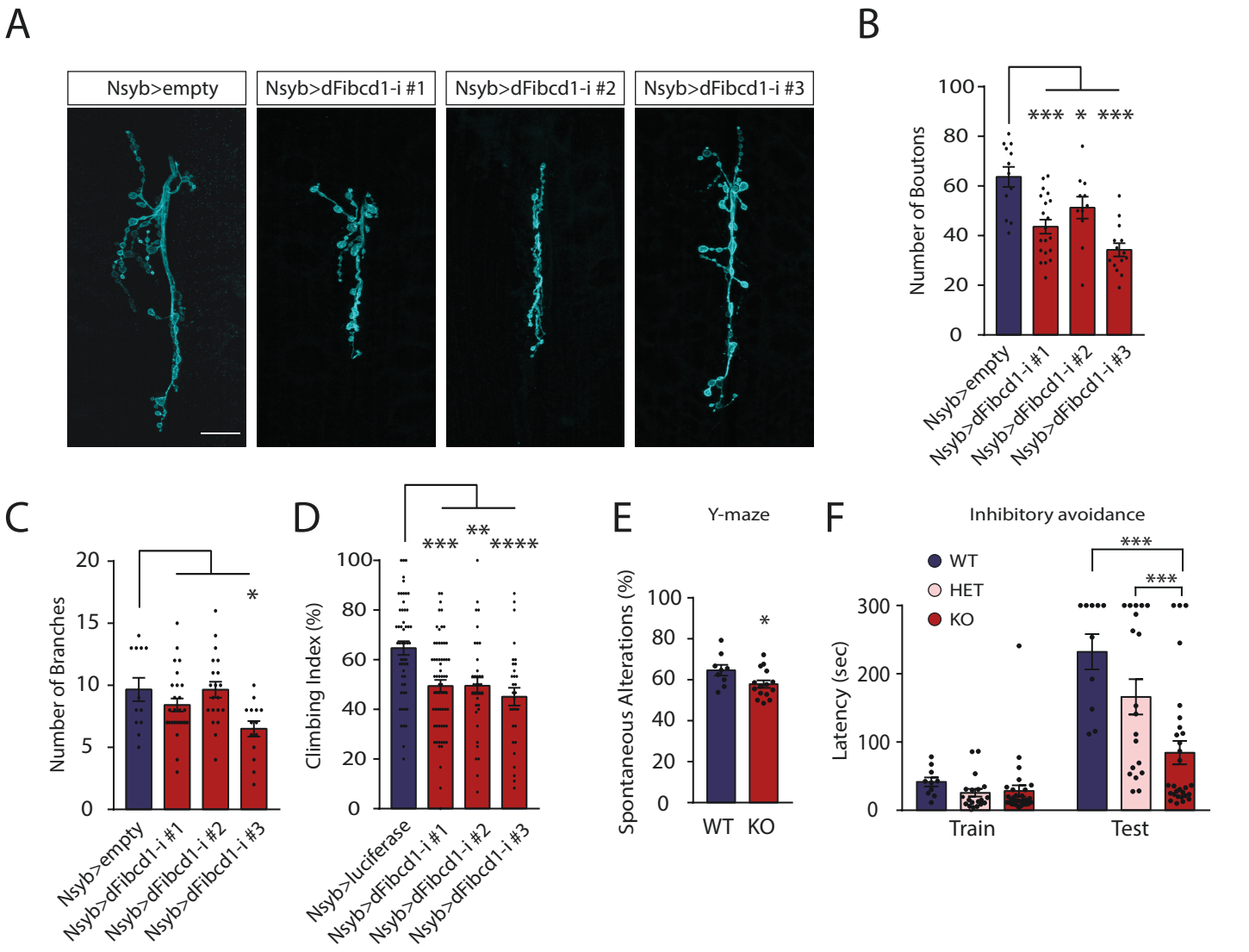
A
Nsyb>empty
Nsyb>dFibcd1-i #1
Nsyb>dFibcd1-i #2
Nsyb>dFibcd1-i #3
B
Number of Boutons
100
80
60
40
20
0
*** * ***
Nsyb>empty
Nsyb>dFibcd1-i #1
Nsyb>dFibcd1-i #2
Nsyb>dFibcd1-i #3
C
Number of Branches
20
15
10
5
0
*
Nsyb>empty
Nsyb>dFibcd1-i #1
Nsyb>dFibcd1-i #2
Nsyb>dFibcd1-i #3
D
Climbing Index (%)
100
80
60
40
20
0
*** ** ****
Nsyb>luciferase
Nsyb>dFibcd1-i #1
Nsyb>dFibcd1-i #2
Nsyb>dFibcd1-i #3
E
Y-maze
Spontaneous Alterations (%)
100
80
60
40
20
0
*
WT
KO
F
Inhibitory avoidance
WT
HET
KO
Latency (sec)
300
200
100
0
***
***
Train
Test

Figure 2: **Neurological deficits in FIBCD1-deficient mice and flies**

(A) Immunofluorescent images (representative of 3 independent experiments) of control and neuronal (Nsyb) *CG10359* (*dFibcd1*) RNAi-mediated knockdown *D. melanogaster,* 3rd instar larvae NMJ (NMJ6/7) stained with anti-horseradish peroxidase antibody. Empty control and RNAi-mediated knockdown of *CG10359* (*dFibcd1-i*) lines #1, 2 and 3 shown. Scale bar = 20µm. (B) Quantification of (A), control and *CG10359* knockdown lines NMJ neuron bouton number. (C) Quantification of (A), control and *CG10359* knockdown lines NMJ neuron axon branch points. (D) Negative geotaxis assay of adult Drosophila control and RNAi lines #1, #2 and #3 compared to control lines expressing RNAi targeting luciferase. Climbing index represent the percentage of flies that crossed the 5 cm vial mark within 5 seconds after gentle tapping to the bottom of the vial. N is the number of tested vials: N (luciferase) = 53; N (line #1) = 63; N (line #2) = 36; N (line #3) = 31. For flies per vial, see Figure S2C. (E) Percentage of mouse spontaneous alterations in the Y-maze. N is the number of animals; N(WT) = 9; N(KO) = 15. (F) Latency to enter the dark (foot shock) chamber during the inhibitory avoidance task at training and testing (24 hours post-training) periods. *Fibcd1* WT, heterozygous (HET) and KO mice shown. N(WT) = 8; N(HET) = 19; N(KO) = 15. Data is represented as mean and error bars represent SEM. * = $p \leq 0.05$; ** = $p \leq 0.01$; *** = $p \leq 0.001$.

Figure 3

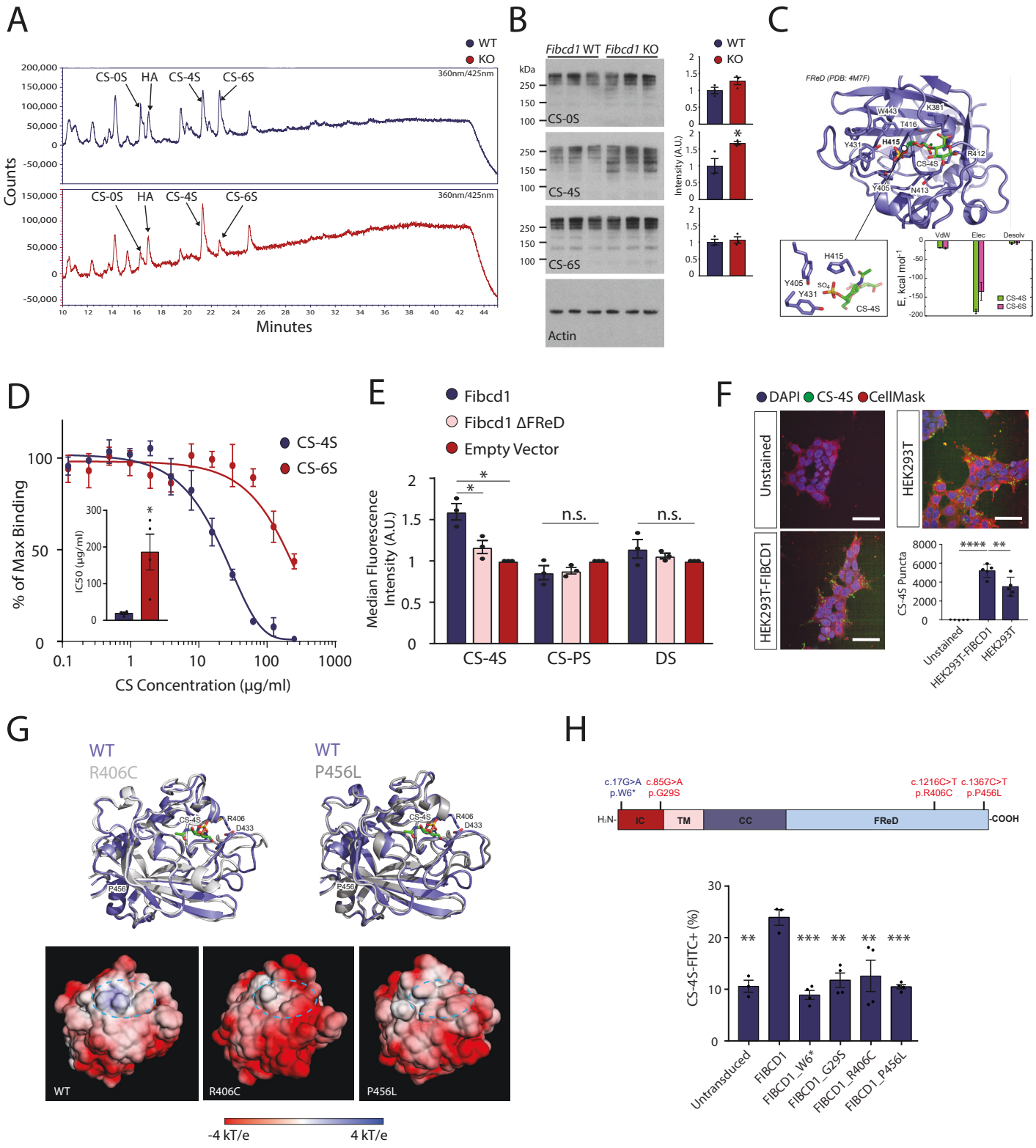
A
WT
KO
CS-0S
HA
CS-4S
CS-6S
360nm/425nm
Counts
Minutes
B
Fibcd1 WT
Fibcd1 KO
kDa
CS-0S
CS-4S
CS-6S
Actin
Intensity (A.U.)
C
FReD (PDB: 4M7F)
W443
K381
T416
Y431
H415
R412
CS-4S
Y405
N413
VdW
Elec
Desolv
E, kcal mol-1
D
CS-4S
CS-6S
% of Max Binding
IC50 (µg/ml)
CS Concentration (µg/ml)
E
Fibcd1
Fibcd1 ΔFReD
Empty Vector
Median Fluorescence Intensity (A.U.)
n.s.
CS-4S
CS-PS
DS
F
DAPI
CS-4S
CellMask
Unstained
HEK293T
HEK293T-FIBCD1
CS-4S Puncta
G
WT
R406C
WT
P456L
CS-4S
R406
D433
P456
WT
R406C
P456L
-4 kT/e
4 kT/e
H
c.17G>A p.W6*
c.85G>A p.G29S
c.1216C>T p.R406C
c.1367C>T p.P456L
H2N-
IC
TM
CC
FReD
-COOH
CS-4S-FITC+ (%)
Untransduced
FIBCD1
FIBCD1_W6*
FIBCD1_G29S
FIBCD1_R406C
FIBCD1_P456L

Figure 3: **FIBCD1 is an endocytic receptor for hippocampal glycosaminoglycans**

(A) HPLC traces (representative of 3 independent experiments) of variously sulphated GAGs (as labelled) in adult *Fibcd1* WT (top, blue) and KO (bottom, red) CA1 pyramidal cell layer hippocampi. Unsulphated CS = CS-0S; hyaluronic acid = HA; 4-O-sulphated CS = CS-4S; 6-O-sulphated CS = CS-6S. (B) Immunoblot analysis (left) and quantification of signal intensity (right) of littermate WT (blue) versus *Fibcd1* KO (red) adult hippocampi with antibodies against CS-0S, CS-4S, CS-6S and actin as a loading control. Each lane represents an independent animal (N = 3). Protein marker sizes are indicated. (C) Top binding pose for *in silico* docking of CS-4S to FIBCD1 FReD (PDB 4M7F). Inset (left) is the orientation of CS-4S within the FReD binding pocket and (right) binding free energy of CS-4S vs CS-6S. Van der Waals (vdW), electrostatic (Elec) and desolvation (Desolv) components of binding free energy charge. (D) Competitive ELISA with increasing concentrations of CS-4S (blue circles) or –6S (red circles) incubated with recombinant FIBCD1 FReD and acetylated BSA. Inset is IC50 concentrations for CS-4S and CS-6S. N is number of biological replicates; N = 4. (E) Flow cytometric analysis of N2a cells expressing full-length mFIBCD1, mFIBCD1ΔFReD or empty vector control incubated with FITC-tagged chondroitin-4-sulfate (CS-4S), poly-sulphated chondroitin sulphate (CS-PS) or dermatan sulphate (DS). N = 3. (F) Internalisation of FITC-tagged CS-4S by FIBCD1-overexpressing HEK293T lines compared to untransduced cells and unstained cells. Left, representative images; right, quantification. Data is plotted as total puncta per condition. Cells are further stained with CellMask (membrane) and Hoechst (nuclei). N = 5. Scale bar = 50µm. (G) Top, superposition ribbon diagrams of the WT FReD domain (dark blue) with R406C (left) and P456L (right) mutants (in grey). The loops surrounding the ligand binding site (389-399 and 423-448) exhibit the largest structural rearrangement in both mutants. Bottom, comparison of the electrostatic potential mapped onto the solvent-accessible surface between WT and the two variant FReDs. (H) Top, depiction of FIBCD1 cDNA and location of patient variants (red) and W6* control (blue). Bottom, flow cytometric analysis of untransduced

HEK293T cells, or expressing constructs with full-length wild-type human FIBCD1, FIBCD1 with the W6* early stop variant as control (FIBCD1_W6*), or the three patient variants (as labelled) incubated with FITC-tagged CS-4S represented as percentage of CS-4S-FITC relative to unstained control. N represents biological replicates ; N = 4. Data are represented as mean and error bars represent SEM. Statistics were calculated by 1-way ANOVA, comparing to the FIBCD1 condition. Data represents the mean and error bars represent SEM. * = $p \leq 0.05$; ** =$p \leq 0.01$; *** =$p \leq 0.001$; **** $p \leq 0.0001$.

Figure 4

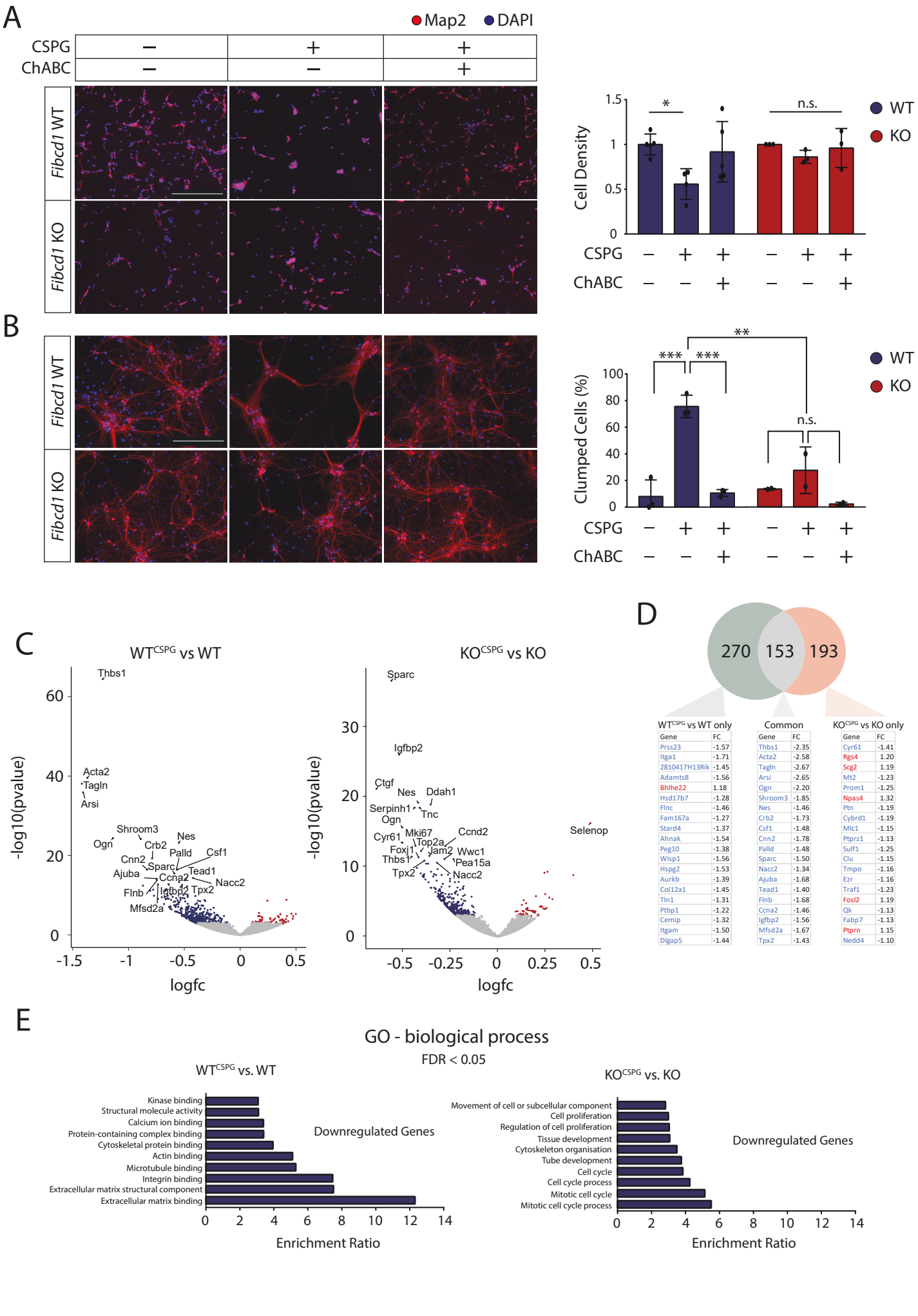

WTCSPG vs WT only		Common		KOCSPG vs KO only	
Gene	FC	Gene	FC	Gene	FC
Prss23	-1.57	Thbs1	-2.35	Cyr61	-1.41
Itga1	-1.71	Acta2	-2.58	Rgs4	1.20
2810417H13Rik	-1.45	Tagln	-2.67	Scg2	1.19
Adamts8	-1.56	Arsi	-2.65	Mt2	-1.23
Bhlhe22	1.18	Ogn	-2.20	Prom1	-1.25
Hsd17b7	-1.28	Shroom3	-1.85	Npas4	1.32
Flnc	-1.46	Nes	-1.46	Ptn	-1.19
Fam167a	-1.27	Crb2	-1.73	Cybrd1	-1.19
Stard4	-1.37	Csf1	-1.48	Mlc1	-1.15
Ahnak	-1.54	Cnn2	-1.78	Ptprz1	-1.13
Peg10	-1.38	Palld	-1.48	Sulf1	-1.25
Wisp1	-1.56	Sparc	-1.50	Clu	-1.15
Hspg2	-1.53	Nacc2	-1.34	Tmpo	-1.16
Aurkb	-1.39	Ajuba	-1.68	Ezr	-1.16
Col12a1	-1.45	Tead1	-1.40	Traf1	-1.23
Tln1	-1.31	Flnb	-1.68	Fosl2	1.19
Ptbp1	-1.22	Ccna2	-1.46	Qk	-1.13
Cemip	-1.32	Igfbp2	-1.56	Fabp7	-1.13
Itgam	-1.50	Mfsd2a	-1.67	Ptprn	1.15
Dlgap5	-1.44	Tpx2	-1.43	Nedd4	-1.10

Figure 4: **FIBCD1 mediates responses of primary hippocampal cultures to CSPGs.**

(A) Left, Representative images of immunofluorescent staining (MAP2, red; DAPI, blue) of primary hippocampal cultures at 2 days *in vitro* (DIV), plated on +/- CSPG coating with and without prior digestion with ChABC, as indicated. Right, quantification of DIV2 images, showing the number of protruding cells per field normalised to untreated condition. N(WT) = 3; N(KO) = 2. (B) Left, representative images of DIV14 neurons, same conditions as in (A). Right, quantification of DIV14 images, representing the percentage of cells per field that are clumped. N represents biological replicates; N(WT) = 3; N(KO) = 2. Scale bar = 250µm. (C) Volcano plots of differential gene expression of transcriptomes at DIV3 hippocampal cultures comparing (left) WT^{CSPG} vs WT and KO^{CSPG} vs KO (FDR < 0.05) (right). Significantly upregulated and downregulated genes are shown in red and blue, respectively. The top 20 DEGs are labelled. (D) Above, Venn diagram of significant DEGs unique to WT^{CSPG} vs WT (green, 270 genes), KO^{CSPG} vs KO (orange, 193 genes) and common between the two (grey, 153 genes). Below, lists of the 20 most significant DEGs and their fold change for each comparison, showing downregulated DEGs in blue and upregulated in red. (E) GO term enrichment analysis for significantly downregulated genes (FDR < 0.05) in (left) WT^{CSPG} vs WT and (right) KO^{CSPG} vs KO. Data are represented as mean and error bars represent SEM. * = p≤0.05; ** =p≤0.01; *** =p≤0.001.

Figure 5

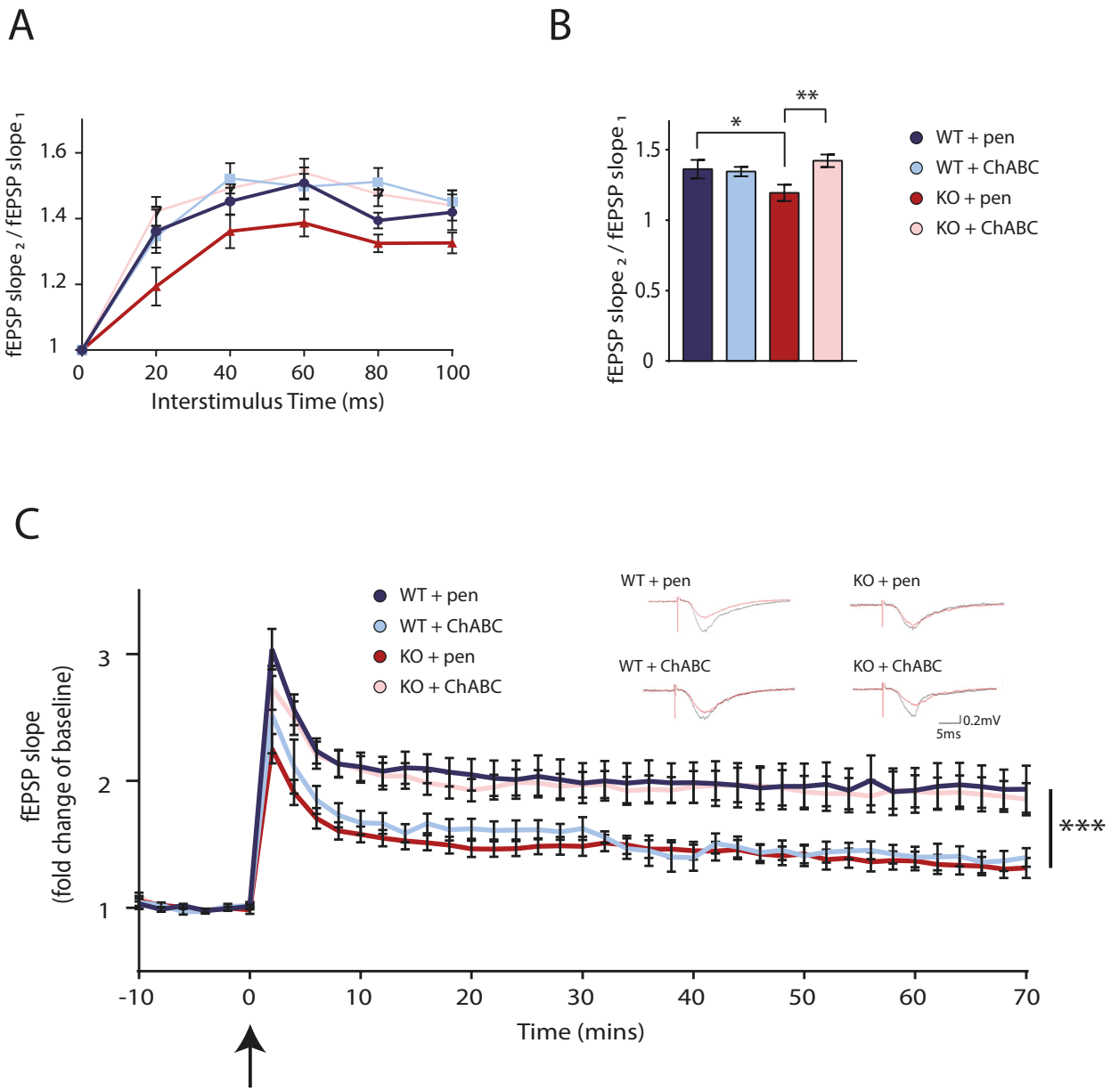
A
fEPSP slope 2 / fEPSP slope 1
1.6
1.4
1.2
1
0
20
40
60
80
100
Interstimulus Time (ms)
B
fEPSP slope 2 / fEPSP slope 1
1.5
1
0.5
0
*
**
WT + pen
WT + ChABC
KO + pen
KO + ChABC
C
fEPSP slope
(fold change of baseline)
3
2
1
WT + pen
WT + ChABC
KO + pen
KO + ChABC
WT + pen
KO + pen
WT + ChABC
KO + ChABC
0.2mV
5ms
***
-10
0
10
20
30
40
50
60
70
Time (mins)

Figure 5: **Impaired synaptic remodelling in FIBCD1-deficient mice is rescued by ChABC treatment**

(A-B) Paired-pulse facilitation in CA3-CA1 Schaffer collateral pathway of acute hippocampal slices from *Fibcd1* WT and KO mice. Pre-treatment with enzymes penicillinase (+pen) or Chondroitinase ABC (+ChABC) as labelled. N (WT+pen) = 17; N (KO+pen) = 20; N (WT+ChABC) = 19; N (KO+ChABC) = 25. (C) Long-term potentiation in CA3-CA1 Schaffer collateral pathways of acute hippocampal slices. Theta burst stimulation (TBS) is at time 0 indicated by the arrow. N (WT+pen) = 9; N (KO+pen) = 15; N (WT+ChABC) = 6; N (KO+ChABC) = 12. Inset are representative traces. Data are represented as mean and error bars represent SEM. * = $p \leq 0.05$; ** = $p \leq 0.01$; *** = $p \leq 0.001$.

Supplemental Figure 1

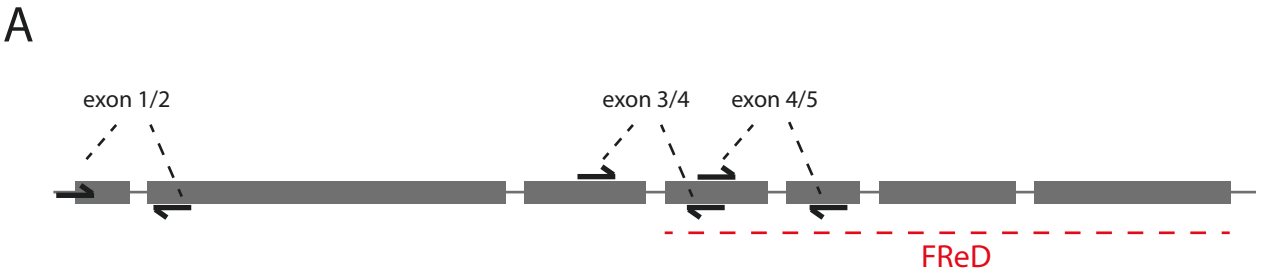

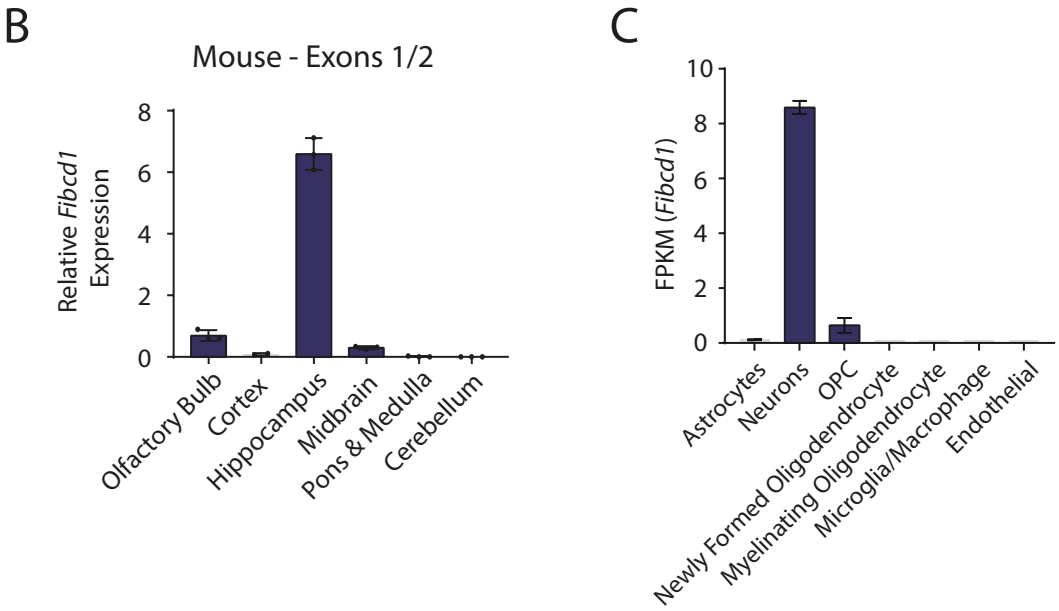

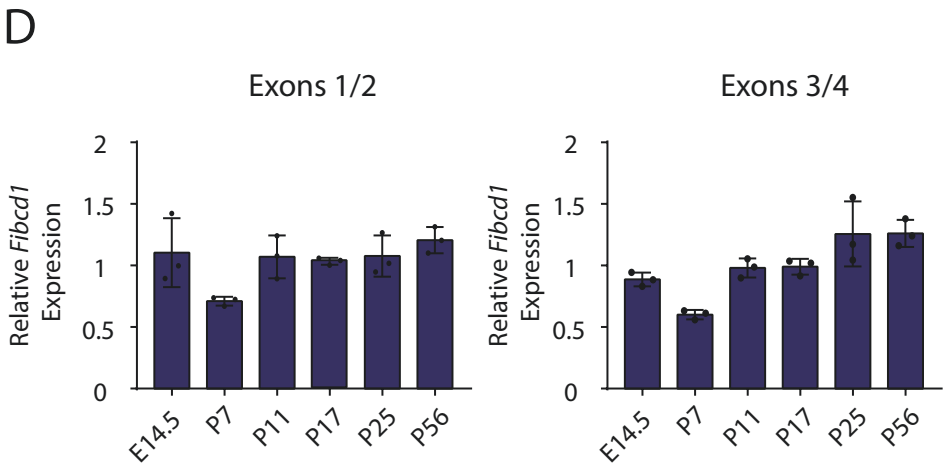

Figure S1: ***Fibcd1*** **expression in the adult and developing mouse brain.**

(A) Schematic of mouse *Fibcd1* exons (grey rectangles) and introns (grey lines), and location of primer pair binding ('exons 1/2, 3/4 and 4/5') used for RT-qPCR. Exon sizes are to scale; introns and primer lengths are not. The exons coding for FIBCD1 FReD is indicated by a red dashed line. (B) Relative mRNA expression levels of mouse *Fibcd1* (primers binding to exon 1 and 2) normalised to *Gapdh* in the indicated brain regions, analysed by RT-qPCR N represents biological replicates; N = 3. (C) *Fibcd1* expression in bulk populations of sorted mouse brain cell population, from *brainrnaseq.org.* OPC = oligodendrocyte precursor cell. (D) Relative mRNA expression levels of mouse *Fibcd1* (primers binding to exon 1 and 2 and exons 3 and 4) normalised to *Gapdh* in the hippocampus of the indicated time points, analysed by RT-qPCR. N = 3. Data are presented as mean and error bars represent SD.

Supplemental Figure 2

A

```
CLUSTAL O(1.2.4) multiple sequence alignment


FRed_DROME      TATRQLPSSCSYSFLS---NHGILKVQLTPESESFYVSCD-----EDWTVILSRTSDDVN    52
FRed_HUMAN      CATGSRPRDCLDVLLSGQQDDGVYSVFPTHYPAGFQVYCDMRTDGGGWTVFQRREDGSVN    60
FRed_MOUSE      CANGSRPRDCLDVLLSGQQDDGVYSIFPTHYPAGFQVYCDMRTDGGGWTVFQRREDGSVN    60
                 *. . * .*   :**   :.*: .:  *    .* * **      .***:  * ...**

FRed_DROME      FERGWLDYRDGFGNLAGDFFIGLNKLHALTSSALHELRIVMEDFSGNVAYAGYSLFAI--    110
FRed_HUMAN      FFRGWDAYRDGFGRLTGEHWLGLKRIHALTTQAAYELHVDLEDFENGTAYARYGSFGVGL    120
FRed_MOUSE      FFRGWEAYREGFGKLTGEHWLGLKRIHALTTQAAYELHVDLEDFDNGTAYAHYGSFGVGL    120
                * ***  **:***.*:*:.::**:::****:.* :**:: :***....*** *. *.:

FRed_DROME      ---GSEKELYPLVLLGKFQDNLTPSAGDSLSYHAGAKFSTVDQDNDNCLECNCALRHKGA    167
FRed_HUMAN      FSVDPEEDGYPLTVA-----DYSGTAGDSLLKHSGMRFTTKDRDSDH-SENNCAAFYRGA    174
FRed_MOUSE      FSVDPEEDGYPLTVA-----DYSGTAGDSLLKHSGMRFTTKDRDSDH-SENNCAAFYRGA    174
                   . *:: ***.:      : : :*****  *:* :*:* *:*.*:  * ***  ::**

FRed_DROME      GWFNNCAKSNLFGEYTTQNQP-GETGIWWDTFSGQ-NSLKRVRWMIRPIS      215
FRed_HUMAN      WWYRNCHTSNLNGQYLRGAHASYADGVEWSSWTGWQYSLKFSEMKIRPVR      224
FRed_MOUSE      WWYRNCHTSNLNGQYLRGAHASYADGVEWSSWTGWQYSLKFSEMKIRPVR      224
                 *:.** .*** *:*    :     *: *.:::*   ***  .  ***:
```

	DROME	HUMAN	MOUSE
DROME	100	41.63	40.19
HUMAN	41.63	100	96.88
MOUSE	40.19	96.88	100

B

RNAi Line	Tub>Gal4 (Fullbody KD)	Nsyb>Gal4 (Neuronal KD)
UAS>CG10359 VDRC^{102670} (Line #1)	Viable	Viable*
UAS>CG10359 VDRC^{4128} (Line #2)	Semi-lethal	Viable*
UAS>CG10359 IR^{BL63703} (Line #3)	Lethal	Viable*

* results in smaller larvae and skewed mendelian ratio

C

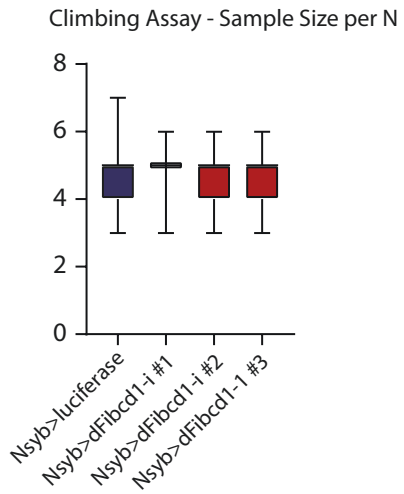

Figure S2: **Description of *dFibcd1*.**

(A) Alignment of human, mouse and fly (DROME) FReD protein sequence. Inset, percent identity matrix (% homology) between Drosophila, human and mouse FReD protein sequences. (B) Summary of 3 RNAi lines crossed to full body GAL4 driver (tubulin) or neuron-specific (Nsyb) and the effects on viability. (C) Number of flies analysed for the climbing assay in Fig 2D. Box plots depict data mean and upper and lower quartile.

Supplemental Figure 3

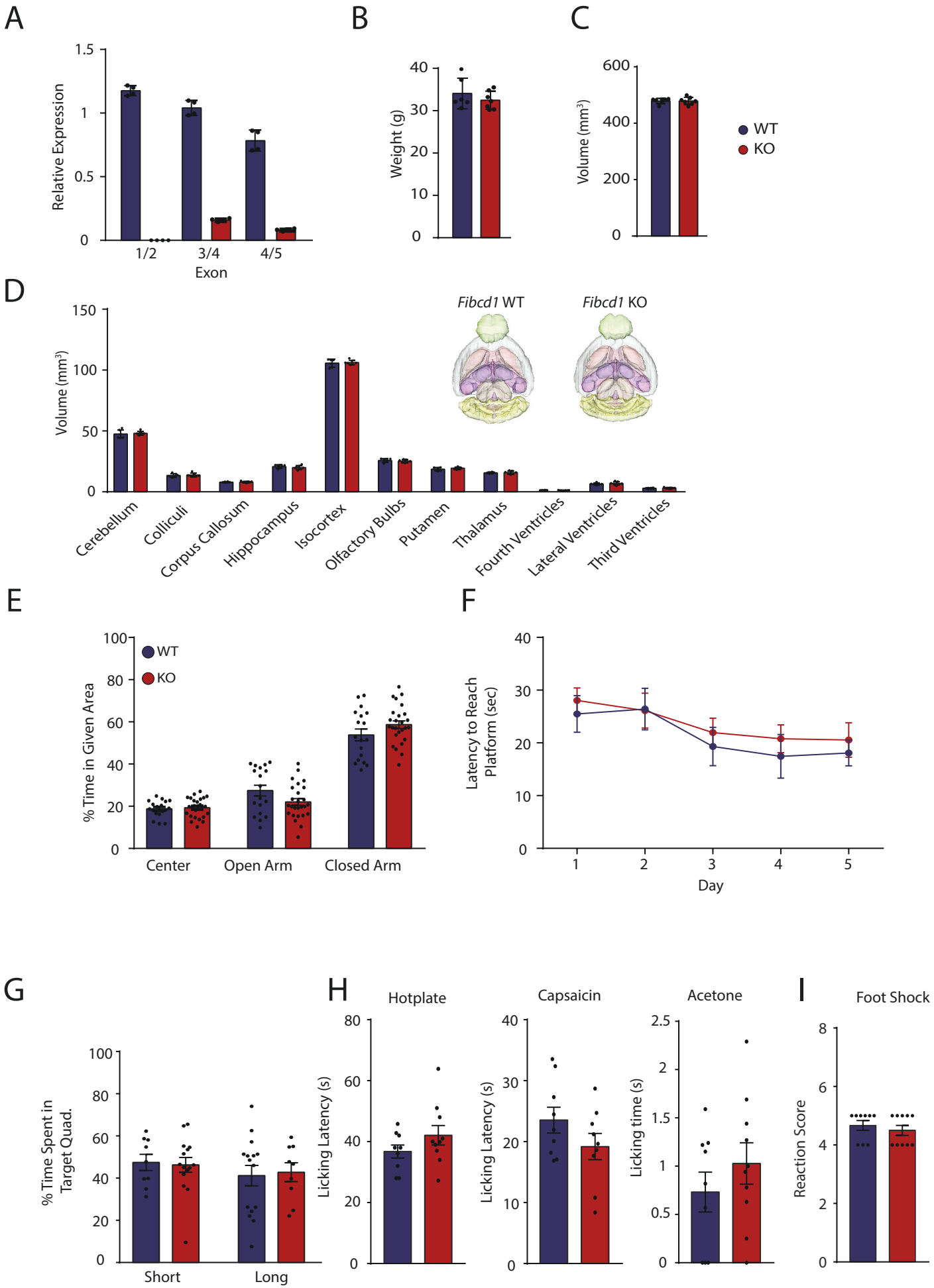

Figure S3: **Phenotyping of FIBCD1-deficient mice**

(A) RT-qPCR of *Fibcd1* WT and KO adult mouse hippocampi using primer pairs binding to indicated exons (see Fig. S1A). N represents individual mice; N = 4. (B-D) Body weight (B), total brain volume (C) and brain volumes of denoted brain regions (D) of the indicated genotypes as assessed by MRI volumetric analysis. N = 5. Inset are 3D representative MRI renditions of control (left) and *Fibcd1* KO (right) adult brains with analysed brain regions pseudo-coloured. Error bars represent SD. (E) Percentage of time mice spent in the centre, open and closed arms of the Elevated Plus Maze (EPM) are shown for *Fibcd1* WT (blue) and KO (red). N = 18 (WT); 27 (KO). (F-G) Mouse performance quantified by time to reach the target platform (F) and time spent in the target quadrant (G), in Morris Water Maze (MWM) hippocampal-dependent spatial learning task over 5 days. N = 5 (WT); 9 (KO). (H) Acute pain responses to hotplate, acetone drop, or intraplantar capsaicin injections, quantified as time to first response or time spent licking or biting the injected paw, respectively. N= 9 (WT); N = 10 (KO). (I) Reaction score to electrical foot shock stimulation. N = 10 (WT); N = 10 (KO). Data are represented as mean and error bars represent SD.

Supplementary Figure 4

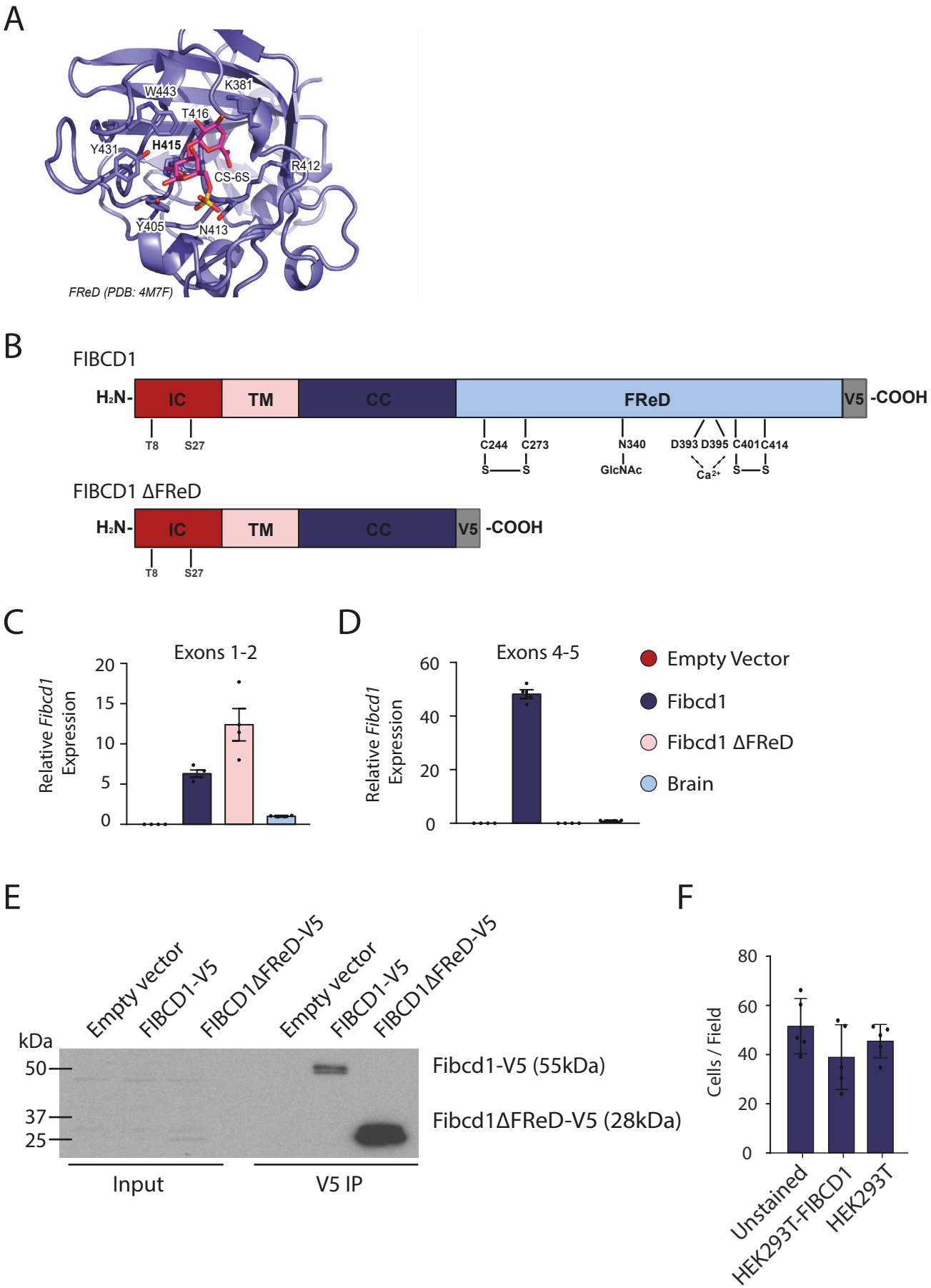

Figure S4: **Docking site of CS-6S in FIBCD1 FReD and validation of mFIBCD1 overexpressing N2a cell lines.**

(A) Top binding pose for *in silico* docking of CS-6S to FIBCD1 FReD (PDB 4M7F). (B) Schematic representation of FIBCD1 domains, IC-intracellular domain (red), TM-transmembrane domain (pink), CC-coiled coil domain (dark blue), FReD (light blue), and location of V5-tag (grey) in full-length mFIBCD1 cDNA and truncated mFIBCD1 lacking the FReD (FIBCD1 ΔFReD). (C) Relative mRNA expression levels of *Fibcd1* in the N2a cells overexpressing full-length (*Fibcd1*) or truncated *FIBCD1* (*Fibcd1 ΔFReD*) and adult mouse WT brain for comparison, analysed by RT-qPCR. N represents biological replicates N = 2. Primers binding to exon 1 and 2 before the FReD domain (B) or to exon 4 and 5 spanning the sequence encoding part of the FReD. Note the complete absence of endogenous *Fibcd1* expression in the 'empty vector' (red bar) control and the complete absence of expression when using primers against exon 4/5 (D), which span the FReD (see Figure S1A) in the *Fibcd1* ΔFReD construct (C, pink bar), validating the generated cell lines. *Gapdh* was used as housekeeping control and values obtained from a control brain sample were set to 1. (E) Validation of transgenic N2a cell line at the protein level by immunoprecipitation with anti-V5 antibody as bait. Input (left) and V5-immunoprecipitated (right) lysates from N2a cells expressing V5-tagged full-length mFIBCD1 (mFIBCD1-V5, predicted size of 55kDa), V5-tagged mFIBCD1 lacking the FReD (V5-FIBCD1 ΔFReD, predicted size of 28kDa) or the empty vector as negative control. Protein marker sizes are indicated. (F) Number of HEK293T cells per field during the CS-4S internalisation experiments, linked to Fig. 3F. N = 5. Data are plotted as mean and error bars represent SD.

Supplementary Figure 5

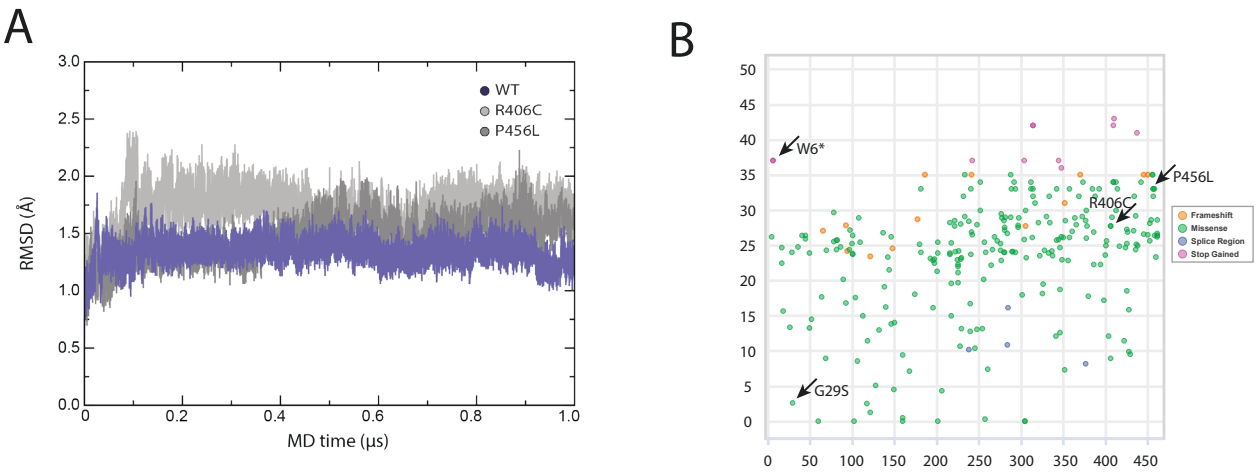

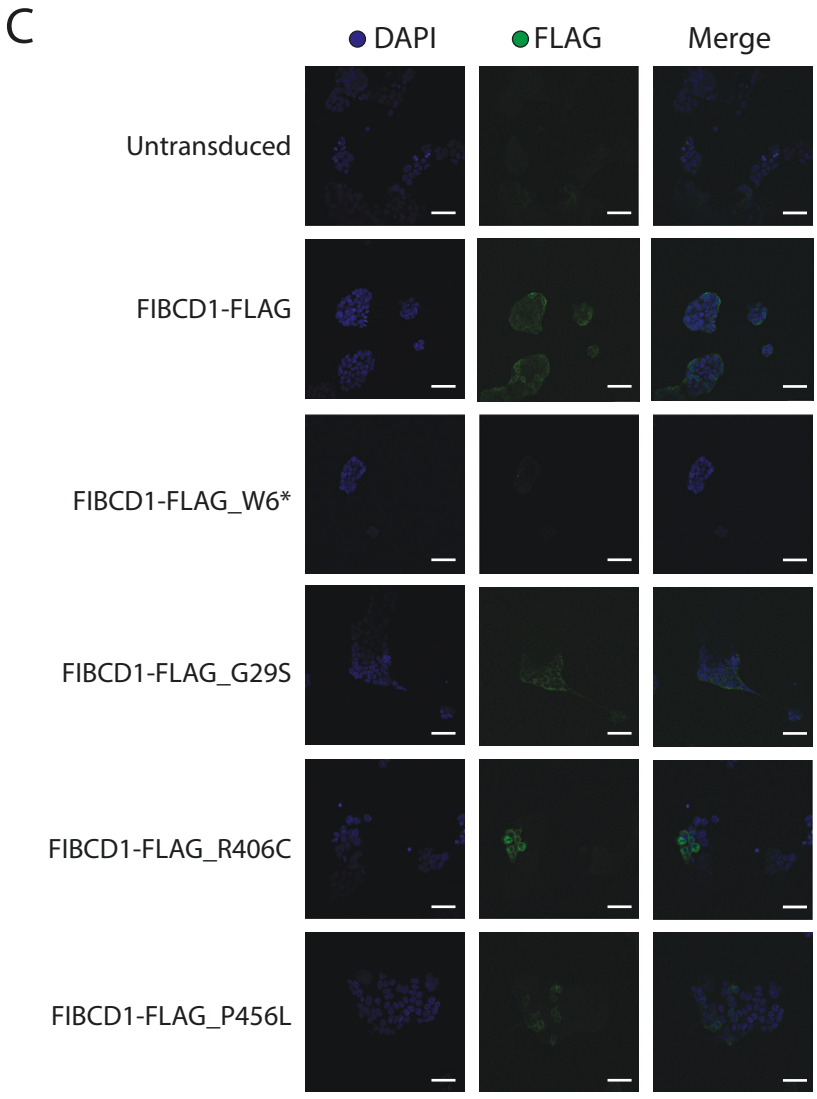

Figure S5: Additional human FIBCD1 data.

(A) Time course of the backbone RMSD from the starting configuration for WT (blue), R406C (pink) and P456L (red) MD simulations. (B) Missense, frameshift, splice region and stop gain variants extrapolated from gnomAD present in the population, colour code is indicated in the figure. Each dot represents one distinct variant, amino acid position and CADD score indicated on x and y axis. Indicated with arrows are the variants discussed in the present study. (C) Validation of FLAG-FIBCD1 expression in stably expressing HEK293T cells by immunofluorescence. Note the absence of signal in untransduced cells and cells expressing truncated (W6*) FIBCD1. Shown is DAPI (blue), anti-FLAG (green) and merge. Scale bar = 50um.

Supplementary Figure 6

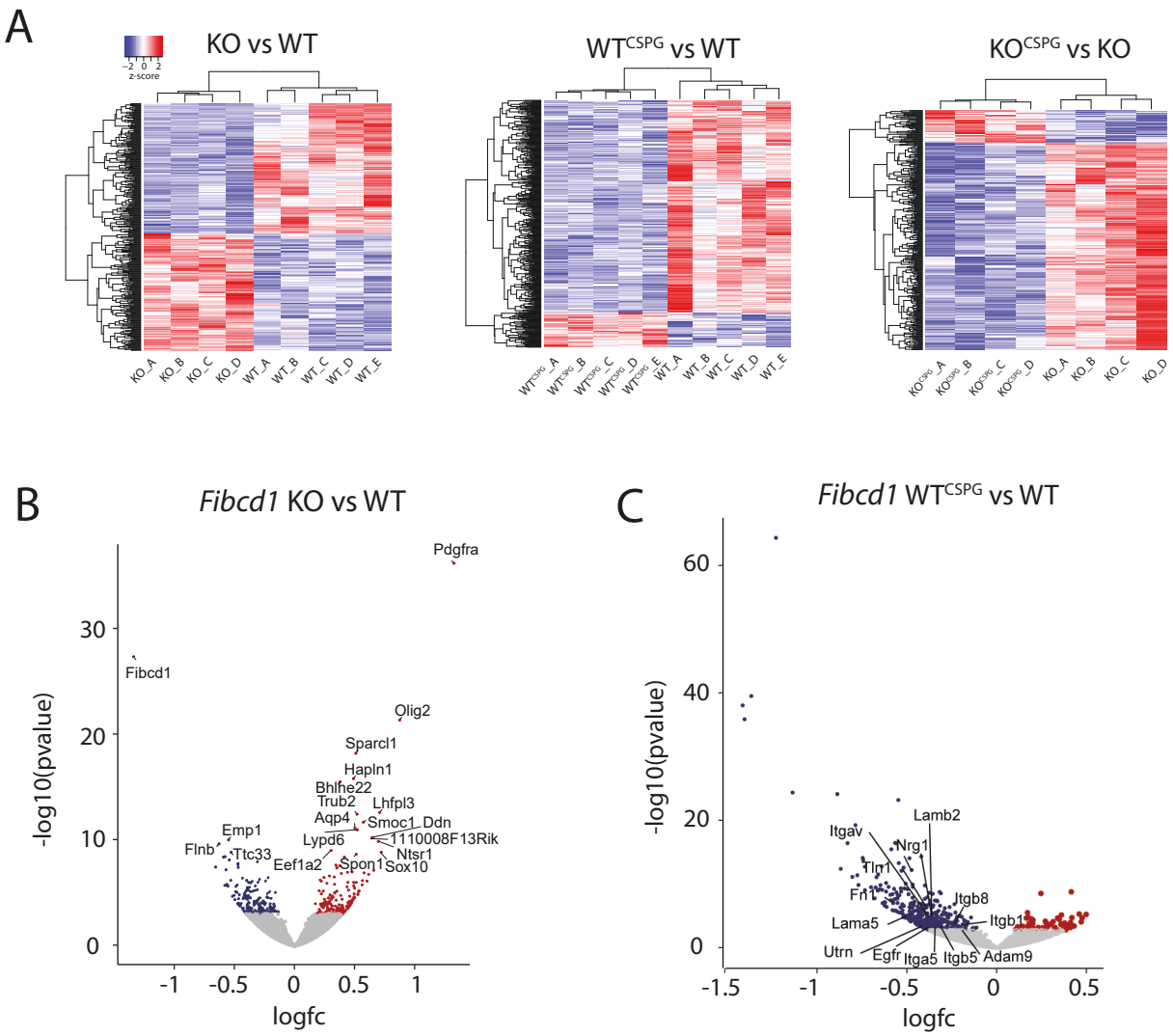

Figure S6: **Additional RNA-seq analysis**

(A) z-score hierarchical clustering for each sample in *Fibcd1* KO vs WT, WT^{CSPG} vs WT and KO^{CSPG} vs KO. Colours represent scaled expression values, with blue for low and red for high expression levels. Legend is indicated. (B) Volcano plot depicting DEGs at DIV2 hippocampal cultures, comparing *Fibcd1* KO vs WT, showing significantly upregulated (red) and downregulated (blue) genes. Top 20 DEGs are labelled. (C) Volcano plot depicting DEGs at DIV2 hippocampal cultures comparing WT^{CSPG} vs WT, all genes that fall into "integrin binding" GO term category are labelled.

Supplementary Figure 7

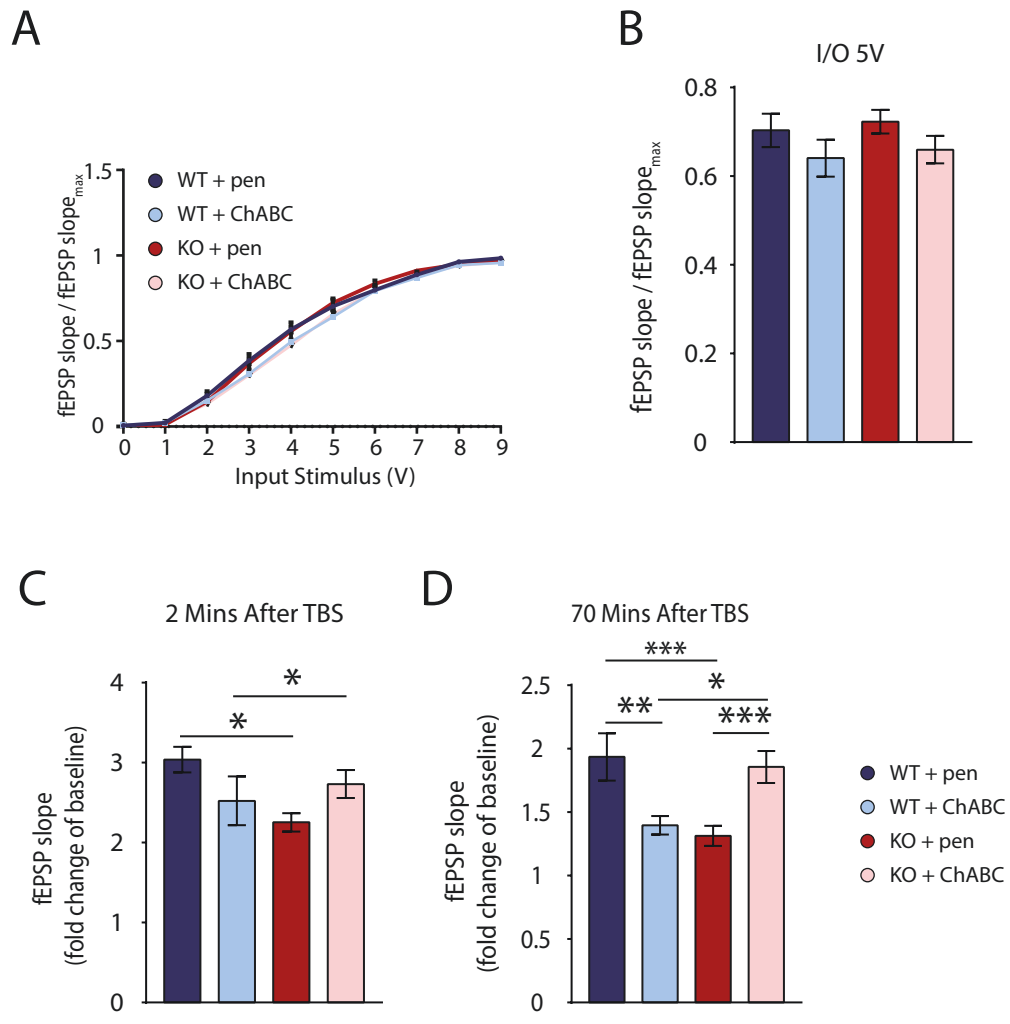

Figure S7: **Additional electrophysiological assessment of mouse hippocampal slices**

(A-B) Input/output assessment of synaptic transmission in CA3-CA1 Schaffer collateral pathway of adult mouse hippocampal slices. *Fibcd1* WT (blue) and KO (red) hippocampal slices, pre-treated with penicillinase (pen) or Chondroitinase ABC (ChABC). N (WT+pen) = 22; N (KO+pen) = 27; N (WT+ChABC) = 21; N (KO+ChABC) = 30. (C-D) LTP fold change of baseline at 2 (C) and 70 (D) minutes post theta-burst stimulation (TBS) in adult mouse hippocampal slices. N (WT+pen) = 9; N (KO+pen) = 15; N (WT+ChABC) = 6; N (KO+ChABC) = 12. * = $p \leq 0.05$; ** = $p \leq 0.01$; *** = $p \leq 0.001$. Data are plotted as mean and error bars represent SEM.

4. Discussion

FIBCD1 state of the art

FIBCD1 is a poorly studied protein. To date, searching for the keyword "FIBCD1" in PubMed returns 14 results, the vast majority of which relate to a function of FIBCD1 in binding fungal moieties. FIBCD1 was first identified as a cDNA clone of unknown function and high sequence homology to L- and M-type ficolins, which are secreted, lectin-type pattern recognition receptors of the innate immune system (Schlosser *et al*, 2009). Schlosser and colleagues demonstrated that FIBCD1 assembles into homotetrameric structures and, when overexpressed in human cell lines, localises to the cell membrane. Next, the authors raised antibodies against FIBCD1's ectodomain and performed a series of immunohistochemical stains in various human tissues and demonstrated FIBCD1 expression in the brush borders of the duodenum and colon as well as the ducts of the salivary glands. A later paper from the same research group demonstrated *FIBCD1* expression also in the brain, trachea, small intestine, spleen, testis, placenta and in the lung mucosal membrane, particularly after fungal infection (Jepsen *et al*, 2018). Schlosser and colleagues purified recombinant FIBCD1 by affinity chromatography using an acetate-coated matrix, followed by ELISA experiments which showed FIBCD1 binding to structures containing acetyl groups (such as acetylcholine and acetylated BSA). This was consistent with FIBCD1's high homology to ficolins, which are also acetyl group-binding proteins. Hypothesising FIBCD1 to function in the innate immune system's recognition of pathogen associated molecular patterns (PAMPs), FIBCD1's binding to a number of PAMPs such as chitin, lipopolysaccharide (LPS) and peptidoglycan was assessed. FIBCD1 was shown to bind with high affinity to chitin but no other tested PAMP, leading the authors to hypothesise that FIBCD1 is an innate immune receptor for fungi. Finally, using radio- and fluorescently tagged acetylated BSA, FIBCD1 was shown to mediate the endocytosis of acetylated structures. The secretion of the radiolabel into the culture supernatant after endocytosis suggested that structures internalised by FIBCD1 were degraded within the cell, potentially in the lysosome.

Although Schlosser and colleagues demonstrated a chitin-binding function of FIBCD1, expression in the duodenum and colon, concluding FIBCD1 to be an innate immune system receptor for fungi, the *in vivo* function of FIBCD1 remained to be investigated. Based on its chitin binding function and high homology to ficolins, it was hypothesised that FIBCD1 mediates responses of the immune system to fungal infection and/or functions at the interface of epithelial borders and endogenous fungal species. To investigate this, Moeller and colleagues generated a transgenic FIBCD1 mouse ($FIBCD1^{Tg}$) with overexpression driven in intestinal tissues under the *Villin* promoter (Moeller *et al*, 2019). The transgenic mice had no obvious differences from WT littermates. The authors first

used a model of intestinal helminth infection by feeding the mice with chitin-containing embryonated *Trichuris muris* eggs, a widely used model for such infections. While FIBCD1 was shown to bind to the *T.muris* eggs, there was no difference between the FIBCD1^{Tg} mice and wild type littermates in protective type 2 immune responses or clearance of the fungal infection. However, sequencing of baseline (i.e. non-infected) gut microbiome revealed changes in the composition of fungal species in the FIBCD1^{Tg} gut compared to WT littermates. In particular, a reduction in the population of the *Candida* genus and increase in *Phoma* genus was noted in the FIBCD1^{Tg} mice. No changes in bacteria species were observed. Finally, the authors demonstrated that FIBCD1^{Tg} exhibited slowed fungal re-colonisation after depletion and reduced intestinal inflammation, concluding FIBCD1 to be a previously unknown microbial pattern recognition receptor (Moeller *et al*, 2019). A follow up study indicated a role of FIBCD1 in regulating lung immune responses to the mould *Aspergillus fumigatus* (Bhattacharya *et al*, 2021). The authors demonstrated immune-compromised FIBCD1 KO mice to be more resistant to invasive pulmonary aspergillosis, as shown by reduced morbidity, mortality and fungal burden. The underlying mechanisms remain not understood.

Before our study, the only indication of an endogenous binding ligand of FIBCD1 was published in 2014 (Shrive *et al*, 2014), that reported the crystal structure of FIBCD1's extracellular, ligand-binding fibrinogen-recognition domain (FReD) in native and ligand-bound conformations. While the paper largely focussed on examining FIBCD1's binding to N-acetylmannosamine (ManNAc), the study identified potential binding sites for sulphated, acetylated ligands such as glycosaminoglycans (Shrive *et al*, 2014).

The remaining studies thus far of FIBCD1 biology relate to cancer. In primary patient samples, overexpression of FIBCD1 was shown to correlate with poor prognosis in gastric cancer (Jiang *et al*, 2018) and hepatocellular carcinoma (Wang *et al*, 2020). While it's unclear if these changes in FIBCD1 expression are causative or merely correlative, genes that modulate the extracellular matrix have been well studied in the context of cancer. Particularly, those that increase a cancerous cell's motility through the matrix, thus facilitating metastasis. While interesting, the link between FIBCD1 and cancer biology remain tenuous and further studies are needed to determine a causative role of FIBCD1 in gastric cancer, hepatocellular carcinoma, or other.

Molecular pathology of FIBCD1-deficiency

In the present study, we have provided evidence for a role of FIBCD1 in the CNS and an association of FIBCD1 loss of function variants to a severe NDD in 2 unrelated patients. While mutations in the synthesis of GAGs and CSPGs have been previously associated to NDDs (e.g. (de Vrij *et al*, 2019)) we believe the present study is the first report of mutations in a receptor for GAGs or CSPGs associated to

human disease. Using animal models, we have noted some pathologies associated to FIBCD1-deficiency that each could be contributing to disease symptoms.

The patients presented with symptoms of severe NDD. Patient 1, a 12 year old boy, was diagnosed by his clinician with severe ASD, attention deficit hyperactivity disorder (ADHD) and anxiety. While sitting and walking milestones were reached normally, he remains nonverbal. Additionally, he was noted as possessing some craniofacial dysmorphias, namely, a triangular shaped head, hypertelorism, almond-shaped eyes, posteriorly rotated and low set ears and epicanthal folds. The dysmorphias are significant as they indicate the patient's NDD to be of genetic rather than environmental cause. Additional clinical diagnoses include recurrent allergic rhinitis and sinusitis. Whole exome sequencing and filtering revealed biallelic variants of unknown significance in *FIBCD1*. Patient 2, a 3 year old girl, was diagnosed with severe NDD and exhibited delayed social and cognitive abilities. Sitting and walking milestones were delayed and she is also nonverbal. She was noted to be microcephalic, to have micrognathia and low set ears. Radiological findings included a thickened cortex, bilateral enlarged frontal gyri, ventriculomegaly and associated decrease in the white matter volume. Finally, she had a patent ductus arteriosus that resolved after 6 months and recurrent pneumonias. Whole exome sequencing, filtering and follow up analysis revealed homozygous variants of unknown significance in *FIBCD1*, *UNC13B* and *RIC1* due to an inheritance of uniparental disomy of chromosome 9 with mosaicism. RIC1 has been reported to cause CATIFA syndrome, with a distinctive correlation of craniofacial dysmorphias such as cleft lip, cataract, tooth eruption abnormalities and facial dysmorphias, which our patient does not have. Similarly, *UNC13B* has been described to cause focal epilepsy, again not found in our patient.

We examined the expression of FIBCD1 in a number of human and mouse tissues. The expression data from the two species was largely in agreement. In the brain, the highest expressing region was the hippocampus which, in the mouse, was largely restricted to the hippocampal stratum pyramidale layer, where the cell bodies of hippocampal pyramidal neurons are located. Additionally, we showed that FIBCD1 is expressed in the hippocampus throughout development, starting at E14.5 into adulthood. The continued expression of FIBCD1 throughout development suggests that lack of FIBCD1 could manifest in developmental abnormalities. The identification of young NDD patients and the brain structural abnormalities noted in P2 are consistent with this hypothesis, as well as the fact that KO of dFibcd1 in *D.melanogaster* is lethal. However, there were no obvious differences in the gross architectures of the KO mice compared to WT littermates suggesting that the mouse brain developed normally even without FIBCD1 expression. Further, the fact that the KO mouse electrophysiological phenotypes observed in the Schaffer-collateral pathway could be fully rescued

suggests that the tracts developed normally. These differences could suggest a slight divergence in FIBCD1 function between the species.

We have developed a cell-based assay to assess the function of FIBCD1 by incubating overexpressing human cells with FITC-tagged chondroitin sulphate (CS). We have used flow cytometry to assess association of the cells to the tagged CS or microscopy to image internalisation. We have determined that the three patient variants identified (c. G29S; c. R406C; c. P456L) as well as a control (c. T6*) reduced the percentage of cells associating to tagged CS compared to cells expressing full length WT FIBCD1 cDNA. Using the crystal structure of FIBCD1's FReD (Shrive *et al*, 2014), we modelled the effects of the two variants present in the FReD (c. R406C and c. P456L) on protein folding. These variants did not have dramatic effects on the predicted folding of the FReD. However, we showed that the surface electrostatic charge of the FReD to be altered by these two variants. In particular, the highly positively charged CS binding pocket (where the negatively charged CS docks) was determined to be abrogated. Therefore, we conclude that the c.R406C and c.P456L variants result in FIBCD1 loss of function by disturbing the charge of the binding pocket and abrogating FIBCD1:CS associations. We were unable to model the c. G29S variant as the crystal structure for the remaining FIBCD1 domains has not been published. Therefore we do not know why this variant is loss of function. Residue 29 is located within the intracellular domain of FIBCD1 which has been previously hypothesised to participate in intracellular signalling. Further, amino acid 29 is close to a predicted phosphorylation site on FIBCD1 (residue 27 (Schlosser *et al*, 2009)). Therefore, it could be that the c.G29S variant interferes with intracellular signalling functions of FIBCD1 or, potentially, localisation or folding of FIBCD1 proteins within the cell.

We have shown increased levels of CS-C in the KO mouse hippocampus compared to WT littermates. Considering the high expression of FIBCD1 in the hippocampus and the endocytic function of FIBCD1, we hypothesise that the role of FIBCD1 is to facilitate the endocytosis of CS-C in the hippocampus for lysosomal degradation. Thus absence of FIBCD1 expression in the KO mouse leads to accumulation of CS-C over time. In support of this, we were able to rescue observed deficits in synaptic remodelling in acute hippocampal slices by exogenous application of the enzyme Chondroitinase ABC (ChABC), which digests GAG chains. However, ChABC targets many GAG species and not only CS-C. Additionally, it seems improbable that the ChABC treatment would have restored CS-C levels in the KO back to baseline. Therefore, while the increased levels of CS-C in the KO hippocampus could well be contributing to the pathology of FIBCD1-deficiency, the data remains inconclusive and requires further study.

We have presented evidence of a previously unknown (but hypothesised) signalling function of FIBCD1 upon interaction with its ligand. We assessed transcriptomic changes in primary mouse

hippocampal neurons after plating on CSPGs and noted a number of differentially expressed genes (DEGs) relating to extracellular matrix synthesis and binding. Additionally, we noted a number of DEGs relating to integrin biology. In neurons, integrins function in the maturation of synapses as well as short- and long-term synaptic remodelling. During development, integrins regulate migration and differentiation of neural stem cells and pathfinding of outgrowing neurites. While our data indicates only a degree of co-expression between FIBCD1 and integrins, one can only speculate as to whether there is a direct or indirect interaction between the two signalling proteins that is perturbed upon FIBCD1 loss of function.

The patients described here with FIBCD1-deficiency have been diagnosed with ASD and severe NDD. ASD has been previously linked to ECM dysregulation in studies of post-mortem tissues of individuals with ASD that were shown to have reduced levels of heparan sulphate (HS) in the subventricular zones (Pearson *et al*, 2013), which was corroborated in the BTBR mouse model of ASD (Meyza *et al*, 2012). Further alterations in urinary GAG levels have been noted in samples from ASD patients (Endreffy *et al*, 2016), although the reason for elevated urinary GAGs are unknown. To test if this was the case in our cohort, we collected urine samples from P1 in three consecutive days and compared urinary GAGs by tandem mass-spectrometry but found no difference in urinary GAG levels for specifically sulphated GAGs compared to 3 healthy controls (data not shown).

We report in the FIBCD1 KO mouse elevated levels of CS-A in the hippocampus, which could be due to the absence of FIBCD1's endocytic activity. This would suggest part of the pathology of FIBCD1-deficiency to be the accumulation of CS-A over time. We explored whether FIBCD1-deficiency resembled other diseases associated with GAG accumulation. Mucopolysaccharidoses (MPS) are a class of lysosomal storage disorders caused by mutations in catabolic enzymes. Morquio syndrome (MPS IV) type B is caused by accumulations of CS-A, however, patients with this disorder usually do not have any CNS involvement. Indeed, Morquio patients typically exhibit skeletal developmental defects, delayed growth and scoliosis, none of which have been reported in our patient cohort. Finally, a clinical test for MPS is elevated urinary GAG levels which, as mentioned, we did not find in one of our patients. In conclusion, it appears FIBCD1-deficiency does not resemble other diseases relating to ECM dysregulation. However our cohort size is only 2 patients, more are needed to make an accurate comparison.

Outlook and future directions

Although we have identified FIBCD1 as a novel gene involved in neural biology, there remain some questions as to the exact function of FIBCD1 and the mechanism by which it acts. The following section

will tackle key outstanding questions, potential avenues for future research into FIBCD1 biology and any limitations of the study that have not already been discussed.

All evidence indicates that FIBCD1 resides in the cellular membrane and associates with GAGs, particularly CS-C, facilitating internalisation. The developmental phenotypes observed in humans suggests a need for FIBCD1:GAG interactions (or a yet unknown function of FIBCD1) during early developmental stages, perhaps as a trigger for important intracellular signalling mechanisms. We have attempted to decipher such signalling mechanisms by transcriptome analysis of WT and KO primary neurons plated on CSPGs, identifying integrins as a potential direct or indirect signalling partner of FIBCD1. However, a key limitation of this experiment is that the FIBCD1 KO mice do not model the developmental disruptions observed in the humans, which could be because of a divergence in function between the two species. Transcriptome analysis of primary mouse neurons is therefore unlikely to provide insights into the human-specific aspects of FIBCD1 developmental signalling. To address this, one could generate iPSCs derived from patient somatic cells (e.g. fibroblasts), differentiate into neurons, and assess transcriptome or proteome changes upon stimulation of FIBCD1 with GAGs or CSPGs. Alternatively, since primary patient cells have thus far been impossible to obtain, one could also knock out FIBCD1 in stem cells before differentiation. In the lab, we have successfully generated FIBCD1 KO ESCs which we differentiated and attempted to stimulate with CSPGs, in a similar experimental setup as with the primary mouse neurons. However, we have so far found that the cells are intolerant to plating on CSPG coatings (data not shown), preventing any further analysis.

Previous work has suggested interactions between lectins and integrins in neuronal and non-neuronal contexts. For example, microglial phagocytosis of apoptotic cerebellar granule neurons by microglia was blocked by the addition of RGD peptides (integrin binders) or carbohydrates targeting lectins, suggesting integrins and lectins to both be important for microglial recognition of apoptotic neurons (Witting *et al*, 2000). The lectin L-14 has been shown to directly bind integrins and regulate skeletal muscle differentiation (Gu *et al*, 1994). Interestingly, studies into lectin-based snake venoms have found their mechanism of action is direct integrin binding of the target host cell and have since been repurposed as potent inhibitors of integrins of different subunit composition (Marcinkiewicz *et al*, 2000; Sarray *et al*, 2007). To investigate if FIBCD1 and neuronally expressed integrins interact, one could express and purify the FReD of recombinant FIBCD1, as done previously (Schlosser *et al*, 2009), immobilise it, and pull down extra- and intracellular proteins followed by Western blot or mass spectrometry to determine potential binding partners. For more indirect interaction, one could stimulate or inhibit different integrins (e.g. by activating or blocking antibodies (Tan *et al*, 2011; Fernandez-Valle *et al*, 1994)) in primary neurons plated with and without CSPGs (i.e. with and without FIBCD1 stimulation) and assess for rescue by morphology. An alternative would be genetic knock-down

or activation of integrins. Additionally, the downstream signalling pathways of integrin signalling are fairly well defined, involving phosphorylation of focal adhesion kinase (FAK) and SRC and converging on Rho GTPases RhoA, CDC42 and RAC1 (Dityatev *et al*, 2010), leading to integrin-regulated phenotypes such as axonal outgrowth. Were FIBCD1 and integrin signalling pathways to converge, one could assess the phosphorylation statuses of the aforementioned proteins upon stimulation of FIBCD1 signalling. Further experiments are needed to assess how well the KO mice model the patient phenotypes. P1 was diagnosed with severe ASD; P2 with severe NDD but with autistic-like symptoms (e.g. non-verbal). Autistic phenotyping in the mice could be performed. For example, reduced vocalisations in the KO mice would model the non-verbal status of both of our patients. Another test for social interactions (e.g. 3-chambers social interaction test) with known and stranger mice could be done to assess for autistic-like phenotypes in the KO mice.

As previously discussed, the increased CS-A observed in the KO hippocampus and rescue of synaptic remodelling phenotypes by ChABC digestion suggests that the accumulation of CS-A is inhibitory to remodelling and may contribute to the pathologies of FIBCD1-deficiency. To substantiate this further, one could attempt to rescue the observed learning behaviour deficiencies (spontaneous alterations, fear conditioning) by stereotaxic injection of ChABC into the hippocampi of KO mice. Rescue of the behavioural deficiencies would be consistent with the rescue of pre-pulse inhibition and long-term potentiation observed in the acute hippocampal slices and a stronger indication that accumulation of CS-A contributes to learning dysfunction. However, a key technical challenge of this experiment is the fact that destruction of the ECM by ChABC can abrogate learning phenotypes in mice. This is reflected in our electrophysiology data – slices from WT mice treated with ChABC had abrogated long-term potentiation. There's likely a narrow window of injected ChABC dosage for this experiment to be successful, making this a technically challenging experiment.

Concluding remarks

Neurodevelopmental disorders are a diverse and complex range of diseases. Severe congenital NDDs are rare but provide insight into the complex nature of the human CNS as they give insight into non-redundant mechanisms of neural development. We have leveraged NGS technologies and follow-up experimental work in cellular and organismal models to identify loss of function variants in a gene not previously known to function in the CNS associated to a complex NDD. We have begun to understand the mechanisms by which FIBCD1 acts, namely, by associating primarily with 4-O-sulphated CSs of the brain extracellular matrix. However, there remain some outstanding questions as to downstream mechanisms through with FIBCD1 acts in the CNS. We believe that our work has not only provided

insight into the pathologies of two patients previously lacking a diagnosis, but also helped to understand the basic workings of the nervous system during development and adult life.

REFERENCES

Adams RH, Betz H & Püschel AW (1996) A novel class of murine semaphorins with homology to thrombospondin is differentially expressed during early embryogenesis. *Mechanisms of Development* 57: 33–45

Aisen PS, Saumier D, Briand R, Laurin J, Gervais F, Tremblay P & Garceau D (2006) A Phase II study targeting amyloid-β with 3APS in mild-to-moderate Alzheimer disease. *Neurology* 67: 1757–1763

Alilain WJ, Horn KP, Hu H, Dick TE & Silver J (2011) Functional regeneration of respiratory pathways after spinal cord injury. *Nature* 475: 196–200

Aono S, Keino H, Ono T, Yasuda Y, Tokita Y, Matsui F, Taniguchi M, Sonta SI & Oohira A (2000) Genomic organization and expression pattern of mouse neuroglycan C in the cerebellar development. *Journal of Biological Chemistry* 275: 337–342

Bagnard D, Lohrum M, Uziel D, Püschel AW & Bolz J (1998) Semaphorins act as attractive and repulsive guidance signals during the development of cortical projections. *Development* 125: 5043–5053

Baig S, Wilcock GK & Love S (2005) Loss of perineuronal net N-acetylgalactosamine in Alzheimer's disease. *Acta Neuropathologica* 110: 393–401

Bernard C & Prochiantz A (2016) Otx2-PNN Interaction to Regulate Cortical Plasticity. *Neural Plasticity* 2016 doi:10.1155/2016/7931693 [PREPRINT]

Beurdeley M, Spatazza J, Lee HHC, Sugiyama S, Bernard C, di Nardo AA, Hensch TK & Prochiantz A (2012) Otx2 binding to perineuronal nets persistently regulates plasticity in the mature visual cortex. *Journal of Neuroscience* 32: 9429–9437

Bhattacharya S, Amarsaikhan N, Maupin AJ, Schlosser A, Füchtbauer E-M, Holmskov U, Moeller JB & Templeton SP (2021) FIBCD1 Deficiency Decreases Disease Severity in a Murine Model of Invasive Pulmonary Aspergillosis. *ImmunoHorizons* 5: 983–993

Bicknese AR, Sheppard AM, O'Leary DDM & Pearlman AL (1994) Thalamocortical axons extend along a chondroitin sulfate proteoglycan- enriched pathway coincident with the neocortical subplate and distinct from the efferent path. *Journal of Neuroscience* 14: 3500–3510

Bouzioukh F, Daoudal G, Falk J, Debanne D, Rougon G & Castellani V (2006) Semaphorin3A regulates synaptic function of differentiated hippocampal neurons. *European Journal of Neuroscience* 23: 2247–2254

Bradbury EJ & Burnside ER (2019) Moving beyond the glial scar for spinal cord repair. *Nature Communications* 10: 1–15 doi:10.1038/s41467-019-11707-7 [PREPRINT]

Bradbury EJ, Moon LDF, Popat RJ, King VR, Bennett GS, Patel PN, Fawcett JW & McMahon SB (2002) Chondroitinase ABC promotes functional recovery after spinal cord injury. *Nature* 416: 636–640

Brückner G, Hausen D, Härtig W, Drlicek M, Arendt T & Brauer K (1999) Cortical areas abundant in extracellular matrix chondroitin sulphate proteoglycans are less affected by cytoskeletal changes in Alzheimer's disease. *Neuroscience* 92: 791–805

Bukalo O, Schachner M & Dityatev A (2001) Modification of extracellular matrix by enzymatic removal of chondroitin sulfate and by lack of tenascin-R differentially affects several forms of synaptic plasticity in the hippocampus. *Neuroscience* 104: 359–369

Carulli D, Pizzorusso T, Kwok JCF, Putignano E, Poli A, Forostyak S, Andrews MR, Deepa SS, Glant TT & Fawcett JW (2010) Animals lacking link protein have attenuated perineuronal nets and persistent plasticity. *Brain* 133: 2331–2347

Chahrour M & Zoghbi HY (2007) The Story of Rett Syndrome: From Clinic to Neurobiology. *Neuron* 56: 422–437 doi:10.1016/j.neuron.2007.10.001

Clement AM, Nadanaka S, Masayama K, Mandl C, Sugahara K & Faissner A (1998) The DSD-1 carbohydrate epitope depends on sulfation, correlates with chondroitin sulfate D motifs, and is sufficient to promote neurite outgrowth. *Journal of Biological Chemistry* 273: 28444–28453

Danielson KG, Baribault H, Holmes DF, Graham H, Kadler KE & Iozzo R v. (1997) Targeted disruption of decorin leads to abnormal collagen fibril morphology and skin fragility. *Journal of Cell Biology* 136: 729–743

Davies SJA, Goucher DR, Doller C & Silver J (1999) Robust regeneration of adult sensory axons in degenerating white matter of the adult rat spinal cord. *Journal of Neuroscience* 19: 5810–5822

Deepa SS, Umehara Y, Higashiyama S, Itoh N & Sugahara K (2002) Specific molecular interactions of oversulfated chondroitin sulfate E with various heparin-binding growth factors: Implications as a physiological binding partner in the brain and other tissues. *Journal of Biological Chemistry* 277: 43707–43716

Delekate A, Zagrebelsky M, Kramer S, Schwab ME & Korte M (2011) NogoA restricts synaptic plasticity in the adult hippocampus on a fast time scale. *Proceedings of the National Academy of Sciences of the United States of America* 108: 2569–2574

DeWitt DA, Silver J, Canning DR & Perry G (1993) Chondroitin Sulfate Proteoglycans Are Associated with the Lesions of Alzheimer's Disease. *Experimental Neurology* 121: 149–152

Dick G, Liktan C, Alves JN, Ehlert EME, Miller GM, Hsieh-Wilson LC, Sugahara K, Oosterhof A, van Kuppevelt TH, Verhaagen J, *et al* (2013) Semaphorin 3A binds to the perineuronal nets via chondroitin sulfate type E motifs in rodent brains. *Journal of Biological Chemistry* 288: 27384–27395

Dickendesher TL, Baldwin KT, Mironova YA, Koriyama Y, Raiker SJ, Askew KL, Wood A, Geoffroy CG, Zheng B, Liepmann CD, *et al* (2012) NgR1 and NgR3 are receptors for chondroitin sulfate proteoglycans. *Nature Neuroscience* 15: 703–712

Dityatev A, Schachner M & Sonderegger P (2010) The dual role of the extracellular matrix in synaptic plasticity and homeostasis. *Nature Reviews Neuroscience* 11: 735–746 doi:10.1038/nrn2898

Djerbal L, Lortat-Jacob H & Kwok J (2017) Chondroitin sulfates and their binding molecules in the central nervous system. *Glycoconjugate Journal* 34: 363–376 doi:10.1007/s10719-017-9761-z

Dou CL & Levine JM (1994) Inhibition of neurite growth by the NG2 chondroitin sulfate proteoglycan. *Journal of Neuroscience* 14: 7616–7628

Duan Y, Wang SH, Song J, Mironova Y, Ming G li, Kolodkin AL & Giger RJ (2014) Semaphorin 5A inhibits synaptogenesis in early postnatal- and adult-born hippocampal dentate granule cells. *eLife* 3

Dunah AW, Hueske E, Wyszynski M, Hoogenraad CC, Jaworski J, Pak DT, Simonetta A, Liu G & Sheng M (2005) LAR receptor protein tyrosine phosphatases in the development and maintenance of excitatory synapses. *Nature Neuroscience* 8: 458–467

Dunham I, Kundaje A, Aldred SF, Collins PJ, Davis CA, Doyle F, Epstein CB, Frietze S, Harrow J, Kaul R, *et al* (2012) An integrated encyclopedia of DNA elements in the human genome. *Nature 2012 489:7414* 489: 57–74

Eastwood SL, Law AJ, Everall IP & Harrison PJ (2003) The axonal chemorepellant semaphorin 3A is increased in the cerebellum in schizophrenia and may contribute to its synaptic pathology. *Molecular Psychiatry* 8: 148–155

Eill GJ, Sinha A, Morawski M, Viapiano MS & Matthews RT (2020) The protein tyrosine phosphatase RPTPξ/phosphacan is critical for perineuronal net structure. *Journal of Biological Chemistry* 295: 955–968

Endreffy I, Bjørklund G, Dicső F, Urbina MA & Endreffy E (2016) Acid glycosaminoglycan (aGAG) excretion is increased in children with autism spectrum disorder, and it can be controlled by diet. *Metabolic Brain Disease* 31: 273–278

Enwright JF, Sanapala S, Foglio A, Berry R, Fish KN & Lewis DA (2016) Reduced labeling of parvalbumin neurons and perineuronal nets in the dorsolateral prefrontal cortex of subjects with schizophrenia. *Neuropsychopharmacology* 41: 2206–2214

Faissner A, Clement A, Lochter A, Streit A, Mandl C & Schachner M (1994) Isolation of a neural chondroitin sulfate proteoglycan with neurite outgrowth promoting properties. *Journal of Cell Biology* 126: 783–799

Falk J, Bonnon C, Girault JA & Faivre-Sarrailh C (2002) F3/contactin, a neuronal cell adhesion molecule implicated in axogenesis and myelination. *Biology of the Cell* 94: 327–334

Fang ZX, Hong SQ, Li TS, Wang J, Xie LL, Han W & Jiang L (2019) Genetic and phenotypic characteristics of SCN1A -related epilepsy in Chinese children. *NeuroReport* 30: 671–680

Favuzzi E, Marques-Smith A, Deogracias R, Winterflood CM, Sánchez-Aguilera A, Mantoan L, Maeso P, Fernandes C, Ewers H & Rico B (2017) Activity-Dependent Gating of Parvalbumin Interneuron Function by the Perineuronal Net Protein Brevican. *Neuron* 95: 639-655.e10

Fawcett JW, Oohashi T & Pizzorusso T (2019) The roles of perineuronal nets and the perinodal extracellular matrix in neuronal function. *Nature Reviews Neuroscience 2019 20:8* 20: 451–465

Fernandez-Valle C, Gwynn L, Wood PM, Carbonetto S & Bunge MB (1994) Anti-β1 integrin antibody inhibits schwann cell meylination. *Journal of Neurobiology* 25: 1207–1226

Fisher D, Xing B, Dill J, Li H, Hoang HH, Zhao Z, Yang XL, Bachoo R, Cannon S, Longo FM, *et al* (2011) Leukocyte common antigen-related phosphatase is a functional receptor for chondroitin sulfate proteoglycan axon growth inhibitors. *Journal of Neuroscience* 31: 14051–14066

Franken S, Junghans U, Rosslenbroich V, Baader SL, Hoffmann R, Gieselmann V, Viebahn C & Kappler J (2003) Collapsin response mediator proteins of neonatal rat brain interact with chondroitin sulfate. *Journal of Biological Chemistry* 278: 3241–3250

Freeze HH, Eklund EA, Ng BG & Patterson MC (2012) Neurology of inherited glycosylation disorders. *The Lancet Neurology* 11: 453–466 doi:10.1016/S1474-4422(12)70040-6

Friedlander DR, Milev P, Karthikeyan L, Margolis RK, Margolis RU & Grumet M (1994) The neuronal chondroitin sulfate proteoglycan neurocan binds to the neural cell adhesion molecules Ng-CAM/L1/NILE and N-CAM, and inhibits neuronal adhesion and neurite outgrowth. *Journal of Cell Biology* 125: 669–680

Frischknecht R, Heine M, Perrais D, Seidenbecher CI, Choquet D & Gundelfinger ED (2009) Brain extracellular matrix affects AMPA receptor lateral mobility and short-term synaptic plasticity. *Nature Neuroscience* 12: 897–904

Fujita Y & Yamashita T (2014) Axon growth inhibition by RhoA/ROCK in the central nervous system. *Frontiers in Neuroscience* 8: 338 doi:10.3389/fnins.2014.00338 [PREPRINT]

Gama CI, Tully SE, Sotogaku N, Clark PM, Rawat M, Vaidehi N, Goddard WA, Nishi A & Hsieh-Wilson LC (2006) Sulfation patterns of glycosaminoglycans encode molecular recognition and activity. *Nature Chemical Biology* 2: 467–473

Garber KB, Visootsak J & Warren ST (2008) Fragile X syndrome. *European Journal of Human Genetics* 16: 666–672

Garwood J, Schnädelbach O, Clement A, Schütte K, Bach A & Faissner A (1999) DSD-1-proteoglycan is the mouse homolog of phosphacan and displays opposing effects on neurite outgrowth dependent on neuronal lineage. *Journal of Neuroscience* 19: 3888–3899

del Gaudio D, Shinawi M, Astbury C, Tayeh MK, Deak KL & Raca G (2020) Diagnostic testing for uniparental disomy: a points to consider statement from the American College of Medical Genetics and Genomics (ACMG). *Genetics in Medicine* 22: 1133–1141

Gogolla N, Caroni P, Lüthi A & Herry C (2009) Perineuronal nets protect fear memories from erasure. *Science* 325: 1258–1261

Gonzalez MDL & Silver J (1994) Axon-glia interactions regulate ECM patterning in the postnatal rat olfactory bulb. *Journal of Neuroscience* 14: 6121–6131

Gu M, Wang W, Song WK, Cooper DNW & Kaufman SJ (1994) Selective modulation of the interaction of α7β1 integrin with fibronectin and laminin by L-14 lectin during skeletal muscle differentiation. *Journal of Cell Science* 107: 175–181

Haji-Ghassemi O, Gilbert M, Spence J, Schur MJ, Parker MJ, Jenkins ML, Burke JE, van Faassen H, Martin Young N & Evans S v. (2016) Molecular basis for recognition of the cancer glycobiomarker, LacdiNAc (GalNAc[β1→4]GlcNAc), by Wisteria floribunda Agglutinin. *Journal of Biological Chemistry* 291: 24085–24095

Hayashi N, Mizusaki MJ, Kamei K, Harada S & Miyata S (2005) Chondroitin sulfate proteoglycan phosphacan associates with parallel fibers and modulates axonal extension and fasciculation of cerebellar granule cells. *Molecular and Cellular Neuroscience* 30: 364–377

Hensch TK (2004) Critical period regulation. *Annual Review of Neuroscience* 27: 549–579 doi:10.1146/annurev.neuro.27.070203.144327

Hensch TK (2005) Critical period plasticity in local cortical circuits. *Nature Reviews Neuroscience* 6: 877–888 doi:10.1038/nrn1787

Hikino M, Mikami T, Faissner A, Vilela-Silva ACES, Pavão MSG & Sugahara K (2003) Oversulfated Dermatan Sulfate Exhibits Neurite Outgrowth-promoting Activity toward Embryonic Mouse

Hippocampal Neurons: Implications of dermatan sulfate in neuritogenesis in the brain. *Journal of Biological Chemistry* 278: 43744–43754

van Horssen J, Wesseling P, van den Heuvel LPWJ, de Waal RMW & Verbeek MM (2003) Heparan sulphate proteoglycans in Alzheimer's disease and amyloid-related disorders. *Lancet Neurology* 2: 482–492 doi:10.1016/S1474-4422(03)00484-8

Hou X, Yoshioka N, Tsukano H, Sakai A, Miyata S, Watanabe Y, Yanagawa Y, Sakimura K, Takeuchi K, Kitagawa H, *et al* (2017) Chondroitin Sulfate Is Required for Onset and Offset of Critical Period Plasticity in Visual Cortex. *Scientific Reports* 7: 1–17

Hynes RO (2002) Integrins: Bidirectional, allosteric signaling machines. *Cell* 110: 673–687

Impagnatiello F, Guidotti AR, Pesold C, Dwivedi Y, Caruncho H, Pisu MG, Uzunov DP, Smalheiser NR, Davis JM, Pandey GN, *et al* (1998) A decrease of reelin expression as a putative vulnerability factor in schizophrenia. *Proceedings of the National Academy of Sciences of the United States of America* 95: 15718–15723

Irie F, Badie-Mahdavi H & Yamaguchi Y (2012) Autism-like socio-communicative deficits and stereotypies in mice lacking heparan sulfate. *Proceedings of the National Academy of Sciences of the United States of America* 109: 5052–5056

James SL, Bannick MS, Montjoy-Venning WC, Lucchesi LR, Dandona L, Dandona R, Hawley C, Hay SI, Jakovljevic M, Khalil I, *et al* (2019) Global, regional, and national burden of traumatic brain injury and spinal cord injury, 1990–2016: a systematic analysis for the Global Burden of Disease Study 2016. *The Lancet Neurology* 18: 56–87

Jepsen CS, Dubey LK, Colmorten KB, Moeller JB, Hammond MA, Nielsen O, Schlosser A, Templeton SP, Sorensen GL & Holmskov U (2018) FIBCD1 Binds Aspergillus fumigatus and Regulates Lung Epithelial Response to Cell Wall Components. *Frontiers in Immunology* 9: 1967

Jiang C, Zhu J, Zhou P, Zhu H, Wang W, Jin Q & Li P (2018) Overexpression of FIBCD1 Is Predictive of Poor Prognosis in Gastric Cancer. *American Journal of Clinical Pathology* 149: 474–483

Jones LL, Yamaguchi Y, Stallcup WB & Tuszynski MH (2002) NG2 Is a Major Chondroitin Sulfate Proteoglycan Produced after Spinal Cord Injury and Is Expressed by Macrophages and Oligodendrocyte Progenitors. *Journal of Neuroscience* 22: 2792–2803

Kantor DB, Chivatakarn O, Peer KL, Oster SF, Inatani M, Hansen MJ, Flanagan JG, Yamaguchi Y, Sretavan DW, Giger RJ, *et al* (2004) Semaphorin 5A is a bifunctional axon guidance cue regulated by heparan and chondroitin sulfate proteoglycans. *Neuron* 44: 961–975

Kaplanis J, Samocha KE, Wiel L, Zhang Z, Arvai KJ, Eberhardt RY, Gallone G, Lelieveld SH, Martin HC, McRae JF, *et al* (2020) Evidence for 28 genetic disorders discovered by combining healthcare and research data. *Nature 2020 586:7831* 586: 757–762

Kappler J, Stichel CC, Gleichmann M, Gillen C, Junghans U, Kresse H & Müller HW (1998) Developmental regulation of decorin expression in postnatal rat brain. *Brain Research* 793: 328–332

Karagogeos D (2003) Neural GPI-anchored cell adhesion molecules. *Frontiers in Bioscience* 8 doi:10.2741/1214

Katoh-Semba R, Matsuda M, Kato K & Oohira A (1995) Chondroitin Sulphate Proteoglycans in the Rat Brain: Candidates for Axon Barriers of Sensory Neurons and the Possible Modification by Laminin of their Actions. *European Journal of Neuroscience* 7: 613–621

Khazaei MR, Girouard MP, Alchini R, Tone SO, Shimada T, Bechstedt S, Cowan M, Guillet D, Wiseman PW, Brouhard G, *et al* (2014) Collapsin response mediator protein 4 regulates growth cone dynamics through the actin and microtubule cytoskeleton. *Journal of Biological Chemistry* 289: 30133–30143

Kitagawa H, Tsutsumi K, Tone Y & Sugahara K (1997) Developmental regulation of the sulfation profile of chondroitin sulfate chains in the chicken embryo brain. *The Journal of biological chemistry* 272: 31377–81

Kobayashi M, Sugumaran G, Liu J, Shworak NW, Silbert JE & Rosenberg RD (1999) Molecular cloning and characterization of a human uronyl 2- sulfotransferase that sulfates iduronyl and glucuronyl residues in dermatan/chondroitin sulfate. *Journal of Biological Chemistry* 274: 10474–10480

Kochinke K, Zweier C, Nijhof B, Fenckova M, Cizek P, Honti F, Keerthikumar S, Oortveld MAW, Kleefstra T, Kramer JM, *et al* (2016) Systematic Phenomics Analysis Deconvolutes Genes Mutated in Intellectual Disability into Biologically Coherent Modules. *American Journal of Human Genetics* 98: 149–164

Kolkman MJM, Streijger F, Linkels M, Bloemen M, Heeren DJ, Hendriks WJAJ & van der Zee CEEM (2004) Mice lacking leukocyte common antigen-related (LAR) protein tyrosine phosphatase domains demonstrate spatial learning impairment in the two-trial water maze and hyperactivity in multiple behavioural tests. *Behavioural Brain Research* 154: 171–182

Kramár EA, Lin B, Rex CS, Gall CM & Lynch G (2006) Integrin-driven actin polymerization consolidates long-term potentiation. *Proceedings of the National Academy of Sciences of the United States of America* 103: 5579–5584

Krishnaswamy VR, Benbenishty A, Blinder P & Sagi I (2019) Demystifying the extracellular matrix and its proteolytic remodeling in the brain: structural and functional insights. *Cellular and Molecular Life Sciences* 76: 3229–3248 doi:10.1007/s00018-019-03182-6

Kubaski F, de Oliveira Poswar F, Michelin-Tirelli K, Burin MG, Rojas-Málaga D, Brusius-Facchin AC, Leistner-Segal S & Giugliani R (2020) Diagnosis of mucopolysaccharidoses. *Diagnostics* 10 doi:10.3390/diagnostics10030172

Kubaski F, Osago H, Mason RW, Yamaguchi S, Kobayashi H, Tsuchiya M, Orii T & Tomatsu S (2017) Glycosaminoglycans detection methods: Applications of mass spectrometry. *Molecular Genetics and Metabolism* 120: 67–77 doi:10.1016/j.ymgme.2016.09.005

Lander ES, Linton LM, Birren B, Nusbaum C, Zody MC, Baldwin J, Devon K, Dewar K, Doyle M, Fitzhugh W, *et al* (2001) Initial sequencing and analysis of the human genome. *Nature* 409: 860–921

Lang BT, Cregg JM, Depaul MA, Tran AP, Xu K, Dyck SM, Madalena KM, Brown BP, Weng YL, Li S, *et al* (2015) Modulation of the proteoglycan receptor PTPσ promotes recovery after spinal cord injury. *Nature* 518: 404–408

Lawrence R, Olson SK, Steele RE, Wang L, Warrior R, Cummings RD & Esko JD (2008) Evolutionary differences in glycosaminoglycan fine structure detected by quantitative glycan reductive isotope labeling. *Journal of Biological Chemistry* 283: 33674–33684

Lee H, Raiker SJ, Venkatesh K, Geary R, Robak LA, Zhang Y, Yeh HH, Shrager P & Giger RJ (2008) Synaptic Function for the Nogo-66 Receptor NgR1: Regulation of Dendritic Spine Morphology and Activity-Dependent Synaptic Strength. *Journal of Neuroscience* 28: 2753–2765

Lee HHC, Bernard C, Ye Z, Acampora D, Simeone A, Prochiantz A, di Nardo AA & Hensch TK (2017) Genetic Otx2 mis-localization delays critical period plasticity across brain regions. *Molecular Psychiatry* 22: 680–688

Lindahl B, Westling C, Giménez-Gallego G, Lindahl U & Salmivirta M (1999) Common binding sites for β-amyloid fibrils and fibroblast growth factor-2 in heparan sulfate from human cerebral cortex. *Journal of Biological Chemistry* 274: 30631–30635

Ljunger E, Cnattingius S, Lundin C & Annerén G (2005) Chromosomal anomalies in first-trimester miscarriages. *Acta Obstetricia et Gynecologica Scandinavica* 84: 1103–1107

Marcinkiewicz C, Lobb RR, Marcinkiewicz MM, Daniel JL, Smith JB, Dangelmaier C, Weinreb PH, Beacham DA & Niewiarowski S (2000) Isolation and characterization of EMS16, a C-lectin type protein from Echis multisquamatus venom, a potent and selective inhibitor of the α2β1 integrin. *Biochemistry* 39: 9859–9867

Mauney SA, Athanas KM, Pantazopoulos H, Shaskan N, Passeri E, Berretta S & Woo TUW (2013) Developmental pattern of perineuronal nets in the human prefrontal cortex and their deficit in schizophrenia. *Biological Psychiatry* 74: 427–435

McGeachie AB, Cingolani LA & Goda Y (2011) A stabilising influence: Integrins in regulation of synaptic plasticity. *Neuroscience Research* 70: 24–29 doi:10.1016/j.neures.2011.02.006

McGee AW, Yang Y, Fischer QS, Daw NW & Strittmatter SH (2005) Neuroscience: Experience-driven plasticity of visual cortex limited by myelin and nogo receptor. *Science* 309: 2222–2226

Meathrel K, Adamek T, Batt J, Rotin D & Doering LC (2002) Protein tyrosine phosphatase σ-deficient mice show aberrant cytoarchitecture and structural abnormalities in the central nervous system. *Journal of Neuroscience Research* 70: 24–35

Meyza KZ, Blanchard DC, Pearson BL, Pobbe RLH & Blanchard RJ (2012) Fractone-associated N-sulfated heparan sulfate shows reduced quantity in BTBR T+tf/J mice: A strong model of autism. *Behavioural Brain Research* 228: 247–253

Mikami T, Yasunaga D & Kitagawa H (2009) Contactin-1 is a functional receptor for neuroregulatory chondroitin sulfate-E. *Journal of Biological Chemistry* 284: 4494–4499

Milev P, Friedlander DR, Sakurai T, Karthikeyan L, Flad M, Margolis RK, Grumet M & Margolis RU (1994) Interactions of the chondroitin sulfate proteoglycan phosphacan, the extracellular domain of a receptor-type protein tyrosine phosphatase, with neurons, glia, and neural cell adhesion molecules. *Journal of Cell Biology* 127: 1703–1715

Miller GM & Hsieh-Wilson LC (2015) Sugar-dependent modulation of neuronal development, regeneration, and plasticity by chondroitin sulfate proteoglycans. *Experimental Neurology* 274: 115–125

Miyata S, Komatsu Y, Yoshimura Y, Taya C & Kitagawa H (2012) Persistent cortical plasticity by upregulation of chondroitin 6-sulfation. *Nature Neuroscience* 15: 414–422

Moeller JB, Leonardi I, Schlosser A, Flamar AL, Bessman NJ, Putzel GG, Thomsen T, Hammond M, Jepsen CS, Skjødt K, *et al* (2019) Modulation of the fungal mycobiome is regulated by the chitin-binding receptor FIBCD1. *Journal of Experimental Medicine* 216: 2689–2700

Mosca-Boidron AL, Gueneau L, Huguet G, Goldenberg A, Henry C, Gigot N, Pallesi-Pocachard E, Falace A, Duplomb L, Thevenon J, *et al* (2016) A de novo microdeletion of SEMA5A in a boy with autism spectrum disorder and intellectual disability. *European Journal of Human Genetics* 24: 838–843

Mühleisen TW, Mattheisen M, Strohmaier J, Degenhardt F, Priebe L, Schultz CC, Breuer R, Meier S, Hoffmann P, Rivandeneira F, *et al* (2012) Association between schizophrenia and common variation in neurocan (NCAN), a genetic risk factor for bipolar disorder. *Schizophrenia Research* 138: 69–73

Nagai J, Kitamura Y, Owada K, Yamashita N, Takei K, Goshima Y & Ohshima T (2015) Crmp4 deletion promotes recovery from spinal cord injury by neuroprotection and limited scar formation. *Scientific Reports 2015 5:1* 5: 1–12

Nakanishi K, Aono S, Hirano K, Kuroda Y, Ida M, Tokita Y, Matsui F & Oohira A (2006) Identification of neurite outgrowth-promoting domains of neuroglycan C, a brain-specific chondroitin sulfate proteoglycan, and involvement of phosphatidylinositol 3-kinase and protein kinase C signaling pathways in neuritogenesis. *Journal of Biological Chemistry* 281: 24970–24978

Nakanishi K, Tokita Y, Aono S, Ida M, Matsui F, Higashi Y & Oohira A (2010) Neuroglycan C, a brain-specific chondroitin sulfate proteoglycan, interacts with pleiotrophin, a heparin-binding growth factor. *Neurochemical Research* 35: 1131–1137

Nguengang Wakap S, Lambert DM, Olry A, Rodwell C, Gueydan C, Lanneau V, Murphy D, le Cam Y & Rath A (2020) Estimating cumulative point prevalence of rare diseases: analysis of the Orphanet database. *European Journal of Human Genetics* 28: 165–173

Nikonenko I, Toni N, Moosmayer M, Shigeri Y, Muller D & Sargent Jones L (2003) Integrins are involved in synaptogenesis, cell spreading, and adhesion in the postnatal brain. *Developmental Brain Research* 140: 185–194

Nithianantharajah J & Hannan AJ (2006) Enriched environments, experience-dependent plasticity and disorders of the nervous system. *Nature Reviews Neuroscience* 7: 697–709 doi:10.1038/nrn1970

Novak U & Kaye AH (2000) Extracellular matrix and the brain: Components and function. *Journal of Clinical Neuroscience* 7: 280–290 doi:10.1054/jocn.1999.0212 [PREPRINT]

Okamoto M, Sakiyama J, Mori S, Kurazono S, Usui S, Hasegawa M & Oohira A (2003) Kainic acid-induced convulsions cause prolonged changes in the chondroitin sulfate proteoglycans neurocan and phosphacan in the limbic structures. *Experimental Neurology* 184: 179–195

Pantazopoulos H, Katsel P, Haroutunian V, Chelini G, Klengel T & Berretta S (2021) Molecular signature of extracellular matrix pathology in schizophrenia. *European Journal of Neuroscience* 53: 3960–3987

Pantazopoulos H, Woo TUW, Lim MP, Lange N & Berretta S (2010) Extracellular matrix-glial abnormalities in the amygdala and entorhinal cortex of subjects diagnosed with schizophrenia. *Archives of General Psychiatry* 67: 155–166

Park YK & Goda Y (2016) Integrins in synapse regulation. *Nature Reviews Neuroscience* 17: 745–756 doi:10.1038/nrn.2016.138

Pearson BL, Corley MJ, Vasconcellos A, Blanchard DC & Blanchard RJ (2013) Heparan sulfate deficiency in autistic postmortem brain tissue from the subventricular zone of the lateral ventricles. *Behavioural Brain Research* 243: 138–145

Perosa SR, Porcionatto MA, Cukiert A, Martins JRM, Passeroti CC, Amado D, Matas SLA, Nader HB, Cavalheiro EA, Leite JP, *et al* (2002) Glycosaminoglycan levels and proteoglycan expression are altered in the hippocampus of patients with mesial temporal lobe epilepsy. *Brain Research Bulletin* 58: 509–516

Pietersen CY, Mauney SA, Kim SS, Lim MP, Rooney RJ, Goldstein JM, Petryshen TL, Seidman LJ, Shenton ME, McCarley RW, *et al* (2014) Molecular profiles of pyramidal neurons in the superior temporal cortex in schizophrenia. *Journal of Neurogenetics* 28: 53–69

Pineda D, García B, Olmos JL, Dávila JC, Real MÁ & Guirado S (2005) Semaphorin5A expression in the developing chick telencephalon. In *Brain Research Bulletin* pp 436–440. Elsevier

Pinkstaff JK, Detterich J, Lynch G & Gall C (1999) Integrin subunit gene expression is regionally differentiated in adult brain. *Journal of Neuroscience* 19: 1541–1556

Pizzorusso T, Medini P, Berardi N, Chierzi S, Fawcett JW & Maffei L (2002) Reactivation of ocular dominance plasticity in the adult visual cortex. *Science* 298: 1248–1251

Potapova T & Gorbsky GJ (2017) The consequences of chromosome segregation errors in mitosis and meiosis. *Biology* 6 doi:10.3390/biology6010012 [PREPRINT]

Purushothaman A, Fukuda J, Mizumoto S, ten Dam GB, van Kuppevelt TH, Kitagawa H, Mikami T & Sugahara K (2007) Functions of chondroitin sulfate/dermatan sulfate chains in brain development: Critical roles of E and iE disaccharide units recognized by a single chain antibody GD3G7. *Journal of Biological Chemistry* 282: 19442–19452

Rex CS, Chen LY, Sharma A, Liu J, Babayan AH, Gall CM & Lynch G (2009) Different Rho GTPase-dependent signaling pathways initiate sequential steps in the consolidation of long-term potentiation. *Journal of Cell Biology* 186: 85–97

Ribot J, Breton R, Calvo CF, Moulard J, Ezan P, Zapata J, Samama K, Moreau M, Bemelmans AP, Sabatet V, *et al* (2021) Astrocytes close the mouse critical period for visual plasticity. *Science* 373: 77–81

Ripke S, Neale BM, Corvin A, Walters JT, Farh KH, Holmans PA, Lee P, Bulik-Sullivan B, Collier DA, Huang H, *et al* (2014) Biological insights from 108 schizophrenia-associated genetic loci. *Nature* 511: 421–427

Rogers CJ, Clark PM, Tully SE, Abrol R, Garcia KC, Goddard WA & Hsieh-Wilson LC (2011) Elucidating glycosaminoglycan - protein - protein interactions using carbohydrate microarray and computational approaches. *Proceedings of the National Academy of Sciences of the United States of America* 108: 9747–9752

Rowlands D, Lensjø KK, Dinh T, Yang S, Andrews MR, Hafting T, Fyhn M, Fawcett JW & Dick G (2018) Aggrecan directs extracellular matrix-mediated neuronal plasticity. *Journal of Neuroscience* 38: 10102–10113

Saghatelyan AK, Gorissen S, Albert M, Hertlein B, Schachner M & Dityatev A (2000) The extracellular matrix molecule tenascin-R and its HNK-1 carbohydrate modulate perisomatic inhibition and long-term potentiation in the CA1 region of the hippocampus. *European Journal of Neuroscience* 12: 3331–3342

Santa-Maria I, Hernández F, del Rio J, Moreno FJ & Avila J (2007) Tramiprosate, a drug of potential interest for the treatment of Alzheimer's disease, promotes an abnormal aggregation of tau. *Molecular Neurodegeneration* 2: 1–12

Sarray S, Delamarre E, Marvaldi J, Ayeb M el, Marrakchi N & Luis J (2007) Lebectin and lebecetin, two C-type lectins from snake venom, inhibit α5β1 and αv-containing integrins. *Matrix Biology* 26: 306–313

Scarpa M, Lourenço CM & Amartino H (2017) Epilepsy in mucopolysaccharidosis disorders. *Molecular Genetics and Metabolism* 122: 55–61 doi:10.1016/j.ymgme.2017.10.006 [PREPRINT]

Schlomann U, Schwamborn JC, Müller M, Fässler R & Püschel AW (2009) The stimulation of dendrite growth by Sema3A requires integrin engagement and focal adhesion kinase. *Journal of Cell Science* 122: 2034–2042

Schlosser A, Thomsen T, Moeller JB, Nielsen O, Tornøe I, Mollenhauer J, Moestrup SK & Holmskov U (2009) Characterization of FIBCD1 as an Acetyl Group-Binding Receptor That Binds Chitin. *The Journal of Immunology* 183: 3800–3809

Sharma K, Selzer ME & Li S (2012) Scar-mediated inhibition and CSPG receptors in the CNS. *Experimental Neurology* 237: 370–378 doi:10.1016/j.expneurol.2012.07.009

Shen Y, Tenney AP, Busch SA, Horn KP, Cuascut FX, Liu K, He Z, Silver J & Flanagan JG (2009) PTPσ Is a receptor for chondroitin sulfate proteoglycan, an inhibitor of neural regeneration. *Science* 326: 592–596

Shi Y & Ethell IM (2006) Integrins control dendritic spine plasticity in hippocampal neurons through NMDA receptor and Ca2+/calmodulin-dependent protein kinase II-mediated actin reorganization. *Journal of Neuroscience* 26: 1813–1822

Shintani Y, Takashima S, Asano Y, Kato H, Liao Y, Yamazaki S, Tsukamoto O, Seguchi O, Yamamoto H, Fukushima T, *et al* (2006) Glycosaminoglycan modification of neuropilin-1 modulates VEGFR2 signaling. *EMBO Journal* 25: 3045–3055

Shrive AK, Moeller JB, Burns I, Paterson JM, Shaw AJ, Schlosser A, Sorensen GL, Greenhough TJ & Holmskov U (2014) Crystal structure of the tetrameric fibrinogen-like recognition domain of fibrinogen C domain containing 1 (FIBCD1) protein. *Journal of Biological Chemistry* 289: 2880–2887

Smith PD, Coulson-Thomas VJ, Foscarin S, Kwok JCF & Fawcett JW (2015) "GAG-ing with the neuron": The role of glycosaminoglycan patterning in the central nervous system. *Experimental Neurology* 274: 100–114 doi:10.1016/j.expneurol.2015.08.004

Soares Da Costa D, Reis RL & Pashkuleva I (2017) Sulfation of Glycosaminoglycans and Its Implications in Human Health and Disorders. *Annual Review of Biomedical Engineering* 19: 1–26

Sofroniew M v (2009) Molecular dissection of reactive astrogliosis and glial scar formation. *Trends in Neurosciences* 32: 638–647 doi:10.1016/j.tins.2009.08.002

Srinivasan J, Schachner M & Catterall WA (1998) Interaction of voltage-gated sodium channels with the extracellular matrix molecules tenascin-C and tenascin-R. *Proceedings of the National Academy of Sciences of the United States of America* 95: 15753–15757

Staubli U, Vanderklish P & Lynch G (1990) An inhibitor of integrin receptors blocks long-term potentiation. *Behavioral and Neural Biology* 53: 1–5

Sugiyama S, di Nardo AA, Aizawa S, Matsuo I, Volovitch M, Prochiantz A & Hensch TK (2008) Experience-Dependent Transfer of Otx2 Homeoprotein into the Visual Cortex Activates Postnatal Plasticity. *Cell* 134: 508–520

Takahashi N, Sakurai T, Bozdagi-Gunal O, Dorr NP, Moy J, Krug L, Gama-Sosa M, Elder GA, Koch RJ, Walker RH, *et al* (2011) Increased expression of receptor phosphotyrosine phosphatase-β/ζ is associated with molecular, cellular, behavioral and cognitive schizophrenia phenotypes. *Translational Psychiatry* 1

Takaya R, Nagai J, Piao W, Niisato E, Nakabayashi T, Yamazaki Y, Nakamura F, Yamashita N, Kolattukudy P, Goshima Y, *et al* (2017) CRMP1 and CRMP4 are required for proper orientation of dendrites of cerebral pyramidal neurons in the developing mouse brain. *Brain Research* 1655: 161–167

Tan CL, Kwok JCF, Patani R, Ffrench-Constant C, Chandran S & Fawcett JW (2011) Integrin activation promotes axon growth on inhibitory chondroitin sulfate proteoglycans by enhancing integrin signaling. *Journal of Neuroscience* 31: 6289–6295

Thapar A, Cooper M & Rutter M (2017) Neurodevelopmental disorders. *The Lancet Psychiatry* 4: 339–346 doi:10.1016/S2215-0366(16)30376-5

Tsien RY (2013) Very long-term memories may be stored in the pattern of holes in the perineuronal net. *Proceedings of the National Academy of Sciences of the United States of America* 110: 12456–12461

Valdez R, Ouyang L & Bolen J (2016) Public health and rare diseases: Oxymoron no more. *Preventing Chronic Disease* 13

Venter JC, Adams MD, Myers EW, Li PW, Mural RJ, Sutton GG, Smith HO, Yandell M, Evans CA, Holt RA, *et al* (2001) The Sequence of the Human Genome. *Science* 291: 1304–1351

Vissers LELM, Gilissen C & Veltman JA (2016) Genetic studies in intellectual disability and related disorders. *Nature Reviews Genetics* 17: 9–18

Vo T, Carulli D, Ehlert EME, Kwok JCF, Dick G, Mecollari V, Moloney EB, Neufeld G, de Winter F, Fawcett JW, *et al* (2013) The chemorepulsive axon guidance protein semaphorin3A is a constituent of perineuronal nets in the adult rodent brain. *Molecular and Cellular Neuroscience* 56: 186–200

Vorobyov V, Kwok JCF, Fawcett JW & Sengpiel F (2013) Effects of digesting chondroitin sulfate proteoglycans on plasticity in cat primary visual cortex. *Journal of Neuroscience* 33: 234–243

de Vrij FM, Bouwkamp CG, Gunhanlar N, Shpak G, Lendemeijer B, Baghdadi M, Gopalakrishna S, Ghazvini M, Li TM, Quadri M, *et al* (2019) Candidate CSPG4 mutations and induced pluripotent stem cell modeling implicate oligodendrocyte progenitor cell dysfunction in familial schizophrenia. *Molecular Psychiatry* 24: 757–771

Wallace MJ, Batt J, Fladd CA, Henderson JT, Skarnes W & Rotin D (1999) Neuronal defects and posterior pituitary hypoplasia in mice lacking the receptor tyrosine phosphatase PTPσ. *Nature Genetics* 21: 334–338

Walsh MTH, Ryan M, Hillmann A, Condren R, Kenny D, Dinan T & Thakore JH (2002) Elevated expression of integrin αIIb βIIIa in drug-naïve, first-episode schizophrenic patients. *Biological Psychiatry* 52: 874–879

Wang A & He BP (2009) Characteristics and functions of NG2 cells in normal brain and neuropathology. *Neurological Research* 31: 144–150 doi:10.1179/174313209X393555

Wang Y, Sun M, Liu J, Liu Y, Jiang C, Zhu H, Wang W & Wang Y (2020) FIBCD1 overexpression predicts poor prognosis in patients with hepatocellular carcinoma. *Oncology Letters* 19: 795–804

Warr A, Robert C, Hume D, Archibald A, Deeb N & Watson M (2015) Exome sequencing: Current and future perspectives. *G3: Genes, Genomes, Genetics* 5: 1543–1550

Weiss LA, Arking DE, Daly MJ, Chakravarti A, Brune CW, West K, O'Connor A, Hilton G, Tomlinson RL, West AB, *et al* (2009) A genome-wide linkage and association scan reveals novel loci for autism. *Nature* 461: 802–808

Wiesel TN (1982) Postnatal development of the visual cortex and the influence of environment. *Nature* 299: 583–591 doi:10.1038/299583a0

Winberg ML, Noordermeer JN, Tamagnone L, Comoglio PM, Spriggs MK, Tessier-Lavigne M & Goodman CS (1998) Plexin A is a neuronal semaphorin receptor that controls axon guidance. *Cell* 95: 903–916

de Winter F, Kwok JCF, Fawcett JW, Vo TT, Carulli D & Verhaagen J (2016) The Chemorepulsive Protein Semaphorin 3A and Perineuronal Net-Mediated Plasticity. *Neural Plasticity* 2016

Witting A, Müller P, Herrmann A, Kettenmann H & Nolte C (2000) Phagocytic clearance of apoptotic neurons by microglia/brain macrophages in vitro: Involvement of lectin-, integrin-, and phosphatidylserine-mediated recognition. *Journal of Neurochemistry* 75: 1060–1070

Wu X & Reddy DS (2012) Integrins as receptor targets for neurological disorders. *Pharmacology and Therapeutics* 134: 68–81 doi:10.1016/j.pharmthera.2011.12.008

Xiao X, Levy AD, Rosenberg BJ, Higley MJ & Koleske AJ (2016) Disruption of coordinated presynaptic and postsynaptic maturation underlies the defects in hippocampal synapse stability and plasticity in Abl2/arg-deficient mice. *Journal of Neuroscience* 36: 6778–9791

Xu B, Park D, Ohtake Y, Li H, Hayat U, Liu J, Selzer ME, Longo FM & Li S (2015) Role of CSPG receptor LAR phosphatase in restricting axon regeneration after CNS injury. *Neurobiology of Disease* 73: 36–48

Yamaguchi Y (2000) Lecticans: Organizers of the brain extracellular matrix. *Cellular and Molecular Life Sciences* 57: 276–289 doi:10.1007/PL00000690

Yeo TT, Yang T, Massa SM, Zhang JS, Honkaniemi J, Butcher LL & Longo FM (1997) Deficient LAR expression decreases basal forebrain cholinergic neuronal size and hippocampal cholinergic innervation. *Journal of Neuroscience Research* 47: 348–360

Yuan W, Matthews RT, Sandy JD & Gottschall PE (2002) Association between protease-specific proteolytic cleavage of brevican and synaptic loss in the dentate gyrus of kainate-treated rats. *Neuroscience* 114: 1091–1101

Zhang F & Lupski JR (2015) Non-coding genetic variants in human disease. *Human Molecular Genetics* 24: R102–R110 doi:10.1093/hmg/ddv259

Zhou X-H, Brakebusch C, Matthies H, Oohashi T, Hirsch E, Moser M, Krug M, Seidenbecher CI, Boeckers TM, Rauch U, *et al* (2001) Neurocan Is Dispensable for Brain Development. *Molecular and Cellular Biology* 21: 5970–5978

Zimmermann DR & Dours-Zimmermann MT (2008) Extracellular matrix of the central nervous system: From neglect to challenge. *Histochemistry and Cell Biology* 130: 635–653 doi:10.1007/s00418-008-0485-9

Curriculum Vitae

Christopher W. Fell, MSc

D.O.B.: 09/01/1994. Nationality: UK, USA.

Email: cfell@cemm.at; fell.christopherw@gmail.com

---

1) Education

09/2017 – present	**Doctoral Thesis** in Molecular Neuroscience at LBI-RUD/CeMM, Vienna, Austria. Supervisor: Vanja Nagy.
09/2016 – 09/2017	**MSc** in Molecular Genetics at the University of Leicester, UK. Overall grade: Distinction (highest available grade). Thesis: *Novel Tools For Analysis of* Drosophila *Chronobiology*. Grade: Distinction (79%). Exam results: Lecture material: Distinction (85%, top score); Practical material: Distinction (72%).
09/2012 – 07/2015	**BSc** in Biological Sciences (Genetics) at the University of Leicester, UK. Grade: Upper Second-Class.
09/2008-07/2012	**A level** Maths (A), Biology (B), Chemistry (B) at St Bede's School, Redhill, UK. **As level** Maths (A), Chemistry (A), Biology (B), English Literature (B), Critical Thinking (B). 12 **GCSEs**: 3(A*), 8(A), 1(B).

2) Lab experience

11/2018		2 week placement in the lab of **Marius Wernig** (Stanford University, CA, USA) I learned their protocol for primary T cell transdifferentiation to blood iNs (PMID: 29866841).
11/2018		1 week placement in the lab of **Deanna Benson** (Icahn School of Medicine at Mount Sinai, NY, USA), where I learned the Banker 'sandwich' culture method for primary mouse neurons.
11/2017 12/2017	-	5 week rotation in the lab of **Stefan Kubicek** (CeMM, Vienna, AT) where I learned how to plan, execute and analyse high-throughput drug screens.
01/2017 07/2017	-	MSc thesis project in the lab of **Ezio Rosato** (UoL, UK) where we developed a novel genetic reporter for circadian rhythm synaptic activity in *Drosophila*.
09/2014 02/2015	-	BSc thesis project in the lab of **Ed Hollox** (UoL, UK) performing PCR-RFLP on a number of SNPs in the gene *DMBT1* to test for linkage disequilibrium.

3) Fellowships and Grants

08/2020	Contribution to successful FWF 1000 ideas proposal (TAI202): **150,000** €

11/2019 DOC PhD fellowship of the Austrian Academy of Sciences (25525): **144,000** €

4) Conferences and Symposia

11/2021 (upcoming) Poster: Society for Neuroscience 2021, Chicago, USA.

04/2021 Poster: Genomics of Brain Disorders 2021, Wellcome Genome Campus, UK.

03/2021 Organiser: Syngap1 Symposium 2021, Vienna, Austria.

10/2020 Flashtalk: World Wide Neuro online seminar series (available on YouTube: https://www.youtube.com/watch?v=vLvV1M7pad8)

10/2019 Poster: EU Life Scientific meeting, Babraham Institute, Cambridge, UK.

06/2019 Poster: Young Scientist Association PhD Symposium, Vienna, Austria.

06/2018 Poster: Young Scientist Association PhD Symposium, Vienna, Austria.

05/2018 Poster: Ubiquitin and Friends symposium, Vienna, Austria.

List of publications

([†] shared first author ; * co-corresponding)

1) Fell, C.W.[†], Hagelkruys, A.[†], Cicvaric, A., Horrer, M., Liu, L., Li, J.S.S., Stadlmann, J., Polyansky, A.A., Mereiter, S., Tejada, M.A., Kokotović, T., Scaramuzza, A., Twyman, K., Morrow, M.M., Juusola, J., Yan, H., Wang, J., Burmeister, M., Andersen, T.L., Wirnsberger, G., Holmskov, U., Perrimon, N., Zagrovic, B., Monje, F.M., Moeller, J.B., Penninger, J.M.*, Nagy, V.* **FIBCD1 is an endocytic GAG receptor associated to a novel neurodevelopmental disorder.** *Submitted*.
    - Pre-print available on BioRxiv: https://www.biorxiv.org/content/10.1101/2021.09.09.459581v1

2) Fell, C.W. and Nagy, V. **Cellular models and high-throughput screening for genetic causality of Intellectual Disability**. *Trends in Molecular Medicine* (2021) (review).

3) Kokotović, T, M., Langeslag, M., Lenartowicz, E., Manion, J., Fell, C.W., Alehabib, E., Tafakhori, A., Darvish, H., Metscher, B., Bellfroid, E., Neely, G., Kress, M., Penninger, J. M. and Nagy, V. **PRDM12 is required for pain sensation throughout life.** *Frontiers in Molecular Neuroscience* (2021).

4) Vulliard, L., Hancock, J., Kamnev, A., Fell, C.W., Ferreira da Silva, J., Loizou, J., Nagy, V., Dupre, L., Menche, J. **BioProfiling.jl: profiling biological perturbations with high-content imaging in single cells and heterologous populations**. *Bioinformatics* (2021).

5) Kokotović, T [†]. Lenartowicz, E. [†], Langeslag, M., Ciotu, C., Fell, C.W., Scaramuzza, A., Fischer, M., Kress, M., Penninger, J. M., Nagy, V. **Transcription factor Mesenchyme Homeobox Protein 2 (MEOX2) modulates nociceptor function.** *FEBS Journal* (2022).